The Calculation and Inversion of SIROTEM Transient Electromagnetic Responses Over a Layered Earth

by

Richard Stuart Smith
B.Sc. (Hons) (Adelaide)

Thesis submitted for the Degree of Master of Science
The Department of Economic Geology, Faculty of Science
The University of Adelaide

1984

Table of Contents

Abstract

The problem of adjusting conductivity structures so as to reproduce electromagnetic responses obtained in the field is still an active area of research. Most of the current computer programs for calculating responses are expensive to run, as they require large computation times.

This thesis presents means by which the response of a layered earth can be calculated more rapidly. The algorithms have been designed with the Australian prospecting system SIROTEM in mind, and thus all responses are calculated directly in the time domain. One algorithm, an asymptotic expansion, yields the response very rapidly. The asymptotic expansion is valid only at late times, but it is very easy to determine the regions in which it is not valid. The other algorithm, a numerical intergration of an integral, works only when overlying layers are more resistive than the half-space. This is because the poles in the Laplace transform of the voltage response have been ignored. Poles only exist for overlying layers more conductive than the half-space.

Both algorithms can cater for variable ramp rise times, intergration over time windows, and a variety of loop geometries.

These methods have been incorporated within a routine for inverting SIROTEM data. Run times are of the order of a few seconds. Inversions performed on synthetic data, in regions when the methods are valid, illustrate a number of interesting

lessons. This inversion routine can be used for obtaining an initial guess for a slower routine, or alternatively the algorithms can be incorporated within currently existing routines to speed computation time significantly.

Declaration

I certify that this thesis contains no material which has been accepted for the award of any other degree or diploma in any university, and that to the best of my knowledge and belief the thesis contains no material previously published or written by another person except where due reference is made in the text of the thesis.

Richard Smith

Acknowledgement

Due acknowledgement must go to my supervisors Dr. Denis O'Brien and Dr. Peter Brooker for the help and guidance I received during the development of this thesis. I wish to thank them for the aid and advice given by both of them during the years 1982 and 1983 - it is highly appreciated. Thanks must also go to Professor D.M. Boyd, and other members of the Economic Geology Department.

The accuracy of the answers obtained using the algorithms outlined in this thesis were checked by comparison with those of the C.S.I.R.O. developed program GRENDL. The GRENDL runs were made at the courtesy of CRA Exploration (a co-sponsor in the Australian Mineral Industries Research Association - AMIRA). I also wish to thank R.J. Smith of CRA Exploration for his help and encouragement over the previous two years.

Section 1 - Introduction

1.1 The Transient Electromagnetic Prospecting Method

Over the past decade the transient electromagnetic (TEM) method has become increasingly popular as an exploration tool. The method involves exciting the earth with a time varying 'primary' magnetic field which is generated by a current carrying transmitter loop. The variation of the primary magnetic field induces eddy currents in conductors within the earth. The time taken for the decay of these eddy currents depends primarily on the conductivity of the conductor. A 'secondary' magnetic field is produced by these eddy currents. Electromagnetic methods give a measure of the rate of decay of these secondary fields. This is normally done by measuring the electromotive force (emf) induced in the receiver coil by the time rate of change of the flux of the secondary magnetic field through the receiver loop. In the time domain the measurements are made while the primary magnetic field is constant (for example zero) so that the primary induced emf is zero. Measuring the secondary field whilst the primary field is zero allows for greater sensitivity and an enhanced signal to noise ratio - particularly at late times (C.S.I.R.O. (1978)). It has been reported that conductive overburdens do not have the same shielding effect in the time domain as they do in the frequency domain (Spies (1976)).

Early attempts to apply electromagnetic prospecting methods to the Australian environment met with difficulties. For

example, the common occurrence of saline ground water and conductive host rocks shield the effect of conductive orebodies. In 1972 the Commonwealth Scientific and Industrial Research Organization (C.S.I.R.O.) initiated research into the transient electromagnetic technique. The time domain system was chosen as it was thought to be more suitable to the Australian environment (C.S.I.R.O. (1978), McCracken et al (1980), Spies (1976)), and capable of distinguishing between highly conductive orebodies, and conductive host rock and overburden (Buselli (1980a)). The C.S.I.R.O. set out to make improvements on the time domain equipment which was available at the time such as the Russian MPPO-1 system (Buselli (1974)). Since the secondary fields take longer to decay for conductive rocks than resistive rocks it was essential that the new equipment should make measurements at later times - so as to monitor this decay (Buselli (1974)). Furthermore, the Russian MPPO-1 system was susceptible to non-geologic noise such as lightning (sferics), power lines and VLF and R.F. radio transmitters (22, 44 and 800 kHz) (Buselli (1977) and Spies et al (1981)).

The research carried out by the C.S.I.R.O. resulted in the release in 1978 of the SIROTEM prospecting system (Buselli and O'Neill (1977)). The final model released could record the signal at delay times as great as 177.4 milliseconds. The unit was light (16 kg), simple to operate and recorded data automatically onto magnetic tape, as well as providing a printout of the data in the field. Filters reject the noise from radio transmitters and power lines. Digital stacking of up to 4096

readings helps to minimize random noise. In addition to this the SIROTEM unit contains a IM6100 microprocessor capable of rejecting sferic noise, normalizing the voltage response relative to different transmitter currents, and for each reading it calculates the mean percentage error and the apparent conductivity (coincident loops only). Many loop configurations are possible with SIROTEM, but the most commonly used are shown in figure 1.1.

The usefulness of SIROTEM in cases when conductive overburden shields an orebody is illustrated by Buselli (1980b). When SIROTEM is used with coincident transmitter and receiver loops the depth of penetration of the SIROTEM signals is approximately equal to the loop size (Buselli (1981)). Recent results obtained with Backus-Gilbert inversion of SIROTEM data suggest that in resistive cases the depth of penetration may be up to five times the loop size (P.K. Fullager - University of Toronto Seminar, Jan. 1984).

1.2 Modelling of TEM Data

The task of a Geophysicist is to deduce the subsurface structure which produces the TEM response obtained in the field. This can be done with scale model studies, but with increased access to computing facilities numerical modelling is becoming more popular. In numerical and scale modelling the subsurface is approximated by simple shapes, and the form of the subsurface is adjusted until the response obtained adequately represents the field data.

To be able to calculate responses numerically requires that

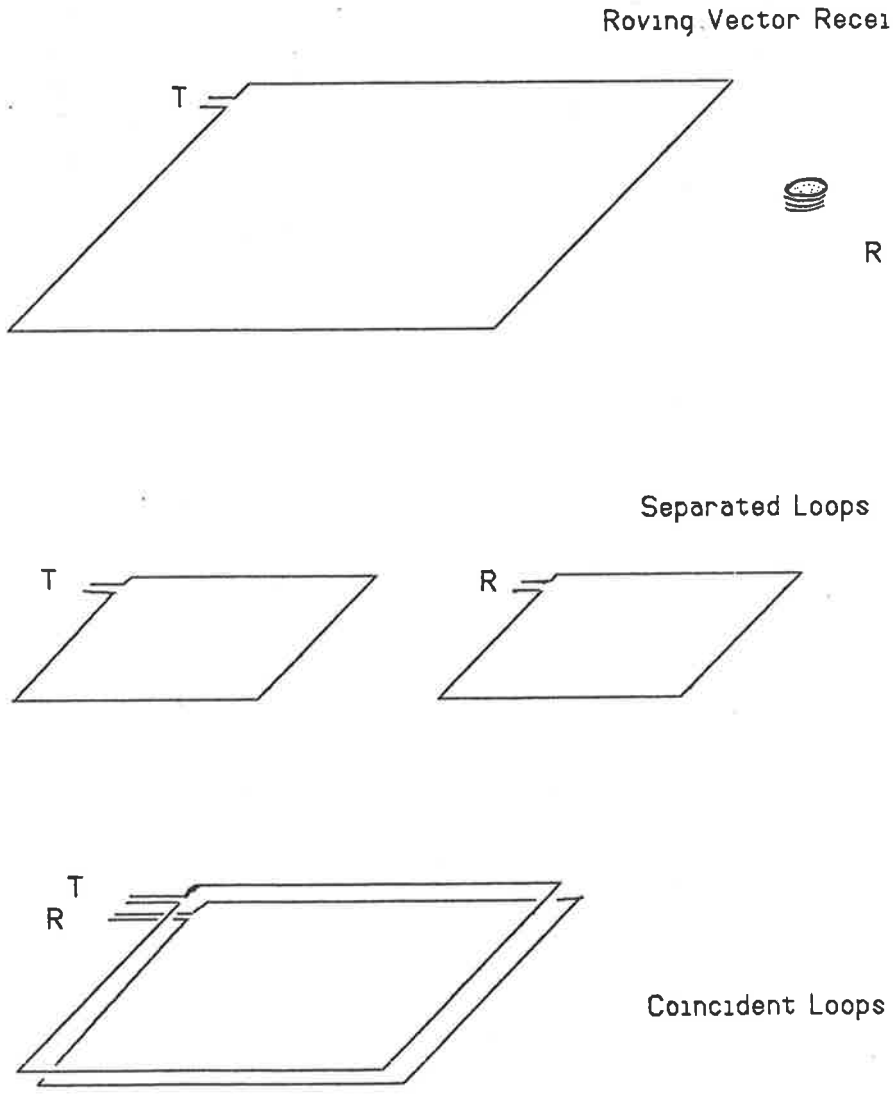

Figure 1.1 Common loop configurations for SIROTEM. (T denotes transmitter, R denotes receiver)

Maxwell's equations be solved subject to: (i) the relevant boundary conditions at interfaces of media with different constitutive parameters, and (ii) the boundary conditions at infinity. Solutions have only been obtained in a limited number of cases such as a horizontally layered earth, or the cases of a conducting sphere and an infinite cylinder in free space (see Ward (1967)). The assumption that conductors are suspended in free space is in general an unrealistic approximation (Singh (1973)), particularly in the Australian environment. When Maxwell's equations have not been solved analytically, numerical solutions must be sought. This is a difficult computational task, and is currently the subject of research (recent examples being Wannamaker, Hohmann and San Filipo (1984), and Das and Verma (1982)). The numerical solutions to Maxwell's equations are in general so time consuming that inversion is only really practical for problems to which analytic solutions have been found. The work discussed in this thesis has been restricted to the TEM response of a horizontally layered ground (see figure 1.2). This problem has been solved analytically, and Wait (1982) gives a good guide to the literature. The response of a layered earth can be written in closed form after Laplace (or Fourier) transformation of the time variable, and Hankel transformation of the radial cylindrical co-ordinate. Thus in principle the problem is solved, however the inversion of the Laplace and Hankel transforms is difficult. Morrison, Phillips and O'Brien (1969) used the trapezoidal quadrature rule for the inverse Hankel transform, and then a Fast Fourier transform for the

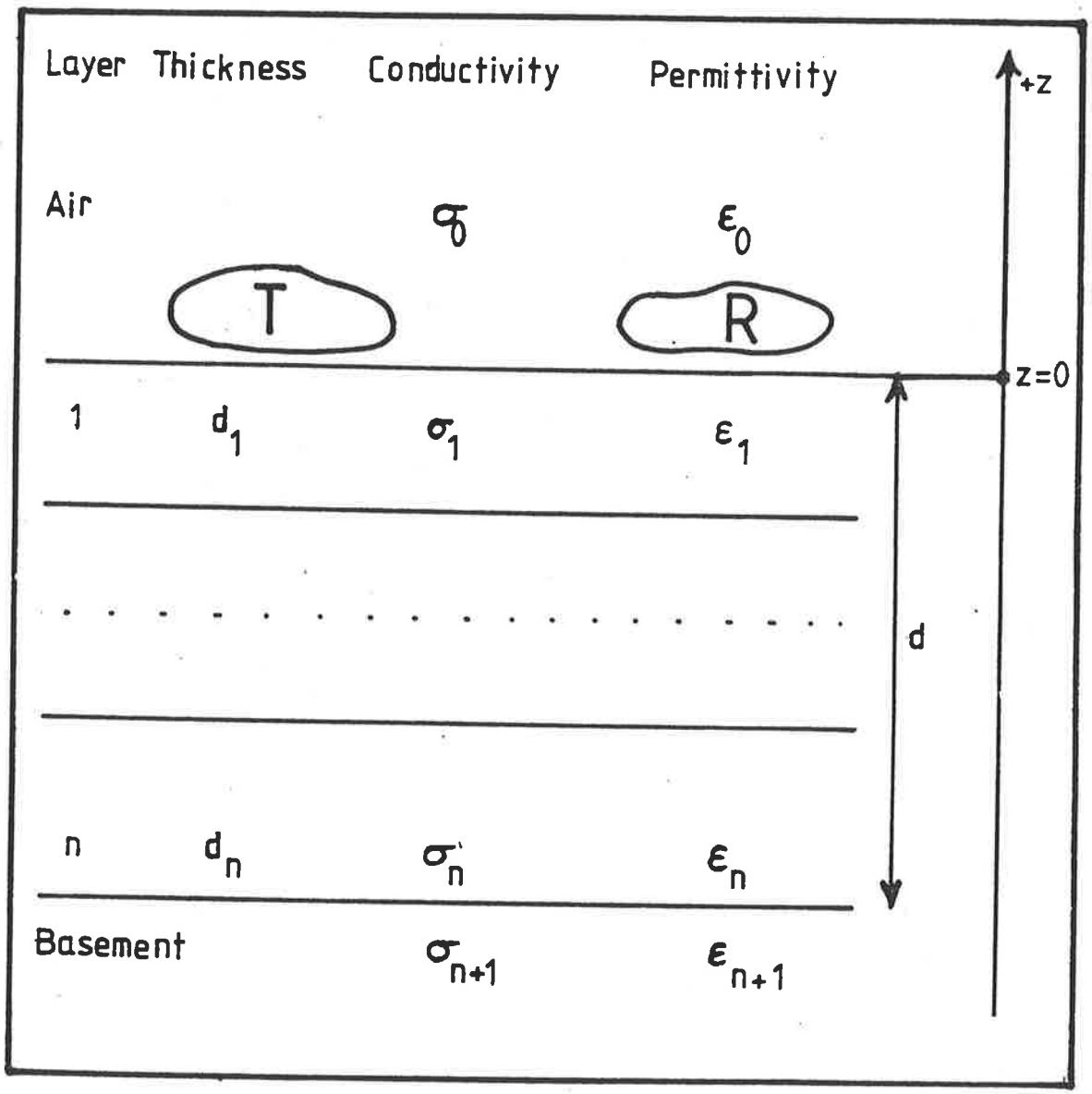

Figure 1.2 The horizontally layered ground discussed in this thesis.

inverse Fourier transform. Lee and Lewis (1974) and Raiche and Spies (1981) have also solved the layered earth problem by subtracting out the half-space response. Lee and Lewis fit cubic splines to the frequency response, and transform the splines analytically to the time domain. According to Lee (1982) their program is inaccurate at late times. Raiche and Spies also subtract out the half-space response, but they perform both inverse transformations with Patterson's (1973) algorithm. According to Knight and Raiche (1982) the method of subtracting out the half space response results in difficulties, as it involves the subtraction of two terms which are the same order of magnitude at late times. The development of digital filters for Hankel transforms of arbitrary order ν allows more efficient programs to be written. Efficiency may be increased further by formulating the Fourier transform as a Hankel transform of order $\nu = 1/2$, and using digital filters. Examples of work with digital filters have been presented by Koefoed et al (1972), Mallick and Verma (1978) and Anderson (1979)).

By reversing the order of the inverse transformations and employing the Gaver-Stehfest (Gaver (1966), Stehfest (1970)) inverse Laplace transform algorithm followed by an adaptive version of Patterson's (1973) numerical intergration algorithm for the inverse Hankel transform Knight and Raiche (1982) made a further improvement in efficiency. It is because the kernel of the integral is known analytically rather than numerically that the Gaver-Stehfest algorithm can be employed, and this allows for gains in the speed, and in the accuracy of the inversion (Knight

and Raiche (1982)). The adaptive Gaussian quadrature for the inverse Hankel transform in Knight and Raiche's routine has since been replaced by a digital filter, and the new algorithm is currently the best available. Further extensions outlined by Raiche (1983) allow the algorithm to calculate the response for ramp function inputs and separated transmitting and receiving loops.

Lee and Lewis (1974) have shown that at early or late times the TEM response approaches that of a half-space whose conductivity is equal to that of the top or bottom layer respectively. Rather than perform time consuming numerical integrations a more rapid means of obtaining a TEM response would be to approximate the integrals by asymptotic expansions. Lee (1982) has developed a two term asymptotic expansion for coincident transmitter and receiver loops over a layered earth. The expansion is only valid at late times. Lee's result subsumes the results of Kamenetski (1969) and Kaufman (1979). Asymptotic expansions are simple to program, and very rapid to calculate. They work best at late times, when it seems that the algorithm of Knight and Raiche is slowest (in its pre-digital filter form).

The algorithms discussed above (such as that of Knight and Raiche) provide a means of calculating layered earth responses at relatively little cost. However a Geophysicist's task is not to calculate the response from a given earth model (the forward problem), but rather, to infer the layered structure from the response of the layered earth (the inverse problem).

In practice the inversion problem is solved by employing an

iterative optimization algorithm which automatically adjusts a layered earth model (from some initial guess) in such a manner so as to minimize a cost function which is a measure of the discrepancy between the response obtained for the adjusted model and the desired response. The 'solution' obtained by such an optimization algorithm will be the local minimizer of the cost function, and except in exceptional circumstances the solution obtained is dependent on the initial guess used in the optimization algorithm. The 'best' solution can only really be obtained after a number of initial guesses have been tried for the optimization program. The choice of these initial guesses must be guided by the geophysicist's intuition, knowledge of geological information, and the results of previous runs of the algorithm. It is therefore essential that if the geophysicist is to gain a feel as to what the solution space looks like, then the inversion (or optimization) runs must be made in real time whilst the user is waiting at an interactive terminal. To achieve this every possible efficiency must be incorporated into the code which calculates the forward problem.

1.3 Layered Earth Inversion

Several layered earth inversion schemes currently exist (such as those developed by Anderson for the EM library of the United States Geological Survey), but the program developed by the C.S.I.R.O. and Macquarie University called GRENDL is the most notable. GRENDL has the following features:

(1) The forward solution is the Knight and Raiche routine discussed above.

(2) The inversion algorithm is a modified Marquardt algorithm (damped least squares) which was developed by Jupp and Vozoff (1975).

(3) The program allows for simultaneous joint inversion of two data sets taken at the same locality. The program currently supports resistivity and TEM layered earth inversion (either or both). Joint inversion has the advantage that it may be capable of resolving the parameters associated with a certain layered structure which one data set would be unable to do alone. This is because TEM and resistivity respond differently to certain layered structures. Thus joint inversion could be useful for resolving thin resistive layers to which TEM sounding is not sensitive.

(4) The parameter statistics of the final model give an estimate of a parameter's effect in ascertaining the final model, and an indication of the error or reliability associated with a particular parameter.

GRENDL provides an excellent means of inverting layered earth data, but it is subject to two weaknesses:

(a) If TEM data is being inverted, then GRENDL runs slowly. This is particularly true for small and medium sized computers, and this makes it difficult to run the program interactively. Therefore it is difficult for the user to develop and apply an intuition to the problem. Seeing the results of an inversion soon after an initial guess has been made provides the user with quick feedback, and thus confirms or denies any suspicions which guided the user towards that initial guess. In such a way an

idea of the form of solution space may be built up.

(b) Like many other inversion schemes the Marquardt algorithm only finds a local minimum of the cost function. The statistics estimates are dependent on the shape of the 'valley' associated with the local minimum of the cost function, and thus they will only be correct if the valley found by the optimization routine is the correct valley (global minimum). Statistical information should only be taken note of if the user is confident that the correct valley in the solution space has been obtained.

Overcoming the problem outlined in (a) above (i.e. making the program quicker) would allow the problem referred to in (b) to be partially overcome. If the algorithm was to be quicker, then many initial guesses could be tried, and thus the user could gain an indication as to how stable and how geologically feasible the solutions obtained are. This would substantially decrease the users reliance on the parameter statistics calculated by the inversion algorithm.

1.4 Possible Refinements

The aim of this thesis is to investigate methods by which the TEM response over a layered earth can be calculated more rapidly. If this is achieved then it may be possible to refine or complement the GRENDL program at a later stage.

The TEM prospecting system considered consists of a horizontal receiving loop (R) and a horizontal transmitting loop (T). The current flowing in the magnetic loop has the following time dependence.

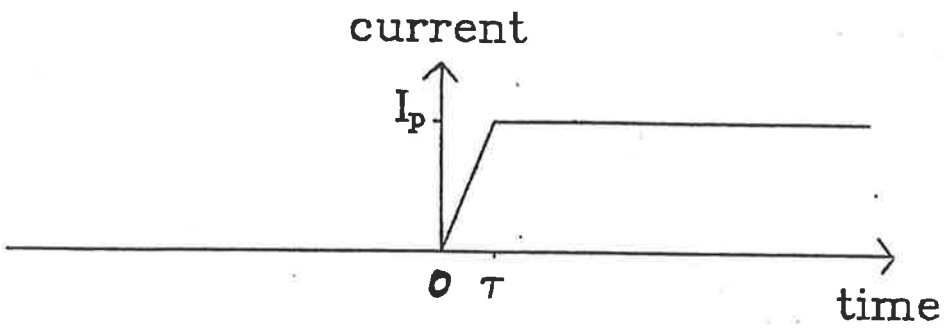

FIGURE 1.3

Thus

$$I(t) = \begin{cases} 0 & t<0 \\ (t/\tau)I_p & 0<t\leq\tau \\ I_p & \tau<t \end{cases}$$

Such a ramp input function can model various prospecting systems such as UTEM (Lamontagne et al (1980)), but for small τ or in the limit as $\tau \to 0$ it models the SIROTEM system (Buselli and O'Neill (1977)).

Define the following scaled dimensionless variables

QUANTITY	UNIT
length	λ
conductivity	σ_{n+1}
time	$\sigma_{n+1}\mu\lambda^2$
permitivity	$\sigma^2_{n+1}\mu\lambda^2$
electric field intensity	volts/λ
current density	amps/λ^2

λ can be any length, but it is most conveniently chosen as the radius of the loop (or one of the side lengths in the case of

rectangular loops).

We wish to compute the dimensionless quantity

$$Z(t) = \lambda\sigma_{n+1} V / I_p$$

Where V is the electromotive force (emf) induced in the receiving loop (Volts), I_p is the peak value of the current in the transmitter loop (Amps) and σ_{n+1} is the basement conductivity (see figure 1.2). Z(t) is related to the mutual impedance of the transmitting and receiving loops over the layered medium.

O'Brien and Smith (1984) (see appendix for details) show that the Mutual impedance can be written

$$Z(t) = 1/(2\pi i) \int_c \exp(st)\, Z(s)\, ds \qquad (1.2)$$

where

$$Z(s) = -1/(4\pi)\, sI(s) \int_0^\infty d1\, P(1)\, K(1,s) \qquad (1.3)$$

The form of I,P and K can be obtained from the appendix. It is sufficient to point out that K depends on the earth's geometrical and electrical properties and can be computed in terms of elementary functions. P (the loop function) depends solely on the loop geometry, and is independent of the electrical properties of the ground. The contour of inte gration must lie to the right of any singularities of Z(s). In the appendix it is shown that in the quasi-static approximation K has a square root branch cut on the line $[-\infty, -1^2]$ and a possibility (in cases of layers more conductive than the basement) of a finite number of

poles in the region $[-1^2,0]$. The singularities are therefore confined to the negative real axis, and the contour may be any vertical line in the right half plane. The order of integration is reversed, and the contour is deformed around the negative real axis. Thus

$$Z(t)= -1/(4\pi) \int_0^{\infty} d1\ P(1) \left\{ \int_{-\infty}^{-1^2} ds\ \exp(st)\ sI(s)\ D(1,s) + \text{residues at poles} \right\} \qquad (1.4)$$

where D is the discontinuity function of K across the branch cut.

$$D(1,s) = 1/(2\pi i) \lim_{v \to 0^+} [K(1,u-iv)-K(1,u+iv)]$$

where $s=u+iv$.

By discarding the effect due to the residue at the poles the order of integration can again be exchanged, and the following result is obtained:

$$Z(t) = (1/\tau)[\ B_1(t) - B_1(t-\tau)\ ] \qquad (1.5)$$

where

$$B_i(t) = (1/\pi^2) \int_0^{\infty} dx\ \exp(-x^2 t)\ x^{2(i-1)}\ S(x) \qquad (1.6)$$

and

$$S(x) = \pi/2 \int_0^{1} dm\ P(mx)\ D(m,x)$$

x and m are defined by:

$$s=-x^2 \quad , \quad 1 = mx$$

Taking the limit as $\tau \to 0$ gives

$$Z(t) = - B_2(t) \tag{1.7}$$

The solution obtained for layered earth responses is given by (1.5) and (1.7). The results derived are subject to the following assumptions:

(1) The time dependence of the current is as shown in figure 1.3.

(2) The transmitter and receiver lie on a flat earth. The transmitter and receiver wires are filamental.

(3) The earth geometry (as shown in figure 1.2) consists of a finite number of layers with differing thickness (d_i) and conductivities (σ_i). The layers are of infinite horizontal extent, and lie above a half space of infinite horizontal and vertical extent.

(4) The quasi-static approximation has been made ($\varepsilon \to 0$). Grant and West (1965) have justified the validity of this approximation. Lee (1981) discusses the validity of the approximation for a uniform half space.

(5) That the residues due to the poles can be ignored. The validity of this approximation is discussed later.

Given this formulation of the problem the purpose of this thesis is to investigate means by which the calculation of TEM layered earth responses can be performed more rapidly. The formulation also offers a number of advantages over previous

formulations. The efficiencies and advantages of the formulation are outlined below.

1.4.1 Asymptotic Expansion

Equations (1.5) and (1.7) are in a form to which Watson's lemma (Olver 1974) can be applied.

$$B_i(t) \sim A_i(t) = (1/2\pi^2)\sum_{r=0}^{\infty} S_r \Gamma((r+1)/2+i)\, t^{-((r+1)/2+i)} \qquad (1.8)$$

where S_r are the Taylor co-efficients of the function S.

$$S(x) = x^2 \sum_{r=0}^{\infty} S_r\, x^r \qquad (1.9)$$

O'Brien and Smith (1984) show how the terms of the expansion can be computed. Computation times are very rapid - being measured in terms of hundredths of a second for the first time, and thousandths of a second for all subsequent times. The saving for later times is because the S_r can be computed once and then stored for later use. The S_r are independent of time, and vary only with the loop and earth geometry. The advantage of this asymptotic expansion is that the region of 'convergence' can be determined. It is therefore possible to decide whether to employ the expansion to calculate the TEM response, or to use the more costly Knight and Raiche routine. The incorporation of the asymptotic expansion into GRENDL should reduce the total computation time for GRENDL significantly.

1.4.2 Numerical Integration

Knight and Raiche decreased the computation time and the instability of layered earth calculations by incorporating the Gaver-Stehfest algorithm for the inverse Laplace transform. The Gaver-Stehfest algorithm requires that the function to be inverted must be known analytically. To achieve this Knight and Raiche must perform the inverse Laplace transform prior to the Hankel transform. As a consequence of this the time variable is contained in the inner integral, and thus inverse Laplace and Hankel transforms must be computed for each time at which the response is required. In the formulation of this thesis the time variable appears only once - in the outer integral of equation (1.6). This is a consequence of the fact that numerical instabilities have already been overcome because of the analytic continuation inherent in the deformation of the contour of integration around the spectrum of the integrand. A direct numerical integration should therefore provide further efficiencies, as the response at all times can be calculated with one evaluation of the inverse Hankel transform (the m integration). In testing this hypothesis standard numerical integration packages can be employed. The method only works when the basement is more conductive than any of the overlying layers. There are two reasons why this is so for resistive overburdens:

(i) The kernel K(1,s) has no poles in the region $[-1^2,0]$, and thus no errors are introduced due to omission of the residues in equation (1.4).

(ii) The function S(x) is smooth, and therefore the outer

integration is easily computed.

For cases of layers more conductive than the basement it is possible for the function K(1,s) to have poles, and the pole terms, although they have no effect on the asymptotic analysis, do become important at early times. Also, there are zeros associated with the discontinuity function D(1,s). They occur in complex conjugate pairs in the complex x plane. As the conductivity contrasts increase these zeros migrate towards the line of integration, and cluster towards the origin. The kernel of S(x) therefore develops nasty peaks, and this makes the numerical integration exceedingly difficult. It is possible to evaluate the function S(x) by using adaptive integration algorithms, but the cost of such calculations is not justified. The numerical integration of (1.5) or (1.7), is therefore only suitable for resistive overburdens.

1.4.3 Integration Over Time Windows

In practical TEM prospecting systems the quantity measured is not Z(t), but rather the average of Z(t) over a finite time interval (window).

$$Z(t_i, t_{i+i}) = 1/(t_{i+1} - t_i) \int_{t_i}^{t_{i+1}} Z(t)dt$$

Normally this average would be calculated numerically, but clearly this is expensive. Formulae (1.5) and (1.7) and (1.8) can all be analytically integrated with respect to time, and thus the integration over time windows can be performed with a negligible increase in the computational cost. There is a marked

difference between data which has been integrated over a window, and data which has not (particularly in the early SIROTEM channels). This, and the effect of altering the ramp rise time (τ) are illustrated later.

1.4.4 Asymptotic Inversion

The asymptotic expansion (equation (1.8)) can be calculated so rapidly that when it is incorporated as the forward problem in an inversion routine it is possible to complete an inversion run on a Cyber 173 in approximately 5 seconds. On smaller machines the inversion would also be completed in real time. As the region of convergence is known, it is possible to devise algorithms which discard data for those channels at which the expansion diverges. The asymptotic formula can therefore be used to develop the geophysicist's intuition concerning the problem, and to provide the user with a feasible initial guess for a more sophisticated program such as GRENDL.

The asymptotic formula has been incorporated into a non-linear least squares optimization program which permits arbitrary linear constraints to be imposed on the parameters. These constraints allow for positivity constraints on the conductivities and thicknesses, and constraints which are dictated by geological evidence and the user's intuition.

Having a TEM fitting program which can be run in real time is a significant step towards quantative modelling of TEM field data. It provides an ability to differenciate between the response of a non-layered conductor and the surrounding layered strata. It also provides a simple means of bedrock mapping, and

the mapping of conductive layers such as coal seams.

Section 2 - Asymptotic Expansions

2.1 General

The asymptotic formula for $B_i(t)$ is as given in equation (1.8).

$$B_i(t) \sim A_i(t) = (1/2\pi^2) \sum_{r=0}^{\infty} S_r \Gamma((r+1)/2+i)\, t^{-((r+1)/2+i)} \tag{2.1}$$

and thus we have

$$Z(t) = (1/\tau) \left[B_1(t) - B_1(t-\tau) \right] \tag{2.2}$$

or, as $\tau \rightarrow 0$

$$Z(t) = - B_2(t) \tag{2.3}$$

The details of calculating the co-efficients S_r is contained in the paper listed in the Appendix. The first two terms of this expansion reduce to the formula given by Lee (1982). For the uniform half-space the expansion reduces to the formulae given by Lee and Lewis (1974) and Raiche and Spies (1981).

The expansion for P(mx) D(m,x) is a divergent power series, and thus the expansion for A_i is an asymptotic series. Therefore the expansions for the 'scaled voltage' (Z(t)) will in general be divergent.

Consider the layered earth and loop geometry shown in figure 2.1.

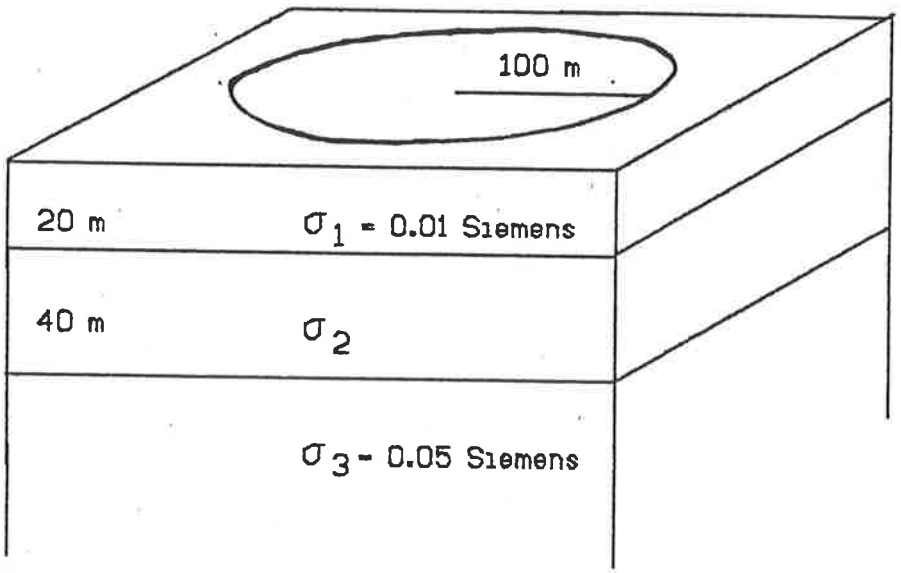

Figure 2.1 The layered earth and loop geometry considered.

The time dependence is a step function input (τ=0).

The magnitude of the first 21 terms in the expansion for the voltage (evaluated at time t=5.754 milliseconds) are shown in Figure 2.2 for three different values of σ_2. For σ_2 = .01 Siemens the expansion can be regarded as essentially convergent, as all the terms calculated are rapidly decaying away to zero. However for σ_2 = .3 Siemens the terms decrease in size until about the eighth term when they start to increase. This situation can be termed 'apparent convergence'. Note that the odd and even terms differ substantially in magnitude. In the case when σ = 1 the termsize increases immediately. In this case

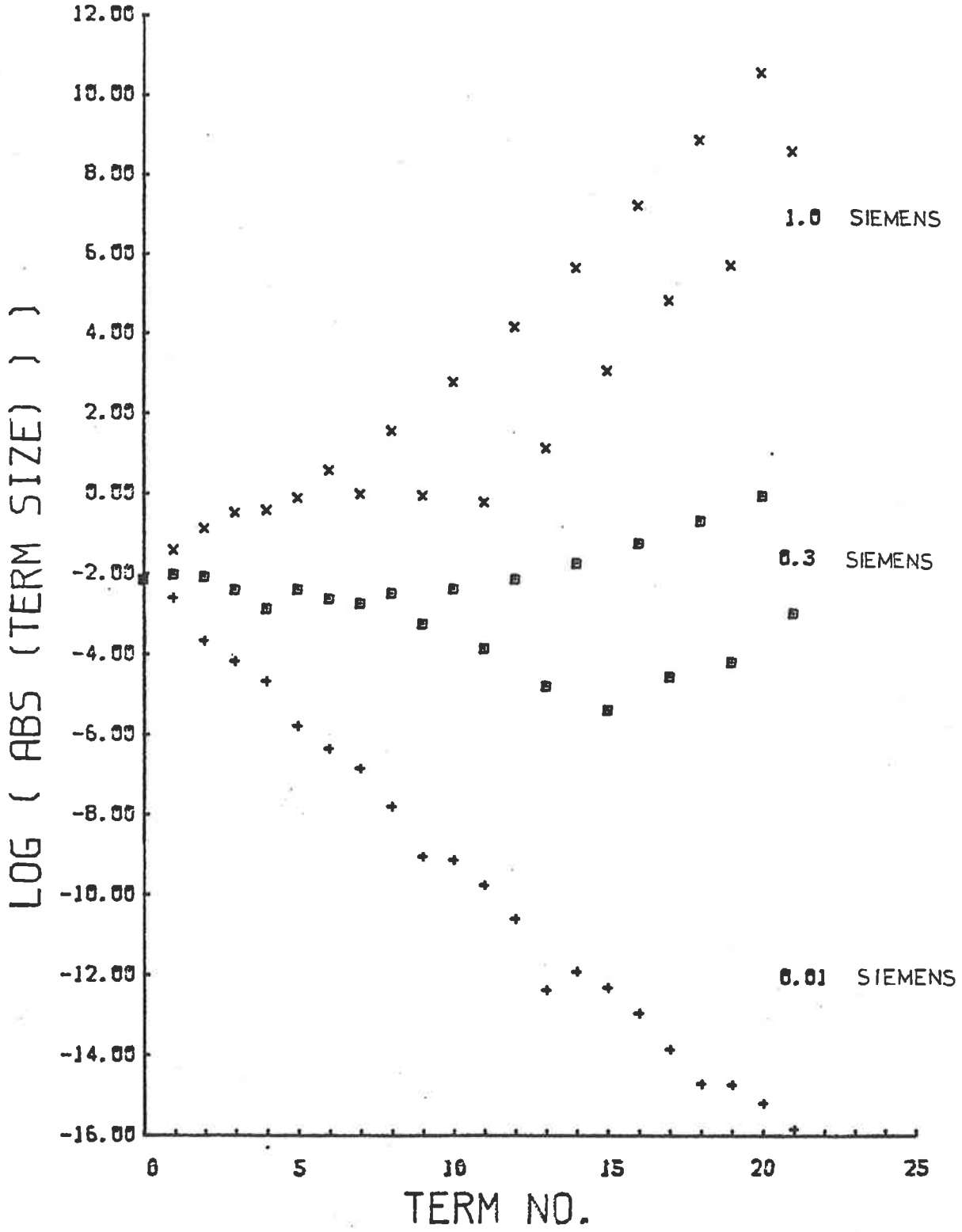

Figure 2.2 The log of the absolute value of the term size plotted against term number for Sigma (2) equal to .01, 0.3 and 1.0 Siemens. For 0.01 Siemens the answer is accurate to within .1%. For the 0.3 Siemen case it is accurate to approximately 6%. For the final case the result is very poor.

the expansion is divergent.

Erdelyi (1956) has shown that the error in using i terms in the asymptotic expansion for

$$\int_0^\infty \exp(-xt) \,/\, (1+t)\, dt \qquad (2.5)$$

is given by the magnitude of the $(i+1)^{th}$ term. By drawing an analogy with equation 2.1 it is possible to gain an indication of the magnitude of the error of the asymptotic expansion by defining the Error factor:

$$\text{Error factor} \quad E_F = \left| T_i / \sum_{j=1}^{i} T_j \right| \times 100$$

where T_j are the individual terms of the expansion and T_{i-1} and T_i are the smallest two consecutive terms. T_i and T_{i-1} are defined such that

$$\left| T_i \,/ \sum_{j=i}^{i} T_j \right| \quad \text{and} \quad \left| T_{i-1} / \sum_{j=1}^{i} T_j \right| < \varepsilon$$

where ε is some small tolerance (e.g. $.5 \times 10^{-4}$). This definition is required, because (as can be seen from figure 2.2), the terms in the expansion oscillate in size, and thus requiring that two consecutive terms be negligible is a more stringent 'convergence' criteria than requiring one be negligible.

Figure 2.3 is a plot of Z(t) obtained by using the asymptotic expansion for different conductive overburdens with a thickness equal to the loop radius. $\tau=0$, and the times are

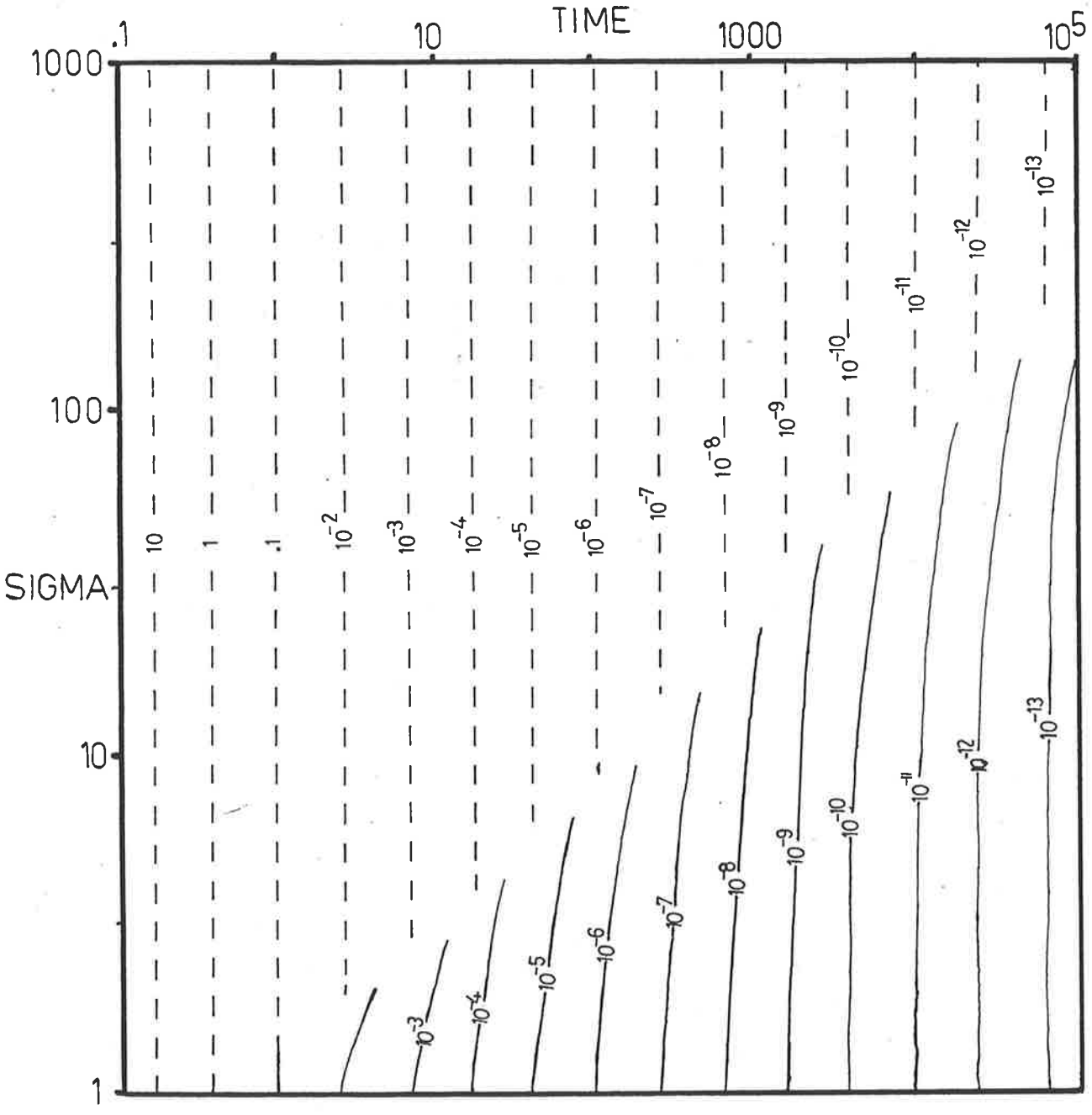

Figure 2.3 Contour map of Z(t) calculated asymptotically for conductive overburdens. The conductivities (Sigma) and the Times are scaled. Dotted lines represent Voltages where the expansion is divergent.

scaled times. The dotted lines represent the scaled voltages where the expansion is divergent. From the contour plot it would be possible to obtain the voltage for any of the times and conductivities plotted on the diagram by multiplying by the scale factor $I_p / \sigma_{n+1}\lambda$. For this particular voltage plot the factor E_F is plotted on figure 2.4. The number of terms required to calculate the voltage is plotted on figure 2.5. The voltages in the same region calculated by the Knight and Raiche (1982) algorithm are shown on figure 2.6. The difference between the asymptotic method and the method of Knight and Raiche (1982) expressed as a percentage of the asymptotic voltage is shown on figure 2.7. Similar plots (figures 2.8 to 2.12) have been done for resistive overburden (coincident circular loops, layer depth is one scaled unit). In the range of cases for which verification has been done the asymptotic expansion provides excellent answers for $E_F < 0.1$. This verifies the hypothesis adopted that the most accurate answer will be obtained after the addition of the smallest two consecutive terms in the series.

The time taken to calculate all the voltages on Map 2.3 by the asymptotic method was .921 seconds of CPU time on a Cyber 173. The Knight and Raiche routine took 1200 seconds of CPU time on a Vax (runs courtesy of CRA). The Knight and Raiche algorithm took longer for the most conductive case compared with the least conductive case (440 seconds compared with 11 seconds). However the asymptotic expansion obtained no meaningful voltages for the most conductive case.

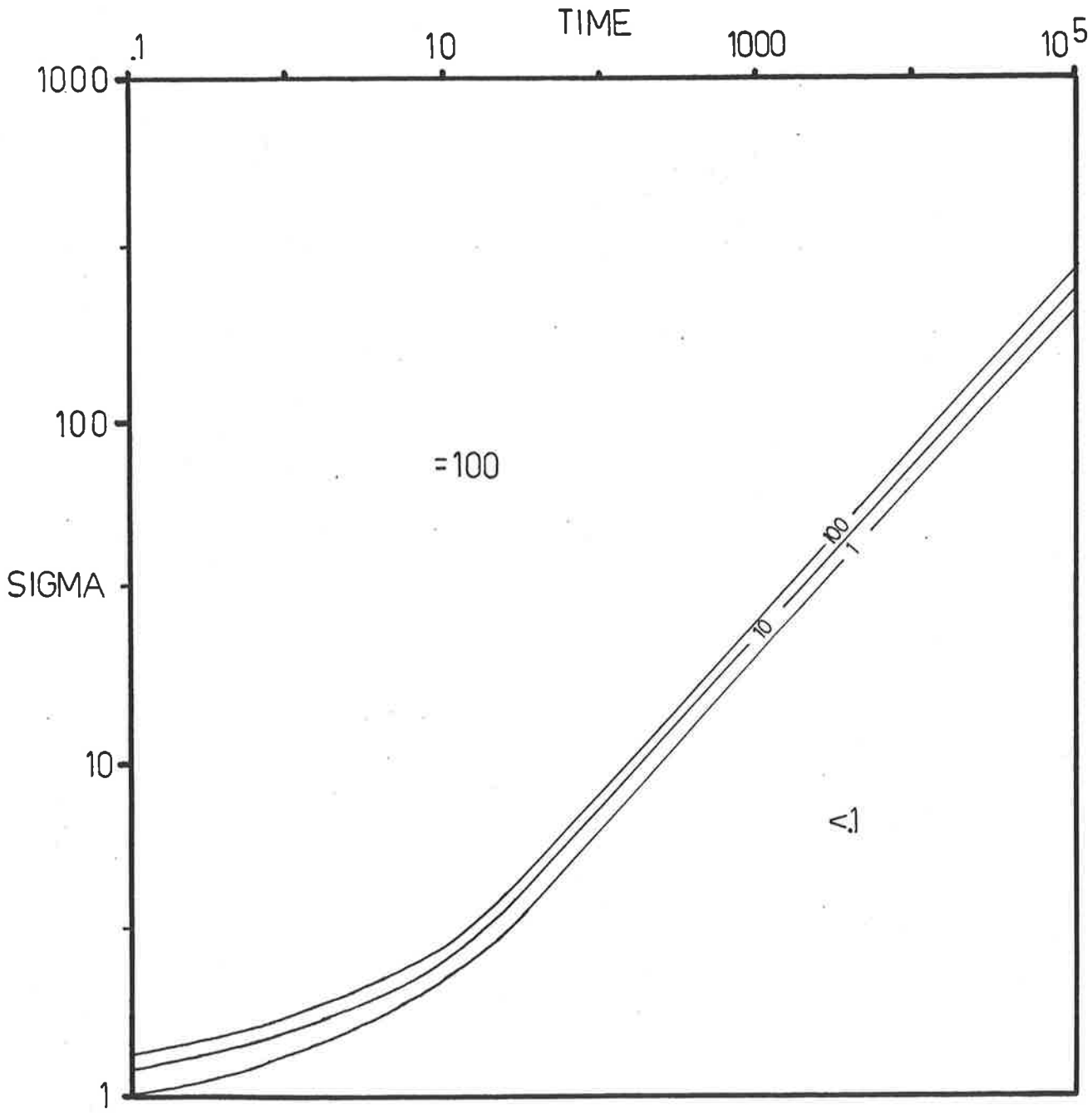

Figure 2.4 Contour map of the Error Factor (E_F) for conductive overburden. The conductivities (Sigma) and the Times are scaled.

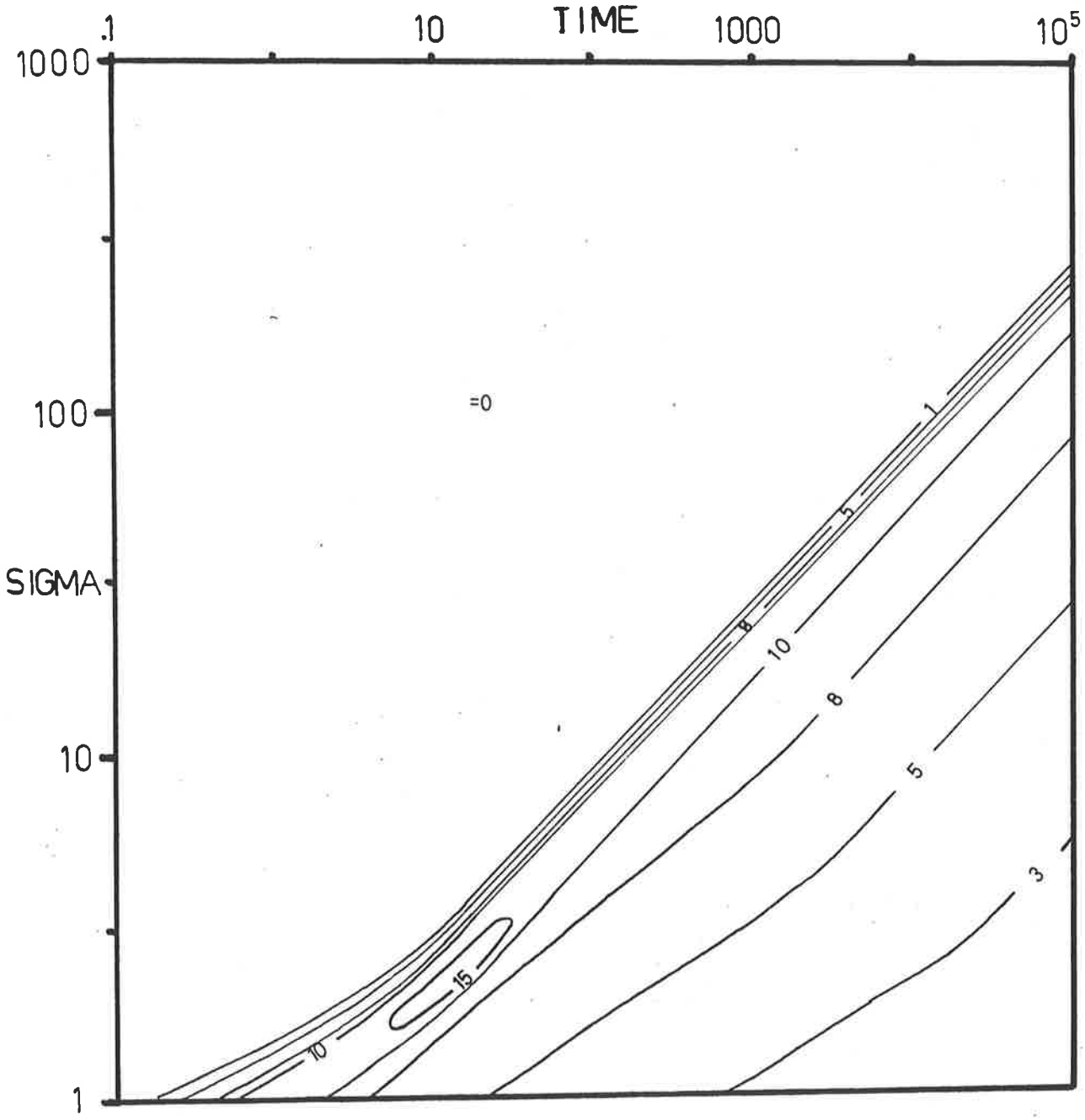

Figure 2.5 Contour map of the number of terms required in the asymptotic expansion (conductive overburden). The conductivities (Sigma) and the times are scaled.

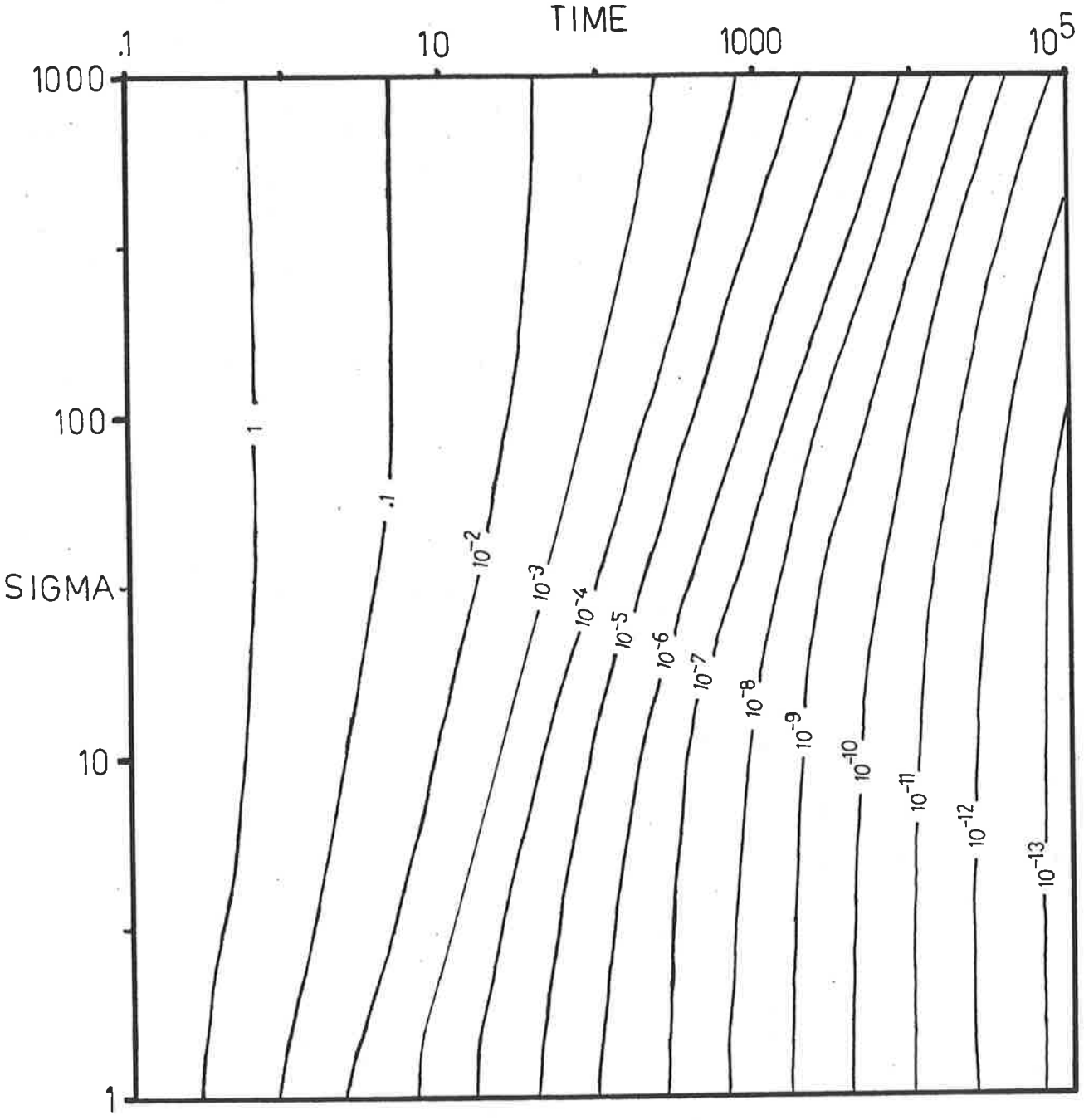

Figure 2.6 Contour map of the Voltage calculated using the algorithm of Knight and Raiche (1982) for conductive overburden. The conductivities (Sigma) and times are scaled.

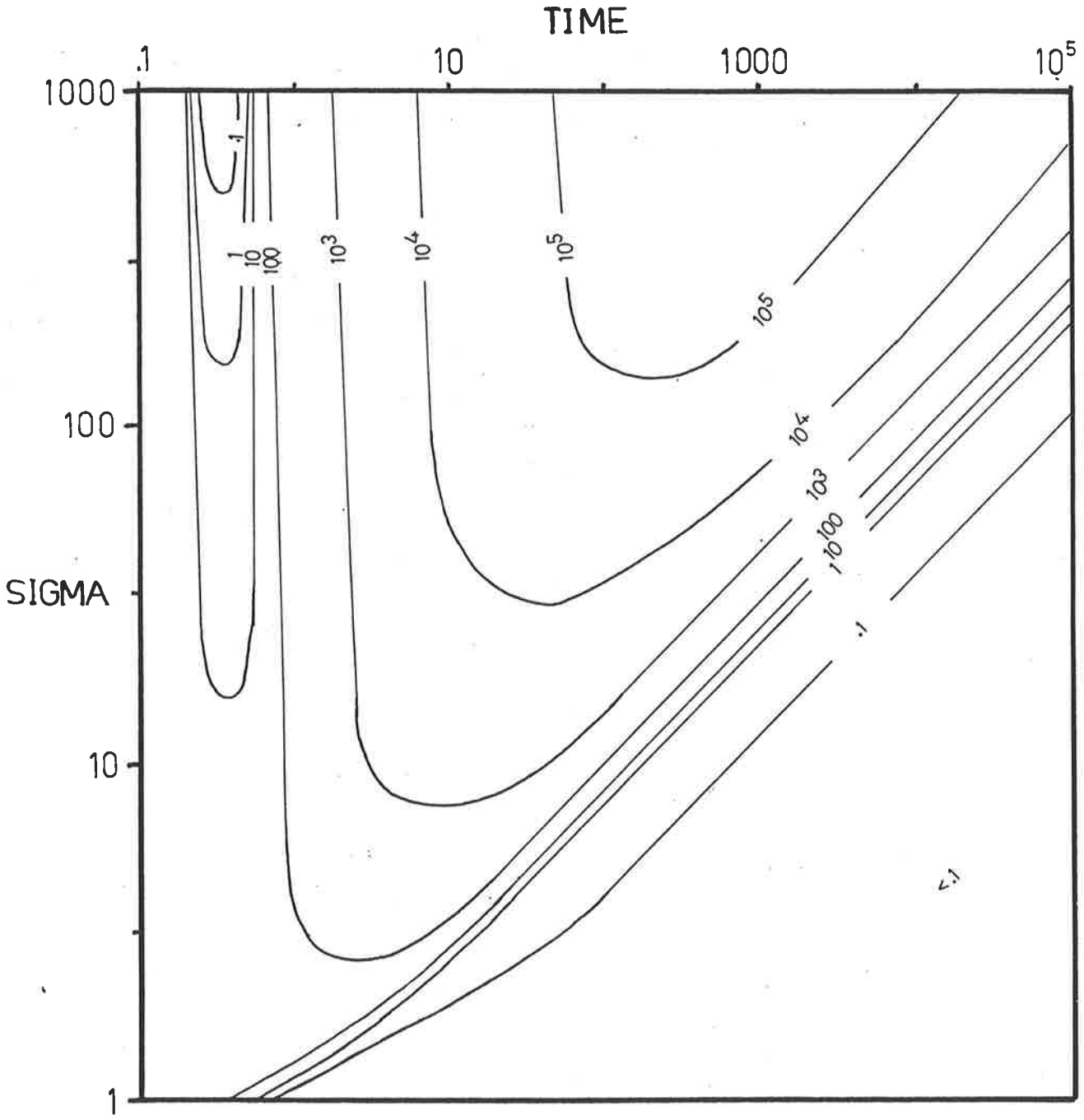

Figure 2.7 The difference between the method of Knight and Raiche (1982) and the asymptotic expansion for conductive overburden. The conductivities (Sigma) and times are scaled.

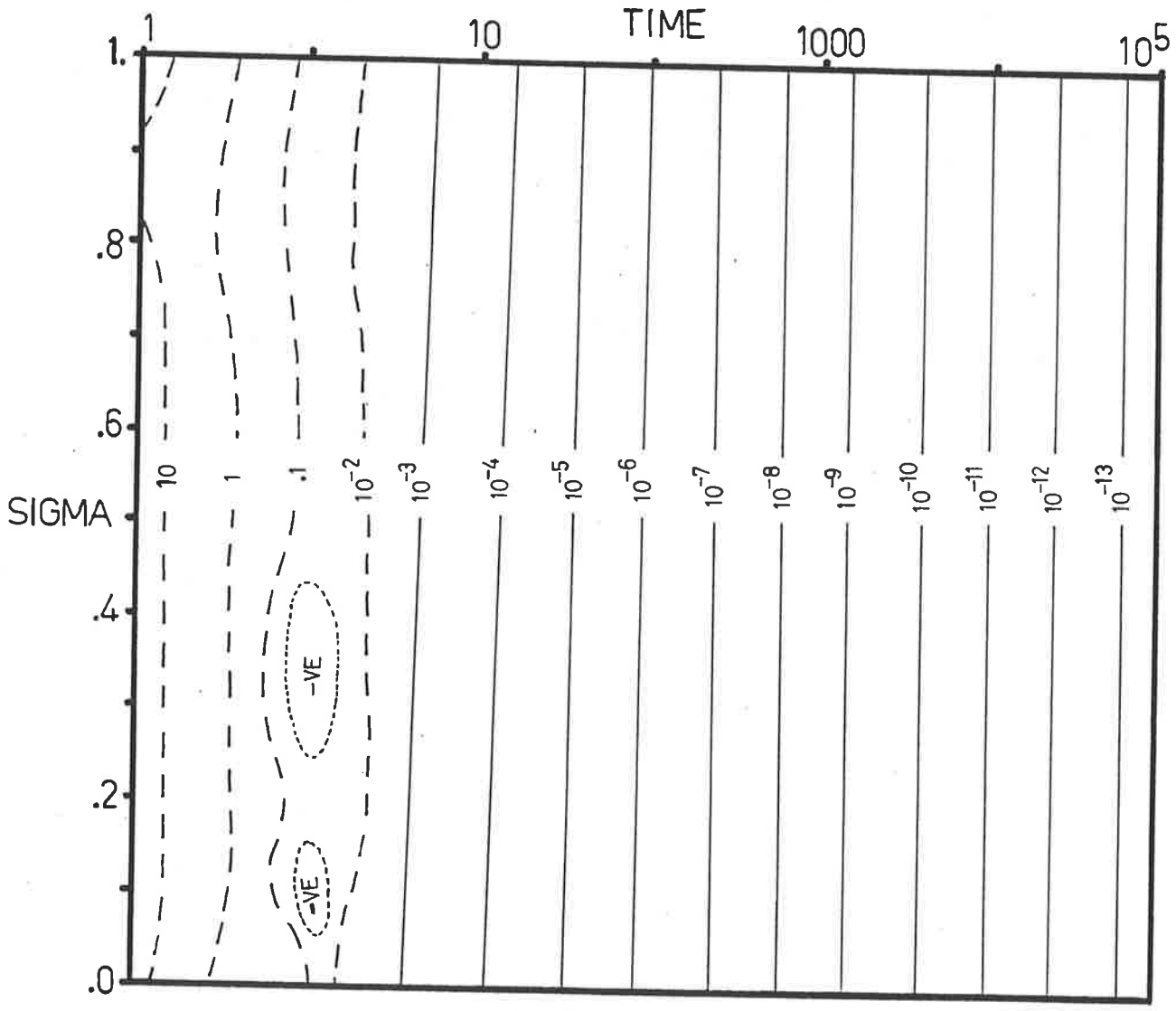

Figure 2.8 Contour map of Z(t) calculated asymptotically for resistive overburdens. The conductivities (Sigma) and the Times are scaled. Dotted lines represent Voltages where the expansion is divergent.

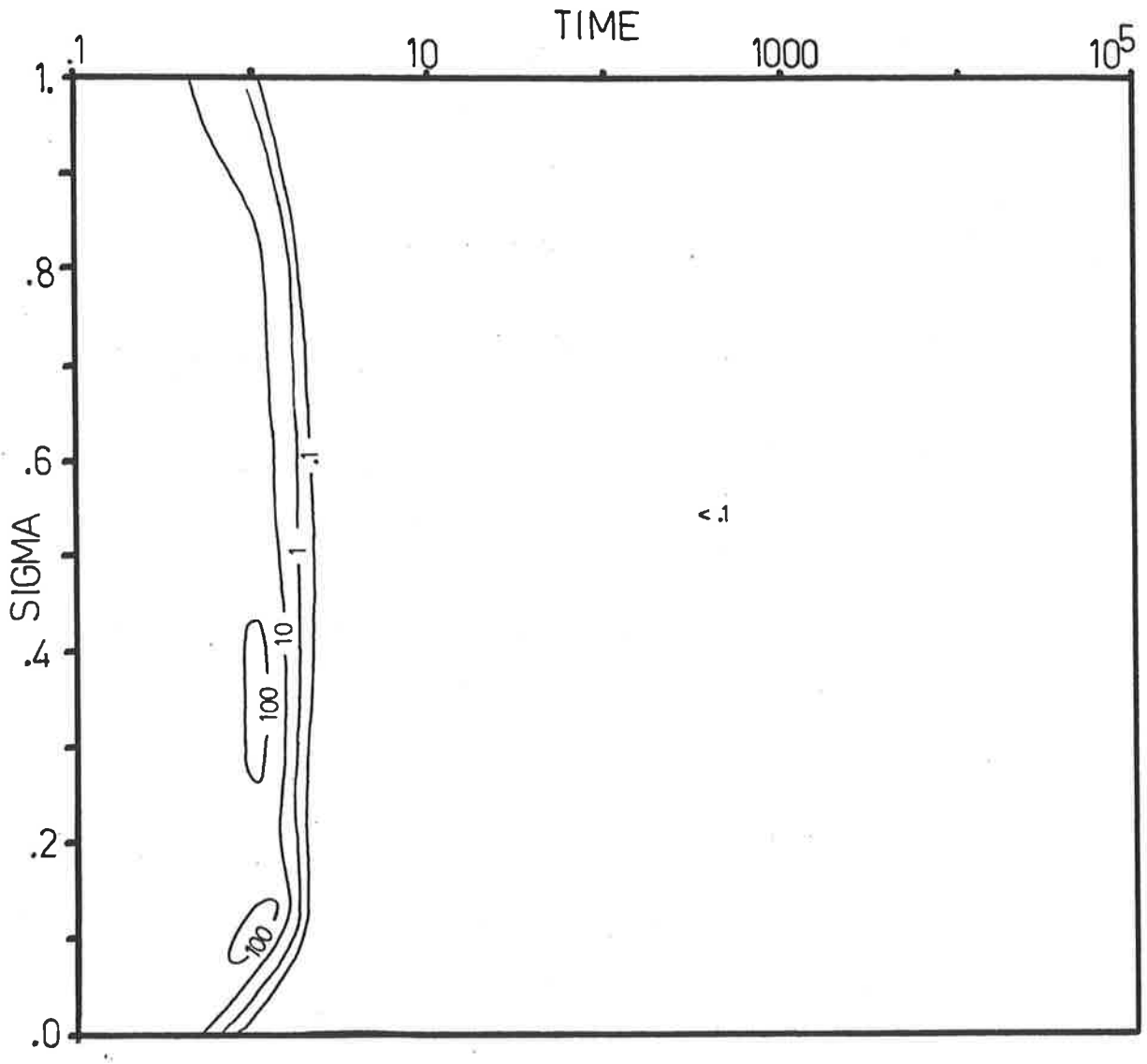

Figure 2.9 Contour map of the Error Factor (E_F) for resistive overburden. The conductivities (Sigma) and the Times are scaled.

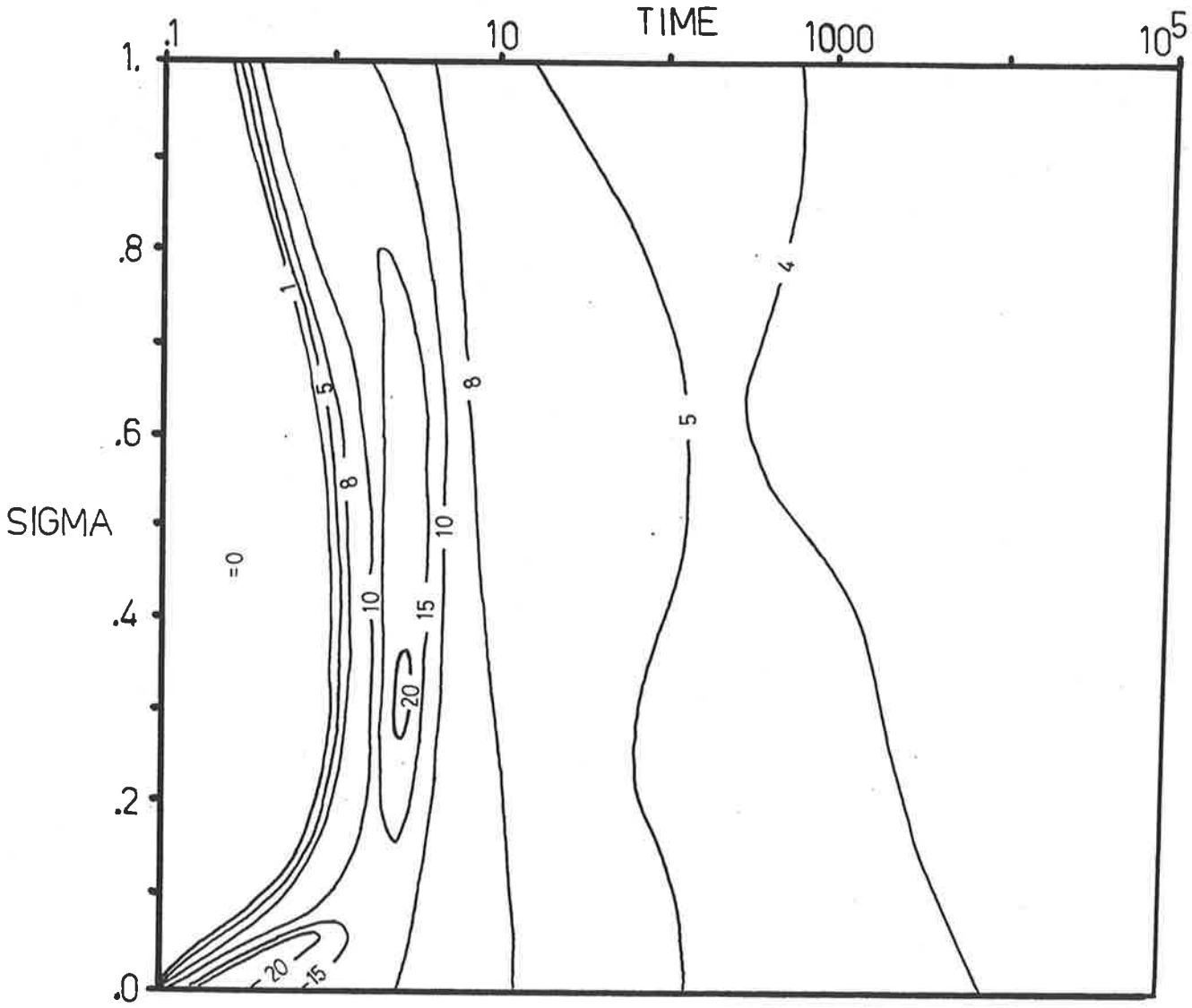

Figure 2.10 Contour map of the number of terms required in the asymptotic expansion (resistive overburden). The conductivities (Sigma) and the times are scaled.

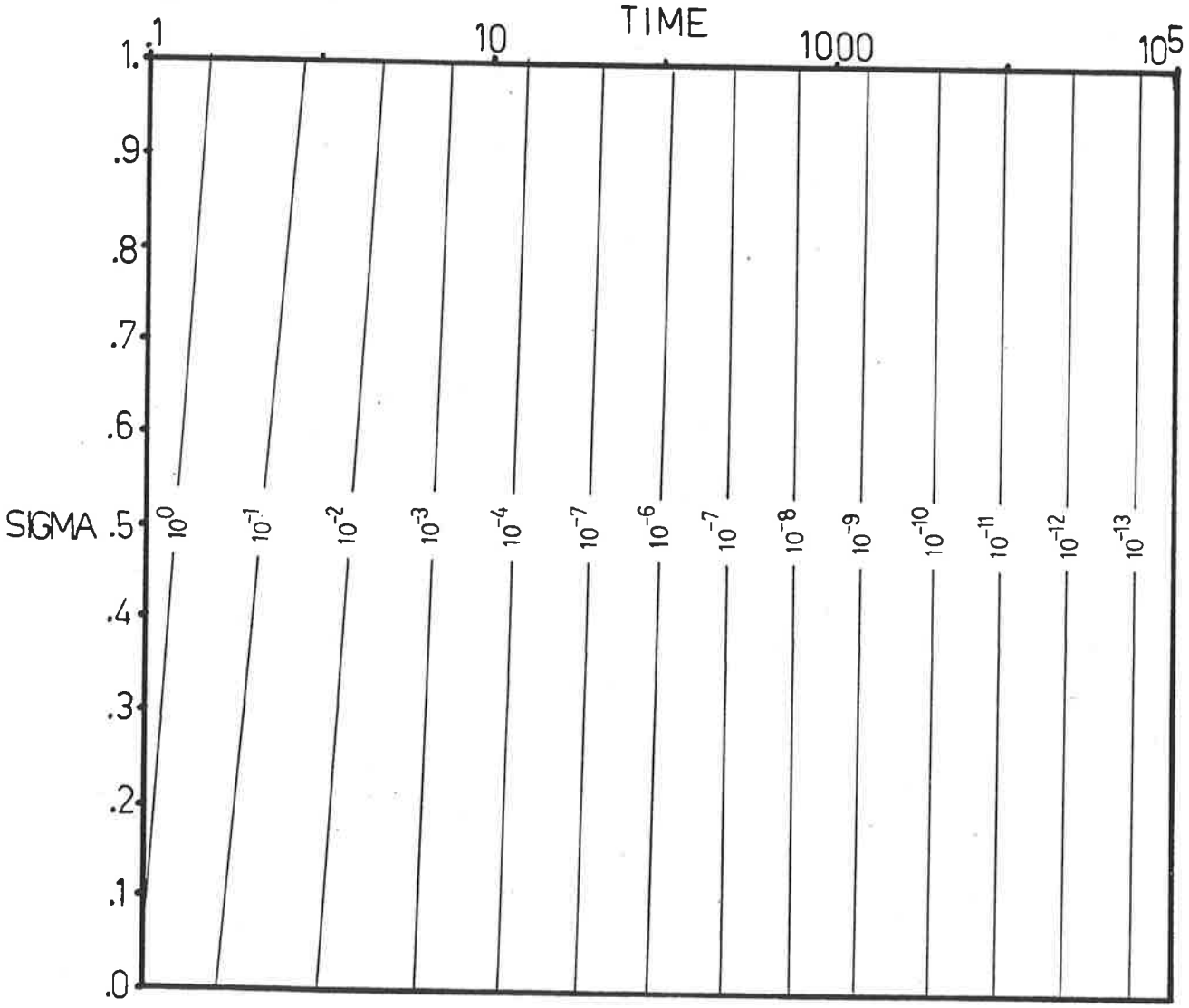

Figure 2.11 Contour map of the Voltage calculated using the algorithm of Knight and Raiche (1982) for resistive overburden. The conductivities (Sigma) and times are scaled.

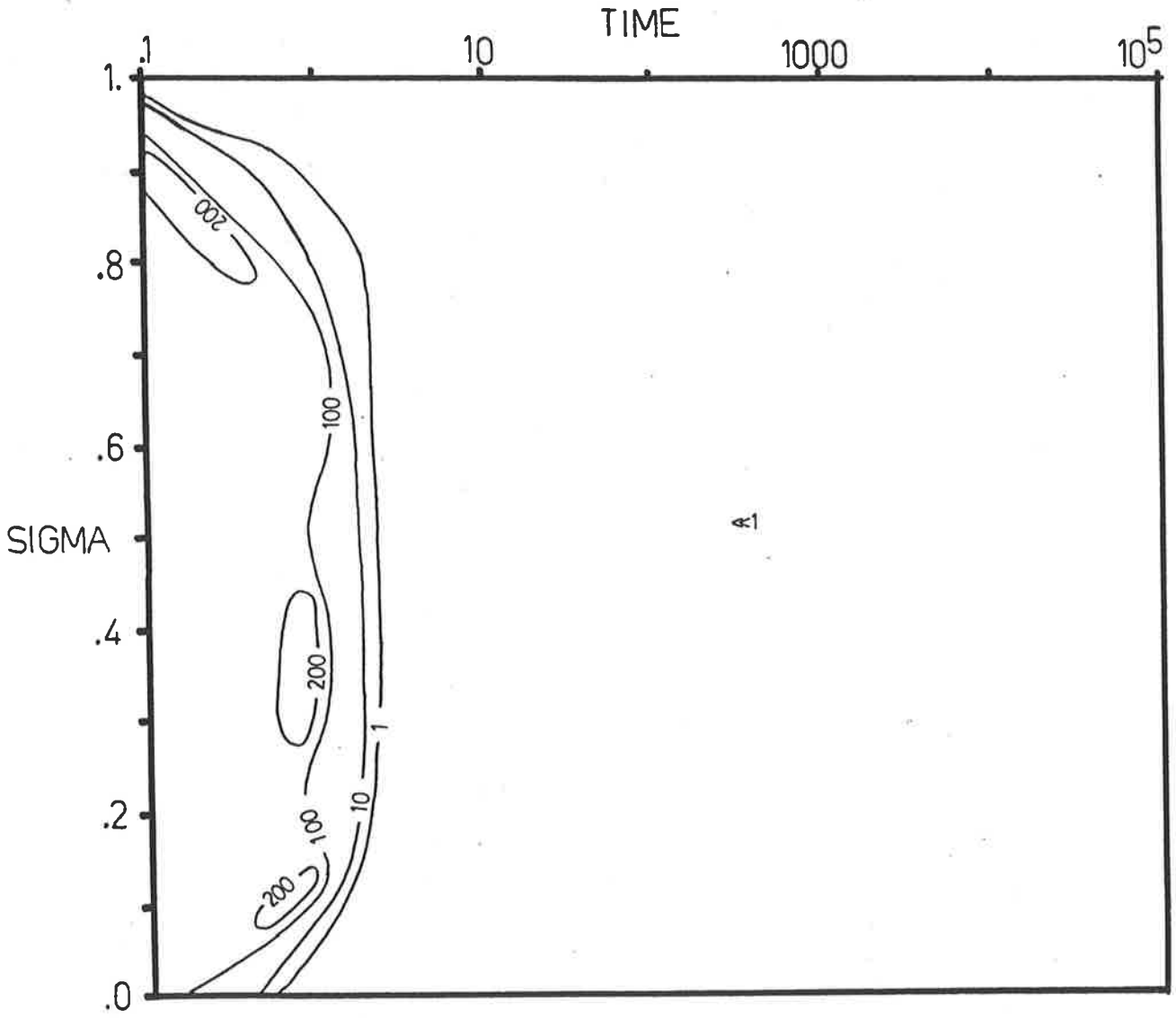

Figure 2.12 The difference between the method of Knight and Raiche (1982) and the asymptotic expansion for resistive overburden. The conductivities (Sigma) and times are scaled.

2.2 Conclusion

The asymptotic approximation to the integral represents an extremely quick method of calculating the voltages. As the region of 'convergence' is known, the gain in run time is obtained with no loss in accuracy, however it is only valid at late times (see figures 2.4 and 2.9). The formula can cater for differing ramp times, and a range of loop geometries. Although this thesis has restricted discussion to circular coincident loops, Smith (1982) has shown that for times when the expansion is valid circular and square loops of the same area have very similar responses (less than 1% discrepancy).

Section 3 - Numerical Integration

When the asymptotic expansion is divergent, it may seem reasonable to integrate equation 1.6 numerically. The advantage offered by the formulation outlined in Section 1 is that the time dependence appears only once - in the outer integral. The S(x) calculated are independent of time, and can be evaluated and stored for use at all times for which the response is desired. This could allow substantial savings in computing times. To investigate whether such a numerical integration is possible we must look at the integrand. Define R(x,m) by the following relation:

$$R(x,m) = P(mx)\ D(m,x).$$

The functional form of P and D are given in the appendix.

Consider circular coincident loops lying on a layer over a half-space. The layer thickness is equal to the loop radius. The function R(x,m) has been calculated as a function of m and x^2 (for ease of programming) and plotted on figure 3.1. 3.1(a) shows the function when the top layer is 100 times more conductive than the basement, and 3.1(b) shows the function when the top layer is 100 times more resistive than the basement. For the resistive case the function is smooth, whilst in the conductive case large spikes occur. To illustrate the manner in which the function changes as the conductivity changes the log of R(x,m) has been plotted for σ = 0.01, 0.1, 1, 5, 10 and 100 (See

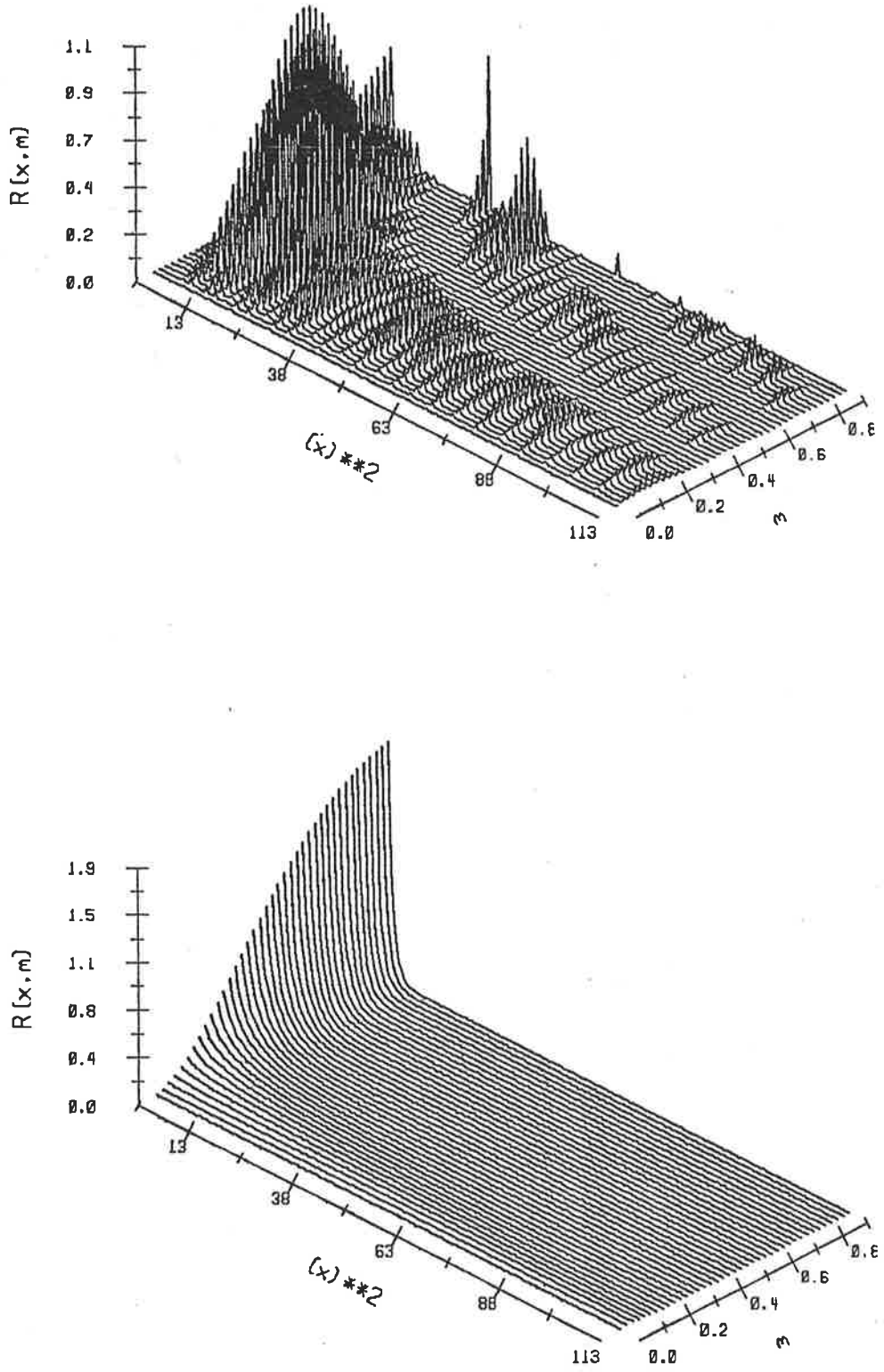

Figure 3.1 (a)(top) R(x,m) for the top layer 100 times more conductive than the halfspace.
(b)(bottom) R(x,m) for the top layer 100 times more resistive than the halfspace.

figures 3.2 to 3.4). For the resistive cases the function is smooth, however when the top layer conductivity increases, ridges due to the complex zeros associated with the function D(m,x) develop. These zeros occur in the complex plane, and as they migrate towards the line of integration, the ridges become sharper and larger, and they cluster towards the origin. Figure 3.5 has been plotted on an expanded scale $0<x^2\leqslant 1$ to show the form of the ridges close to the origin. The position of the 'valleys' in each plot are unchanged, as these are the zeros of the Bessel function contained in the loop function P(mx).

For resistive overburdens the integrations can be done easily. Figure 3.6(a) shows the voltages for a resistive earth (Model #1) made up of three layers with conductivities 0.001, 0.01 and 0.005 Siemens and thicknesses 10, 20 and 30 metres (from top to bottom) above a half space of 0.01 Siemens. The three methods used to calculate the voltages all give identical voltages (to 4 significant figures). The graphs in figure 3.6 were drawn using 20 SIROTEM channels, but so that the graph would not be clustered only 10 channels are displayed. Figure 3.6(b) shows the voltages for Model #2 (two layers, both with thicknesses of 20 metres and conductivities of 0.1 and 0.01 Siemens above a half-space of 1 Siemen). The asymptotic expansion has broken down at 4.97 milliseconds, but the numerical integration and Knight and Raiche's algorithm agree to 4 significant figures. The calculation times for the asymptotic expansion is .24 seconds, whilst the numerical integration can be performed in less than 2 seconds. The numerical integration can

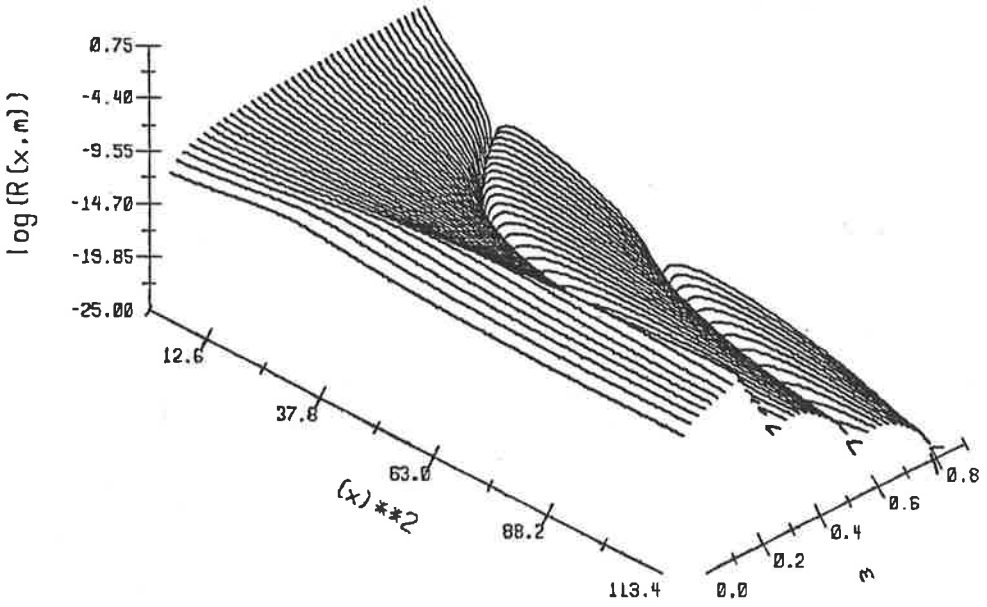

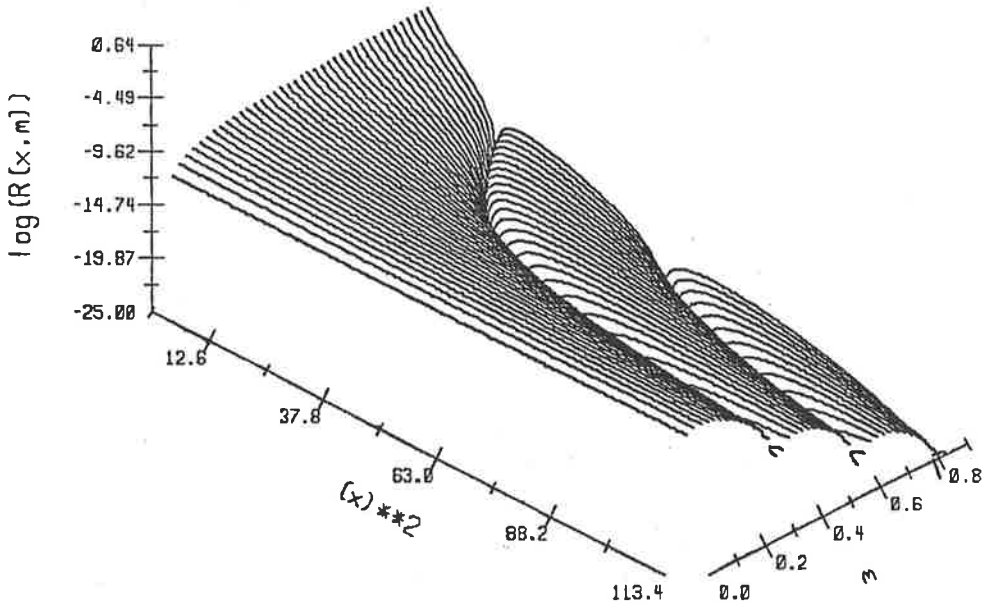

Figure 3.2 (a)(top) log (R(x,m)) for σ_1 equal to 0.1 σ_{n+1}
(b)(bottom) log(R(x,m)) for σ_1 equal to
0.01 σ_{n+1}

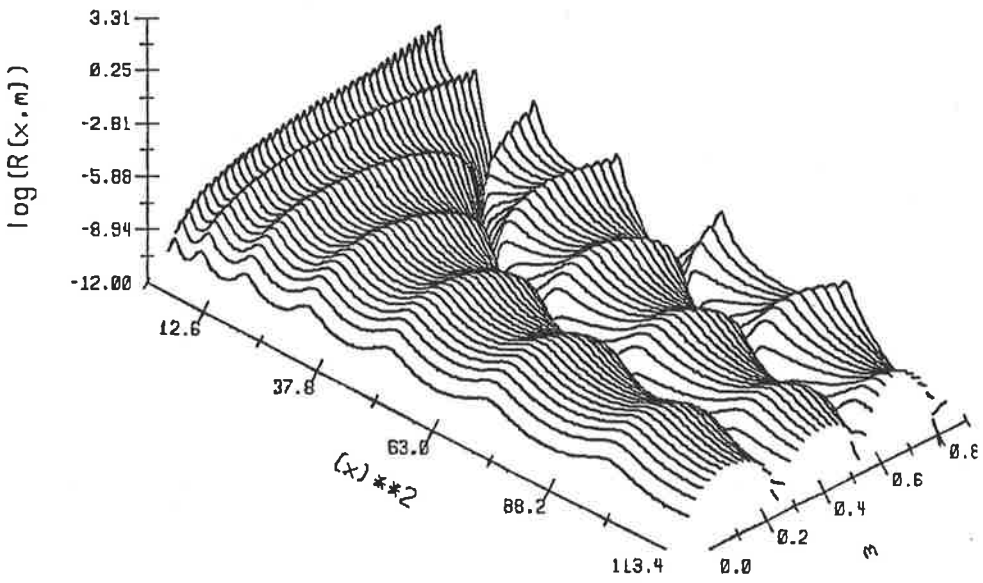

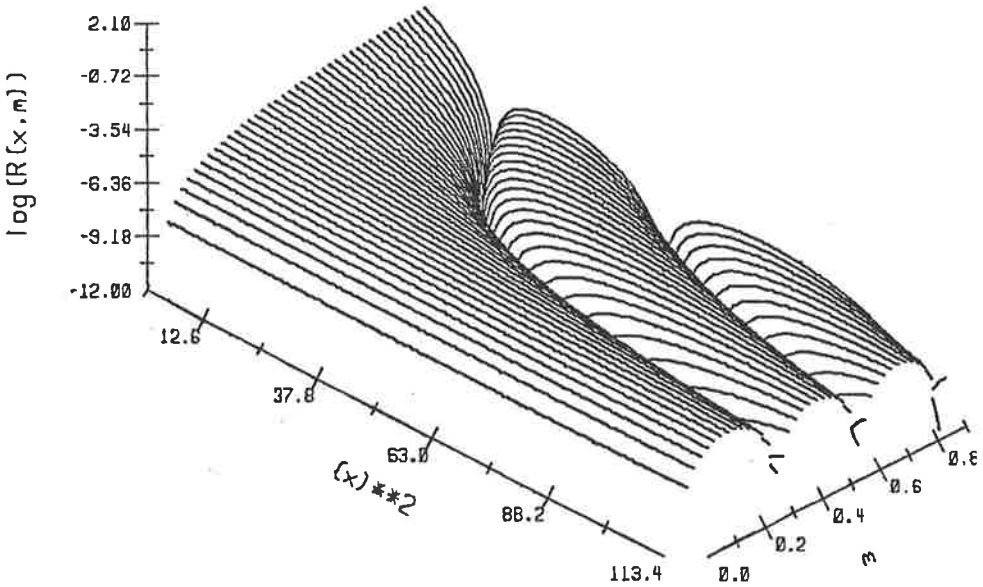

Figure 3.3 (a)(top) log(R(x,m)) for σ_1, equal to 5 σ_{n+1}
(b)(bottom) log(R(x,m)) for σ_1 equal to σ_{n+1}

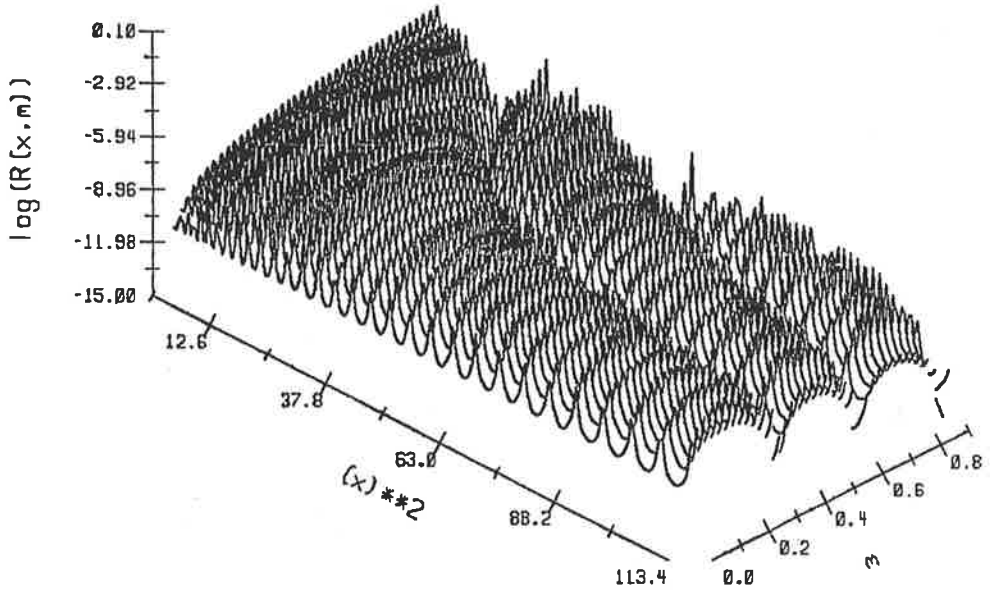

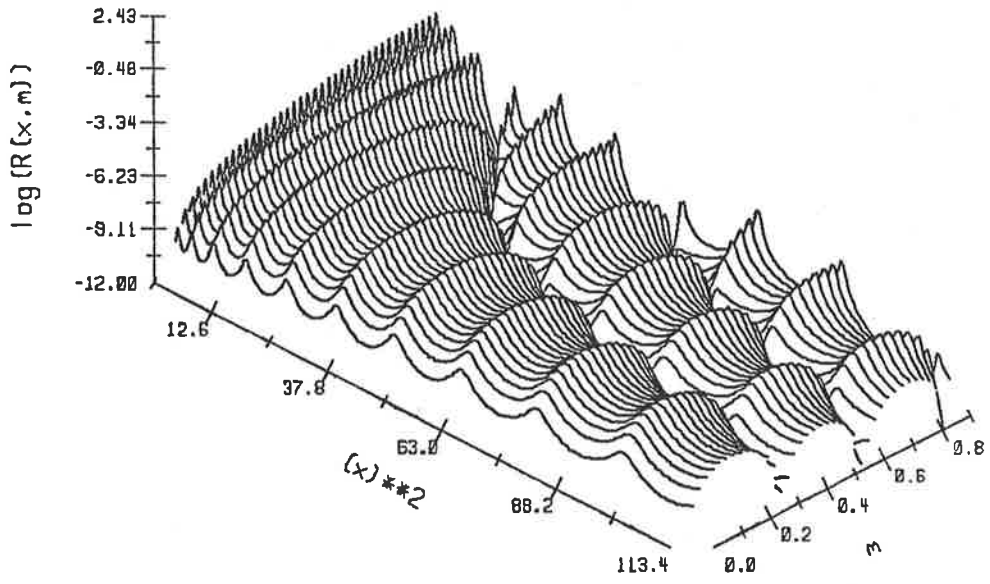

Figure 3.4 (a)(top) log (R(x,m)) for σ_1 equal to 100 σ_{n+1}
(b)(bottom) log (R(x,m)) for σ_1 equal to 10 σ_{n+1}

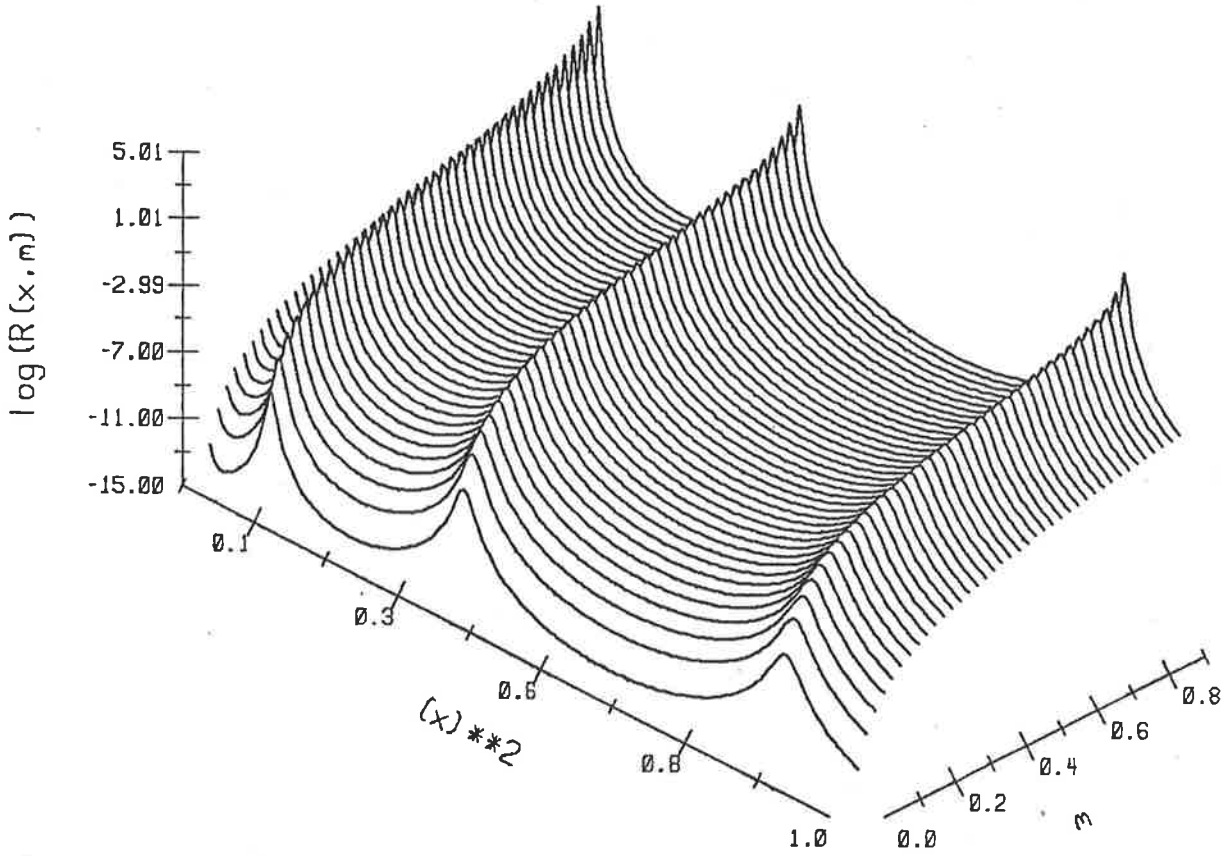

Figure 3.5 log (R(x,m)) plotted on an expanded scale x^2 = [0,1] so as to show the ridges.

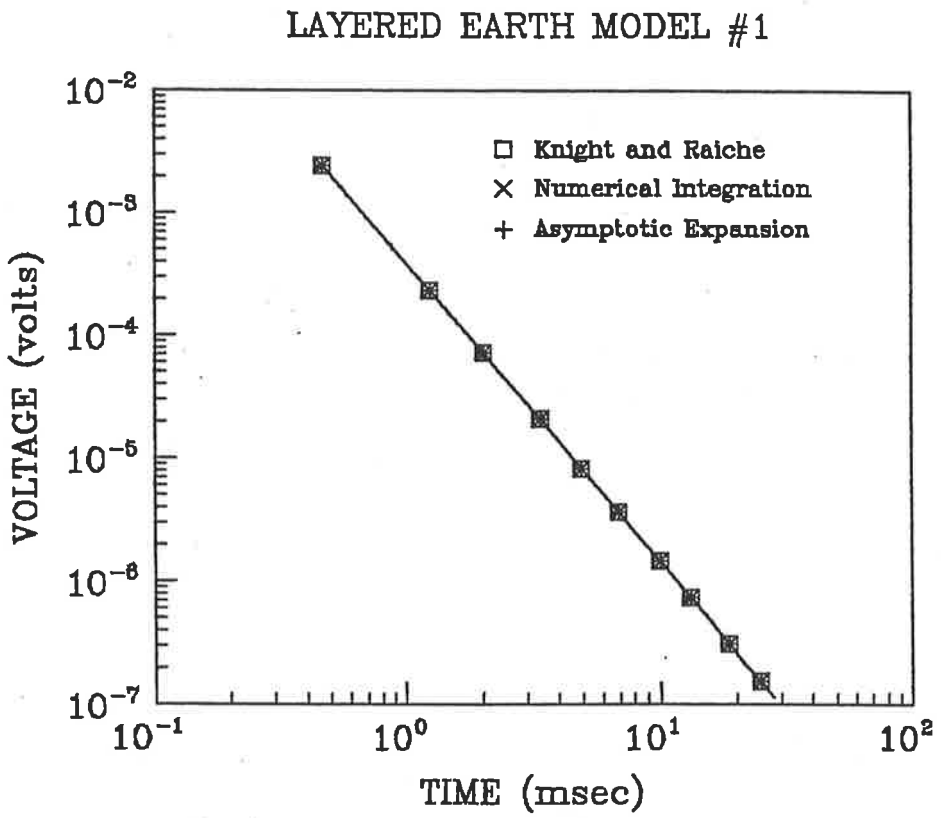

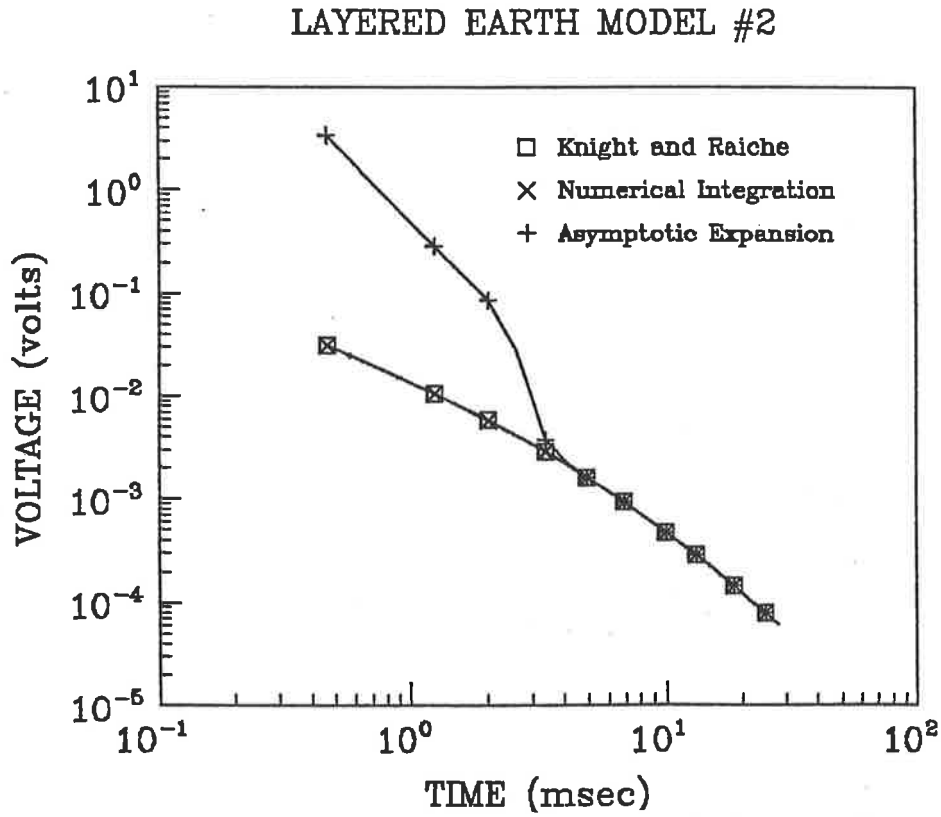

Figure 3.6 (a)(top) the Voltage response for model #1. (b)(bottom) the Voltage response for model #2.

be efficiently performed with a 15 point rule for the m integration on [0,1] (see appendix), and a 15 point Laguerre rule for the x integration (Abramowitz and Slegun (1970) page 923).

For conductive overburdens the ridges in the function R(m,x) make the integration difficult to perform. Adaptive integration must be used so as to place the quadrature nodes near where the function varies rapidly. For the m integration Patterson's (1973) 225 point rule was used, whilst for the x integration an adaptive 3 point Newton-Coates rule was used (O'Brien D.M. (1978 - unpublished)). Results obtained were found to be stable with respect to the relative error requested from the integration routine. The voltages obtained by such numerical integrations were found to disagree with the results obtained from Knight and Raiche (1982), and from the asymptotic expansion when it was not divergent. The error in the numerical integration was attributed to the fact that the poles in the spectrum of K(1,s) have been ignored. As the asymptotic expansion gave valid answers when it was not divergent the effect of ignoring these poles was concluded to have no effect on the asymptotic analysis. The numerical integration of equation 1.6 for TEM responses of geoelectric sections with layers more conductive than the basement is not useful. There are two reasons for this:

(1) The function develops nasty ridges which are difficult and inefficient to integrate, and

(2) the results are unreliable due to the fact that the poles of K(1,s) on $[-1^2,o]$ have been ignored.

However for resistive overburdens R(x,m) is smooth, and can

be evaluated rapidly for many different times. It should therefore be possible to incorporate the numerical integration of equation 1.6 into a program such as GRENDL for such resistive cases.

Section 4 - The Effect of Integration Over Channels and Ramp Rise Time

4.1 Mathematics

For the SIROTEM system, the voltage measured in channel i is the average voltage over a time window from t_i to t_{i+1} (Buselli and O'Neill (1977)). The voltage is thus calculated by evaluating

$$Z(t_i, t_{i+1}) = 1 / (t_{i+1} - t_i) \int_{t_i}^{t_{i+1}} Z(t)\, dt$$

For the asymptotic expansion we obtain:

$$Z(t_i,t_{i+1}) = \begin{cases} \dfrac{A_o(t_i) - A_o(t_{i+1}) - A_o(t_i - \tau) + A_o(t_{i+1}-\tau)}{\tau(t_{i+1} - t_i)} & \tau>0 \\ \dfrac{A_1(t_{i+1}) - A_1(t_i)}{(t_{i+1} - t_i)} & \tau=0 \end{cases}$$

For the numerical integration:

$$Z(t_i, t_{i+1}) = 1/(\pi^2(t_{i+1}-t_i)) \int_0^{\infty} (\exp(-x^2 t_i)-\exp(-x^2 t_{i+1})) \; (-x^2 I(-x^2))\; S(x)dx$$

where the function I has the form given in the appendix.

The integral over a SIROTEM window can therefore be done with little additional computational effort. This eliminates

assumptions made by previous workers that the SIROTEM voltage in a particular channel can be approximated by the voltage at a time somewhere in the middle of the channel.

4.2 The Different Responses

The effect of integration over channel windows, and of varying the ramp rise time is shown on figure 4.1. For a fixed layered earth geometry, and coincident circular loops, the voltage for the first 15 SIROTEM channels has been calculated in four different situations:

(a) The Voltage is that measured at a time in the middle of the window (i.e. not averaged over a window). The ramp rise time is 0.0 milliseconds. The times chosen to represent the channels are those chosen by the GRENDL routine.

(b) The Voltage is integrated over a window. The ramp rise time is 0.0 milliseconds.

(c) The Voltage is not integrated over a window. The ramp rise time is 0.2 milliseconds.

(d) The Voltage is integrated over a window. The ramp rise time is 0.2 milliseconds.

The earth/loop geometry used is a conductive overburden 100 metres thick of 0.0025 Siemens over a basement of 0.001 Siemens. Circular coincident loops of radius 100 metres are used.

Each calculation displays a refinement which allows the actual situation to be modelled more closely. It can be seen that integrating over time channels alters substantially the value of the voltage obtained, particularly in the early channels. The value of 0.2 milliseconds for the ramp rise time

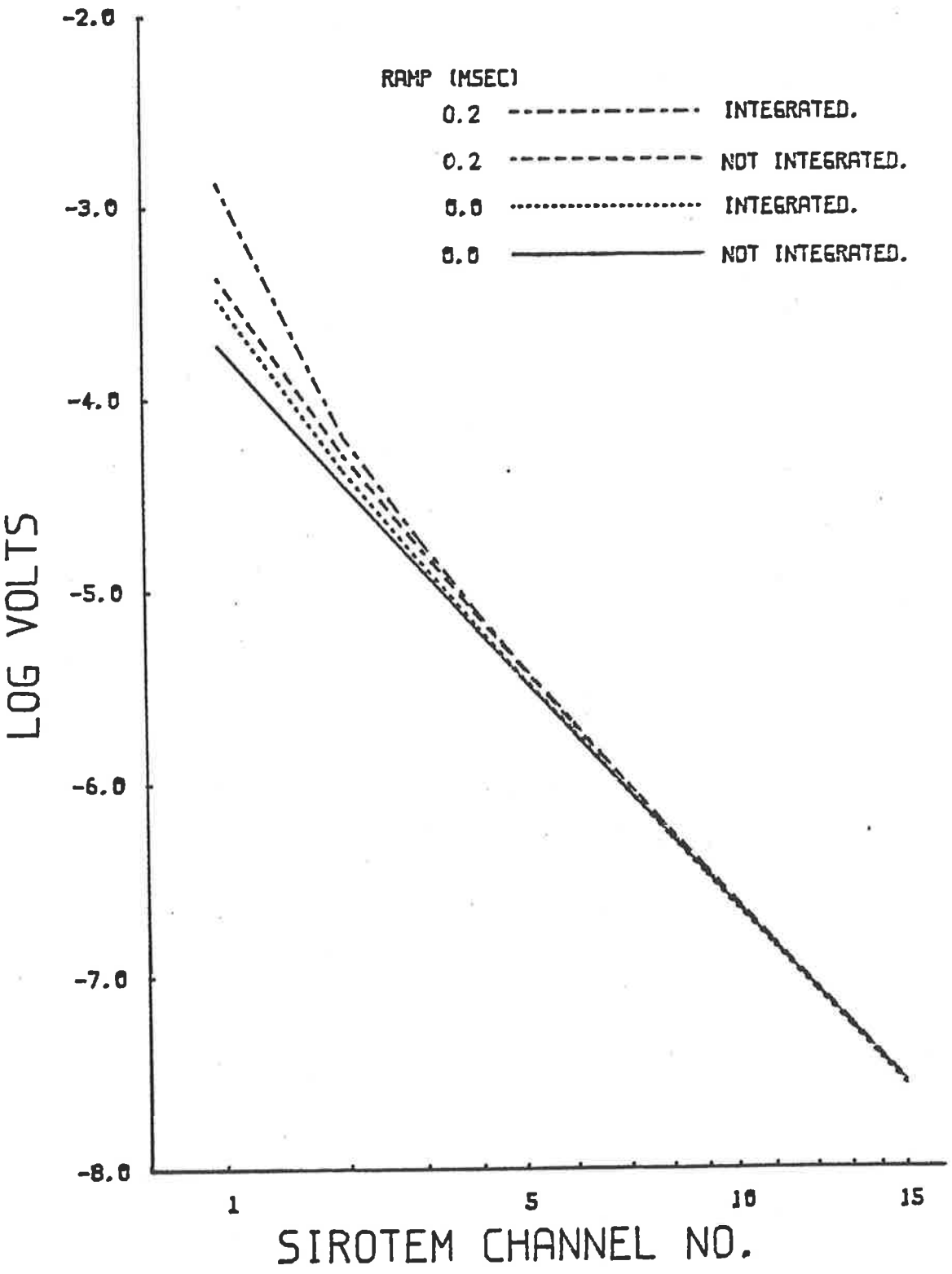

Figure 4.1 The log of the Voltage as a function of SIROTEM channel number (log t). For the four different cases shown.

was chosen arbitrarily to illustrate the point that having an idea of the ramp rise time will allow a better approximation to the voltages obtained with a SIROTEM unit over the prescribed earth. The effect of ramp rise time was also considered by Raiche (1983).

4.3 Fitting the Different Responses

In Section 5 the inversion of layered earth data is discussed. So as to consider what effect the channel integration and ramp rise time have we will apply the techniques discussed in that section to a certain earth model. Synthetic data was generated for a conducting overburden of 0.02 Siemens, 50 metres thick over a basement with conductivity 0.01 Siemens. The loops are coincident and have a 100 metre radius. This is denoted as Model 3, and is shown in figure 4.2.

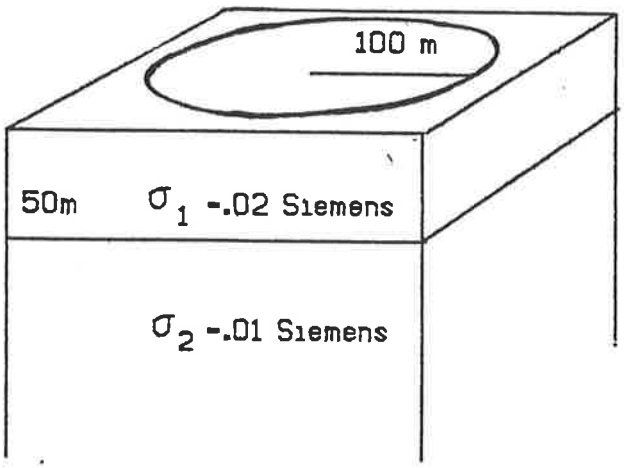

Figure 4.2 The model used for generating the synthetic data.

The ramp rise time was 0.05 milliseconds, and the data was integrated over channel windows. Using the correct answer as an initial guess, this data was inverted; however the ramp time was varied, and the forward problem was utilized both with and then without integration over a window. The inversion results are illustrated on table 4.1. SSQ is the sum of the squares of the discrepancy between the final model data and the data of the model to be inverted. α is a factor which describes the layered earth geometry. This α factor will be discussed more in Section 5. For this earth model the final solution depends critically on the ramp rise time, and whether or not voltages are integrated over a window. If reasonable inversion results for such cases are to be obtained the voltages must be integrated over a window, and the ramp rise time must be known fairly accurately. For SIROTEM the ramp rise time varies with loop size and the conductivity of the earth. This presents a difficulty with the design of the SIROTEM system if quantitative interpretation of SIROTEM data is to be carried out. The improvement gained by integrating over a window and using a ramp function input is clear.

TABLE 4.1

The effect of Ramp inputs and integration over windows

Ramp time (millisec)	Integration	INITIAL GUESS			FINAL SOLUTION			α	SSQ
		d_1	σ_1	σ_2	d_1	σ_1	σ_2		
0.05	YES	50	0.02	0.01	50	0.0200	0.01	-.500	10^{-11}
0.04	YES	50	0.02	0.01	48.255	0.0208	0.00997	-.526	$.3 \times 10^{-3}$
0.06	YES	50	0.02	0.01	54.93	0.0188	0.01	-.485	$.27 \times 10^{-4}$
0.00	YES	50	0.02	0.01	57.44	0.0209	0.00985	-.641	$.15 \times 10^{-1}$
0.05	NO	50	0.02	0.01	68.66	0.0211	0.00934	-.866	.133
0.0	NO	50	0.02	0.01	55.81	0.0247	0.00933	-.9187	.161

Section 5 - Asymptotic Inversion

5.1 The Inverse Problem

The run times for the forward problem allow SIROTEM voltages to be calculated interactively. The rapidity of the calculation and the refinement of integrating over windows makes the forward problem an attractive method of inverting SIROTEM layered earth data. Using the asymptotic expansion alone as the forward problem, run times for the inversion program are about 5 seconds for a 2 layered earth above a half-space. The rapidity of the calculation means that many runs can be done interactively. This will allow the interpreter to gain a feel for the data. When the expansion breaks down at early times the numerical integration can be used, however this slows the run times considerably. By using the asymptotic expansion only, and by restricting the fit of the data to the later times when the asymptotic expansion is valid it is possible to obtain a good initial guess for one of the longer runs. The idea of gaining an approximate solution for use in a longer inversion program is similar to the method advocated by Petrick et al. (1981) with three dimensional resistivity inversion programs.

Regularization programs such as those of Jupp and Vozoff (1975) have been employed to handle the instability of the layered earth inversion problem. The unconstrained non-linear least squares IMSL (International Mathematical and Statistical Library) routine 'ZXSSQ' was tried on the inverse problem. In general this proved unsuccessful, with the routine returning large negative depths and conductivities for some cases.

Inverting to the logarithm of the parameters places positivity constraints on these parameters. This refinement was tried but no significant improvement was achieved. A non-linear least squares algorithm with linear constraints supplied by Holt, J. (personal communication) was incorporated for use in inverting layered earth SIROTEM data. This algorithm therefore allows positivity and geologically feasible constraints to be placed on the parameters. The instability of the problem requires that an interpreter has an understanding of how the initial guess for the routine will effect the final outcome of the inversion. To illustrate this a large number of inversion runs on synthetic data, generated by the forward problem, will be presented.

5.2 Inversion of Synthetic Data

The data was generated by the asymptotic expansion. A single layered earth geometry was chosen such that the asymptotic expansion would be valid at each SIROTEM channel. Because inversion runs could be completed in about 5 seconds a large number of runs can be carried out in an interactive computing session. This allows the interpreter to use the results from the previous run to act as a guide for the next initial guess.

The layered earth and loop geometry used was Model 3 defined in section 4.3 and illustrated on figure 4.2. The ramp rise time is 0.05 milliseconds, and the voltages are integrated over each SIROTEM channel. See Table 5.1 for the voltages obtained.

Although Model 3 may not be representative of field examples which require interpretation, and it may be possible to determine the layer geometry by existing methods (e.g. Raiche and Spies

TABLE 5.1

SIROTEM. Window (millisec)		MODEL 3		MODEL 4	
(from)	(to)	Voltages	Apparent Conductivity	Voltages	Apparent Conductivity
0.25	.6	1.102×10^{-2}	0.0139	9.322×10^{-3}	0.0125
0.65	1.0	1.373×10^{-3}	0.0132	1.209×10^{-3}	0.0119
1.05	1.4	4.511×10^{-4}	0.0125	4.049×10^{-4}	0.0116
1.45	1.8	2.085×10^{-4}	0.0122	1.896×10^{-4}	0.0114
1.85	2.2	1.154×10^{-4}	0.0119	1.059×10^{-4}	0.0113
2.25	3.0	5.936×10^{-5}	0.0117	5.501×10^{-5}	0.0111
3.05	3.8	2.913×10^{-5}	0.0115	2.725×10^{-5}	0.0110
3.85	4.6	1.673×10^{-5}	0.0113	1.576×10^{-5}	0.0109
4.65	5.4	1.062×10^{-5}	0.0112	1.006×10^{-5}	0.0108
5.45	6.2	7.227×10^{-6}	0.0111	6.869×10^{-6}	0.0107
6.25	7.8	4.510×10^{-6}	0.0110	4.306×10^{-6}	0.0107
7.85	9.4	2.642×10^{-6}	0.0109	2.534×10^{-6}	0.0106
9.45	11.0	1.700×10^{-6}	0.0108	1.636×10^{-6}	0.0106
11.05	12.6	1.169×10^{-6}	0.0108	1.128×10^{-6}	0.0105
12.65	14.2	8.434×10^{-7}	0.0107	8.158×10^{-7}	0.0105
14.25	17.4	5.597×10^{-7}	0.0107	5.428×10^{-7}	0.0104
17.45	20.6	3.483×10^{-7}	0.0106	3.387×10^{-7}	0.0104
20.65	23.8	2.338×10^{-7}	0.0106	2.279×10^{-7}	0.0104
23.85	27.0	1.658×10^{-7}	0.0105	1.619×10^{-7}	0.0104
27.05	30.2	1.225×10^{-7}	0.0105	1.198×10^{-7}	0.0103
30.25	36.6	8.345×10^{-8}	0.0105	8.172×10^{-8}	0.0103
36.65	43.0	5.332×10^{-8}	0.0104	5.231×10^{-8}	0.0103
43.05	49.4	3.647×10^{-8}	0.0104	3.583×10^{-8}	0.0103
49.45	55.8	2.623×10^{-8}	0.0104	2.580×10^{-8}	0.0103
55.85	62.2	1.961×10^{-8}	0.0103	1.930×10^{-8}	0.0102
62.25	75.0	1.351×10^{-8}	0.0103	1.332×10^{-8}	0.0102
75.05	87.8	8.746×10^{-9}	0.0103	8.630×10^{-9}	0.0102
87.85	100.6	6.038×10^{-9}	0.0103	5.964×10^{-9}	0.0102
100.65	113.4	4.374×10^{-9}	0.0103	4.323×10^{-9}	0.0102
113.45	126.2	3.287×10^{-9}	0.0102	3.251×10^{-9}	0.0102
126.25	151.8	2.280×10^{-9}	0.0102	2.257×10^{-9}	0.0102
151.85	177.4	1.485×10^{-9}	0.0102	1.471×10^{-9}	0.0101

(1981)), the inversion of this model does illustrate a number of important aspects of layered earth inversion.

At late times the expansion for the voltage becomes dominated by the first term in the series. The first term is proportional to $t^{-5/2}$. Therefore when the results are plotted in log-log space the voltage response will be close to a straight line. This is shown for this particular earth geometry on figure 5.1. The first term of the series is independent of layered earth geometry. Thus, in situations where the late time response is a straight line of slope -5/2 in log-log space it is possible to determine the scale factor $I_p/\sigma_{n+1}\lambda$ from the axis intercept. This will fix the basement conductivity. From figure 5.1 it can be seen that the voltage response is very close to that of a half-space. The effect the top layer has on the voltage response is only seen in the early channels.

5.2.1 Apparent Conductivity

Raiche and Spies (1981) define the apparent conductivity at a certain channel as the conductivity of a half-space which would give the measured voltage response at that channel. By inverting a half-space to the voltage in one channel it is possible to obtain the apparent conductivity for that channel. These and the relevant voltages have been depicted on Table 5.1 (as Model 3). The apparent conductivity at late times tends quite clearly to the half-space conductivity (0.01 Siemens). Thus in this case the basement conductivity is obtained with little difficulty. Above this basement there are obviously conductive layers, however the conductivities and depths of the layers is not clear

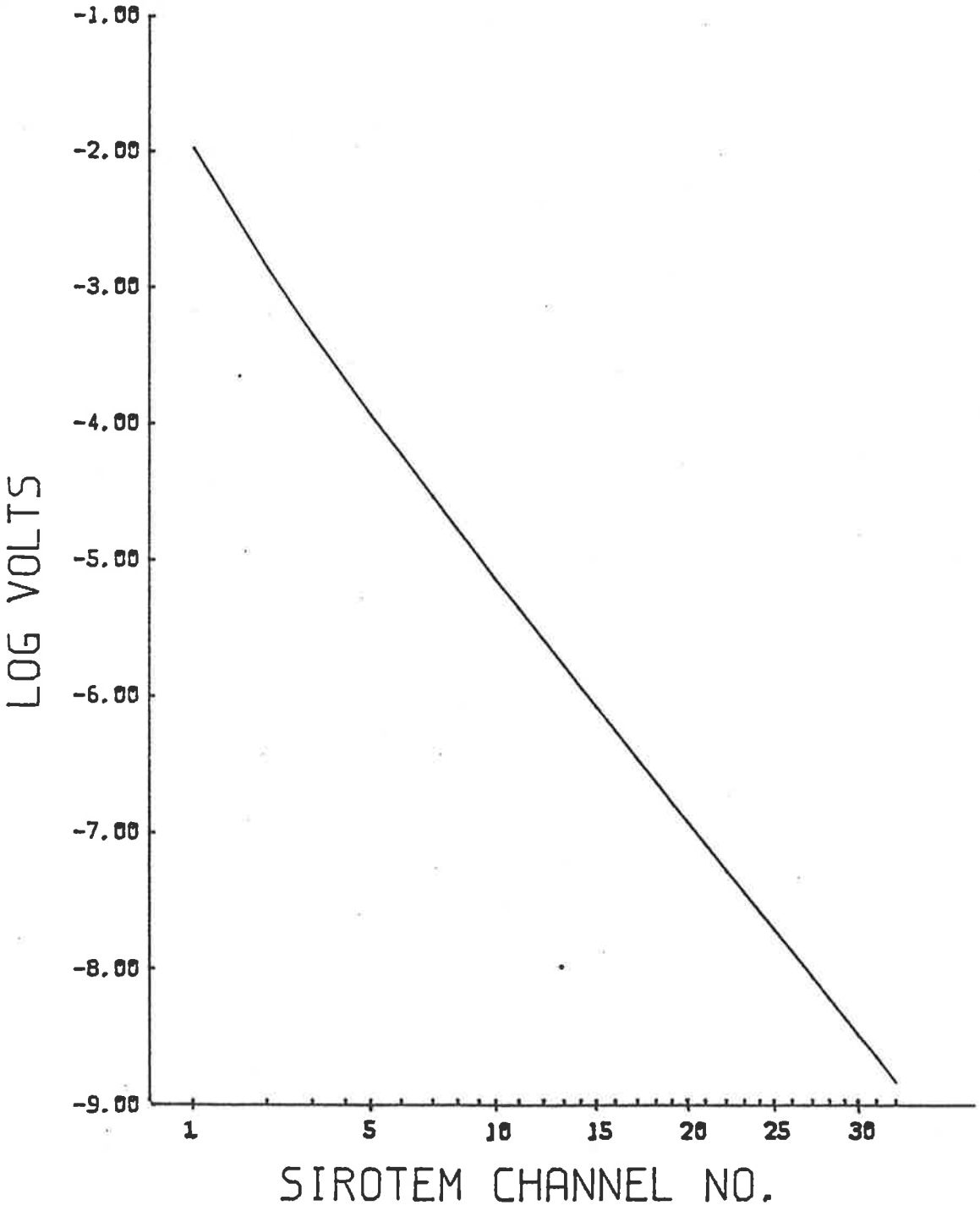

Figure 5.1 The Voltage response for the earth/loop model of Figure 4.2.

from the apparent conductivity data. The apparent conductivity data gives no indication of more than one layer above the basement.

For the inversion routine two types of initial guesses can be made. One involves choosing the top layer conductivity equal to the basement conductivity and making an intelligent guess for the depth. The second involves using the earliest time apparent conductivity for the top layer conductivity and an intelligent guess for the depth. Table 5.2 shows the first guesses, the final parameters returned by the inversion routine and results from subsequent guesses.

The answer with the best fit to the data is the result with the least sum of squares. Clearly one run is never sufficient to obtain the best result. For technique 1 the first guess indicated that σ_1 and d_1 should be larger. This was used in subsequent guesses. For technique 2 the first guess indicated that σ_1 should be larger while d_1 should be smaller.

These runs, and those on Table 5.3, show how the model returned by the inversion routine is strongly dependent on the initial guess.

For n layers above a basement excited by coincident circular transmitter and receiver loops it is possible to show that S_0 and S_1 in Equation 1.9 are given by

TABLE 5.2

	INITIAL MODEL			FINAL MODEL				
	depth	σ_1	σ_2	depth	σ_1	σ_2	α	Sum of Squares
TECHNIQUE 1								
Run 1	20	.014	.01	68	.0174	.009988	-.5074	10^{-3}
Run 2	30	.015	.01	49.98	.02	.01	-.5	10^{-7}
Run 3	40	.015	.01	49.98	.02	.01	-.5	10^{-7}
TECHNIQUE 1								
Run 1	100	.01	.01	82.31	.0161	.01	-.5054	.002
Run 2	82	.0161	.01	82	.0161	.01	-.5054	.002
Run 3	70	.017	.01	68	.0172	.01	-.494	.001
Run 4	60	.021	.01	49.99	.02	.01	-.5	10^{-10}
Run 5	60	.03	.01	49.99	.02	.01	-.5	8×10^{-10}

TABLE 5.3

INITIAL GUESS DEPENDENCE - INVERSION FOR MODEL 3

INITIAL GUESS			FINAL MODEL				
d_1	σ_1	σ_2	d_1	σ_1	σ_2	α	Sum of Squares
100	0.015	0.01	113	0.0147	.00997	-.536	.011
20	0.035	0.02	50	0.0199	.00999	-.500	0.4×10^{-10}
20	0.04	0.01	38.7	0.0228	.00997	-.495	.00004
100	0.02	0.01	109.7	0.01477	.00997	-.528	.0012
20	0.004	0.01	99	0.0152	.00998	-.519	.0013
10	0.01	0.02	10	0.0569	.0101	-.466	.0014
40	0.03	0.01	50	0.02	0.01	-.500	10^{-10}
60	0.03	0.02	113	0.0147	0.00997	-.534	.00109

$$S_0 = 2\pi^2/15 \quad \text{(independent of layered earth geometry)}$$

$$S_1 = \pi/32 \left[-2 \sum_{i=1}^{n} d_i \, (1-\sigma_i)\pi^2\right]$$

$$= -\pi^3 \, \alpha/16$$

$$\text{where } \alpha = \sum_{i=1}^{n} d_i(1-\sigma_i)$$

The subsequent S_i depend on the conductivities and thicknesses in a more complex manner. Note that the top layer conductivity and thickness are poorly determined; however the basement conductivity and α in the next to last column of Table 5.3 are in all cases well determined. For late times in the asymptotic region the expansion will be dominated by the first two terms. It is therefore possible to see why the parameters σ_1 and d_1 are not well determined for this case but σ_2 and α are. Note also that in each case where α is well determined the sum of squares is small. Therefore for late times different layered earth geometrics with the same α and basement conductivities will give similar voltage responses. The inversion routine minimizes the sum of squares, therefore it will in general find the correct α very quickly. The σ_i and d_i are highly correlated, and thus the routine will have difficulty finding the correct combination of σ_i and d_i. The difficulty is compounded by the fact that for small sum of squares the step length in parameter space is small. Therefore many iterations are required to reach the correct answer. Often the routine will find the correct α quickly, but if the σ_i and d_i which make up the α are a long way off their

correct values then the routine will keep iterating slowly, and stop prior to reaching the correct answer (e.g. run 2 of technique 2 Table 5.2). For the cases above which converged to the correct answer the first iteration resulted in the top layer thickness or conductivity being to within 30% of its correct value.

It is important to ensure that guesses are made on either side of the parameters which are finally decided on as being the correct value. This ensures that these parameters are correct. Where possible initial guesses should be in the convergent region of the asymptotic expansion.

5.2.2 An Initial Guess With Many Layers

Table 5.4 shows the results from a set of inversion runs with more than one layer in the initial guess. From the five layer inversion run the conductivity of layer 3 was set to 10^{-4} (the lower bound constraint used for this run). This is a highly resistive layer which the 'smoke ring' of current (Nabighan M. (1979), Lewis and Lee (1978), Hoverstein and Morrison (1982)) travels rapidly through. Its effect on the voltages is minimal, and thus can be ignored. Layer 4 has had its thickness set to zero and this layer also will have little effect considering its conductivity is so close to that of layer five. Using the previous answer with layers 3 and 4 ignored gives a result in which the effect of the third layer would be negligible. It can therefore be ignored. Two subsequent 2 layer runs show that the top layer can be ignored. Finally two one layer runs are required to yield the correct model.

TABLE 5.4

	INITIAL		FINAL			
	Thicknesses	Conductivities	Thicknesses	Conductivities	α	Sum of Squares
5 layers	d_1 20 d_2 20 d_3 20 d_4 20 d_5 20	σ_1 .02 σ_2 .02 σ_3 .02 σ_4 .01 σ_5 .01 σ_6 .01	20.98 28.04 35.92 .1 31.88	.00618 .0381 .0001 .0158 .0145 .01	-.498	$.1 \times 10^{-7}$
3 layers	20 30 30	.0618 .0381 .0145 .01	11.01 44.66 34.82	.0059 .029 .0001 .01	-.457	$.8 \times 10^{-2}$
2 layers	11 40	.006 .03 .01	6.1 39.25	.0001 .2425 .01	-.4991	$.5 \times 10^{-5}$
	10 10	.015 .015 .01	.01 49.98	.001 .02 .01	-.499	$.6 \times 10^{-11}$
1 layer	40	.024 .01	38.2	.0229 .01	-.495	$.23 \times 10^{-4}$
	30	.03 .01	49.94	.02 .01	-.500	10^{-8}

5.2.3 The Effect of Noise

Noise was added to the Voltage data (Table 5.1) by using the CDC Cyber Fortran random number function RANF. The data was corrupted three times and five different noise levels were selected. The initial guess for the inversion was the correct answer, and this was kept constant for all runs. The results are shown in Table 5.5. The figures in brackets are the percent standard deviation ((standard deviation measurement$_i$/measurement$_i$) x 100). The percent standard deviation for σ_1 and d_1 increases more rapidly than the noise level. The percent standard deviation for σ_2 increases more slowly than the noise level, while for α the noise level and percent standard deviation increased at about the same rate. These figures confirm that α and σ_2 are well determined, and that σ_1 and d_1 are poorly determined for this layered earth. This is probably because the effect of the top layer manifests itself in the early channels.

The results for d_1 and σ_1 are encouraging for noise levels of about 1%, as this is of the order of the random noise which may be expected in the field. For the figures presented the initial guess used was the correct answer. If an initial guess away from the correct answer was used then the results would have appeared worse.

5.2.4 The Thin Resistive Layer Problem

The voltage output and apparent conductivity of the model of Figure 5.2 is shown on Table 5.1 (Model 4).

The resistive layer is not seen in the apparent conductivity data (Table 5.1). Apparent conductivity figures will usually not

TABLE 5.5

Percent Noise Level	Depth	σ_1	σ_2	a	Sum of Squares
.1	49.55 ± .639 (1.29)	.02008 ± .00012 (.597)	.010002 ± .0000026 (.025)	.4996 ± .00053 (.105)	10^{-4}
.5	49.79 ± 1.57 (3.15)	.020025 ± .00029 (1.44)	.01000017 ± .000008 (.08)	.4988 ± .0035 (.70)	10^{-3}
1.0	49.27 ± 2.86 (5.80)	.02013 ± .0057 (2.85)	.0100008 ± .00002 (.2)	.498 ± .0055 (1.104)	.0008
5.0	45.28 ± 25.3 (55.8)	.0243 ± .0099 (41.74)	.009995 ± .000071 (.7)	.485 ± .026 (5.34)	.02
10.0	25.48 ± 26.13 (102.55)	.1774 ± .264 (148.36)	.00997 ± .000133 (1.334)	.471 ± .01411 (8.72)	.3

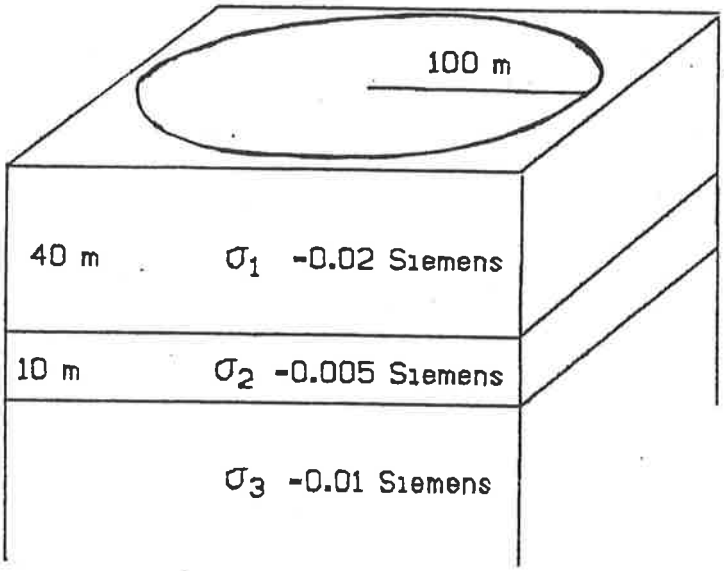

Figure 5.2 Model used for generating the data for the resistive layer problem.

detect thin resistive layers because the smoke ring (Hoverstein and Morrison (1982)) passes through the layer quickly. In general thin resistive layers are of little interest to the Geophysicist. If a TEM interpreter had no 'a priori' information a one layer case would be used to fit the model. The final model obtained from a one layer fit is shown in Table 5.6. The results from using the technique of fitting too many layers is also shown on Table 5.6. The five layer fit gives little indication of a resistive layer, and it is only with 'a priori' information that the interpreter would look closely at the resistive layers.

TABLE 5.6
The thin resistive layer problem

	INITIAL MODEL d_i	INITIAL MODEL σ_i	FINAL MODEL d_i	FINAL MODEL σ_i	α	Sum of Squares
Run 1 1 layer	50	σ_1 .02	31.95	.02096	-.3505	$.4 \times 10^{-7}$
		σ_2 .01		.01		
Run 2 5 layer	20	.02	3.47 (small)	.0171		
	20	.02	19.18	.0180		
	20	.02	20.83	.0195	-.3497	$.175 \times 10^{-5}$
	20	.01	14.27	.0096		
	20	.01	29.38	.0089		
		.01		.01		
Run 3 3 layer	40	.019	35.6	.02017		
	15	.01	8.3	.0101	-.35	$.1 \times 10^{-5}$
	14	.009	30.2	.0096		
		.01		.01		
Run 4 3 layer	30	.03	38.18	.0198	-.35	
	10	.009	.1	.056		$.28 \times 10^{-8}$
	30	.001	26.	.0088		
		.01		.01		
Run 5 2 layer	31	.015	88.127	.0139		
	26	.008	50.55	.0105	-.355	$.75 \times 10^{-3}$
		.01		.01		
Run 6 2 layer	10	.04	10.33	.034		
	50	.008	44.16	.012	-.351	$.53 \times 10^{-6}$
		.01		.01		
Run 7 2 layer	20	.02	38.8	.0198		
	10	.001	23.91	.0086	-.35	$.13 \times 10^{-7}$
		.01		.01		
Run 8 2 layer	38	.02	40.35	.02		
	8.8	.005	8.78	.0039	-.35	$.15 \times 10^{-10}$
		.01		.01		
Run 9 2 layer	38	.02	39.97	.2		
	8.8	.005 (fixed)	9.97	.005	-.35	$.42 \times 10^{-11}$
		.01		.01		

Subsequent 3 and 2 layer models do not aid in resolving the problem. Runs 7 and 8 have guesses very close to the actual answer, but the correct answer is still not obtained. An initial guess where the thin layer conductivity is known and fixed will yield the correct result (Run 9). This serves to illustrate the difficulty in distinguishing resistive layers unless there is good geological control. For a resistive layer between two highly conductive layers the effect would become more marked.

For the synthetic examples discussed above the instability of the TEM problem is shown. The difficulty is amplified by the near non-uniqueness of the problem, as earth geometries with identical α and basement conductivities have similar voltage responses in the asymptotic region. The blind inversion of TEM data can be dangerous as any answer can be obtained for a poor initial guess. Geological control is required; however the control should guide the interpretation not dictate the final answer. The use of geological information is best used to place feasible bounds on parameters. The interpreter must always be careful to distinguish between what is a geological fact and what is interpretation.

The ability to place feasibility bounds on certain parameters is of particular advantage in the constrained non-linear least squares inversion program of Holt (personal communication), as it restricts the parameters to feasible areas in parameter space (Geologically feasible and mathematically feasible - positivity).

5.3 Strategy for Layered Earth Inversion

Prior to using a layered earth inversion algorithm the interpreter must first check that the data is representative of a layered earth. This can be done in a number of ways.

(1) Provided that the earth is non-polarizable (no Induced Polarization (IP) or dispersion effects) negative voltages cannot exist for a coincident loop geometry (Weidelt (1982)). Thus if such negative voltages exist, it will not be possible to adequately represent the induced currents of any earth structure adequately without taking into account IP effects. To attempt to fit the data to a non-polarizable layered earth model will therefore be of little value. It may be possible to obtain a layered earth model which fits the data set in which the late time channels with the sign reversals have been rejected (plus some before, and those after the reversals). However the accuracy of this fit cannot be guaranteed without a priori information of the Cole-Cole model for the conductivity (Pelton et al. 1978) relevant to the layers in question.

(2) Check to see if at late times the voltage response has a -5/2 slope when plotted in log-log space. If so, this will fix the basement conductivity, however it is not always possible to obtain voltages at late enough times to observe the -5/2 slope.

(3) Check that along a traverse there is only a gradual change in the Voltage response. If two perpendicular traverses both exhibit gradual changes then the earth will approximate a layered medium.

(4) Look to the geological mapping of the area or drill hole

information.

Having ascertained that the earth approximates a layered medium the following strategy should be adopted:

(A) If the number of layers is unknown then determine the number of layers by:

Either (i) Ascertaining the minimum number of layers indicated by the apparent conductivity data

or (ii) Fit a half space to the data. Having found the best half space insert additional layers until any additional layer becomes redundant

or (iii) Start with as many layers as possible and eliminate them one by one until a satisfactory solution has been obtained.

(B) Both when the number of layers is known , and when it is unknown, the asymptotic expansion should be used initially, and guesses should be made within the convergent region. The initial guess should be varied so as to allow the inversion routine to cover as large an area of parameter space as possible. This will give it the best chance of obtaining the global minimum.

(C) If the asymptotic expansion breaks down in the early channels these channels should be discarded. The discrepancy between the erroneous voltage given by the asymptotic expansion and the actual voltage will be large and this will dominate the sum of squares and therefore adversely effect the results of the inversion. Using only the late channels the effect of shallow layers will not be felt, however this method should give a quick indication of an initial guess which could be used in the more

costly inversion programs.

(D) The application of the numerical integral of equation 1.6 should only be used when the layers above the half space are resistive.

Alternatively the asymptotic expansion and the numerical integration of equation 1.6 for resistive layers could be incorporated within a routine such as GRENDL to speed the computation. The data should still be checked to see that it is representative of a layered earth. The strategy outlined in (A) can still be used.

In all cases many initial guesses should be used so as to gain an idea of the shape of parameter space. In particular guesses around the answer deemed to be the 'solution' should be tried to test the stability of this solution with respect to variation of the initial guess.

Section 6 - Conclusion

The currently available large loop layered earth inversion schemes are computationally time consuming. The aim of this thesis was to examine means by which the inversion of layered earth data can be made more efficient, and thus interpretation made easier and cheaper.

The analysis in the Appendix of this thesis has resulted in algorithms which have a number of advantages over the methods presented by previous workers (Knight and Raiche (1982), Lee and Lewis (1974), Raiche and Spies (1981) and Morrison, Phillips and O'Brien (1969)):

(a) The time dependence of equation 1.6 means that:

(i) The voltages can be calculated more efficiently. When the asymptotic expansion is valid the coefficients of the expansion are independent of time, and therefore having calculated the coefficients for one delay time they can be re-used for all subsequent delay times. This results in an extremely rapid computation of the response. At times when the asymptotic expansion is not valid, and when the overburden is resistive the integral can be evaluated numerically. This is also efficient, as the time dependence appears only in the outer integral, and thus the S(x) can be evaluated and stored for use at all the required delay times. The asymptotic expansion can be evaluated more quickly than the numerical integration.

(ii) The voltage can be integrated over a time window with little extra computation time being required. The SIROTEM equipment is therefore better represented mathematically. This is of particular value in the early SIROTEM channels.

(b) A variety of loop configurations can be modelled. This means that the voltage response can be calculated for coincident and separated circular loops, and coincident and separated rectangular loops. The sizes of the receiver and transmitter loops may be varied independently. It is also possible to obtain expressions for other loop configurations.

This means that the half-space response can also be obtained for these loop geometries. Therefore using a one variable line search inversion routine it is possible to obtain the apparent conductivity at different SIROTEM channels provided that the loop geometry function P(mx) is known. Apparent conductivity is a useful interpretative tool, as it can give a good guide as to the subsurface structure, and also give an indication of a good initial guess for an inversion algorithm. This formulation provides a means of rapidly calculating the apparent conductivities for loop geometries apart from the coincident loop configuration.

(c) The incorporation of linear constraints in the non-linear least squares inversion routine is useful. The constraints allow the interpreter to place geologically and mathematically feasible bounds on the parameters, and to prevent the routine from deviating too far from an initial guess.

(d) Although Raiche (1983) has also obtained results for a variable ramp rise time the formulation presented here also allows for that sophistication - the usefulness of which is illustrated in section 4.

The asymptotic and the numerical evaluations can be incorporated into an inversion routine as the sole forward algorithms. For channels when neither method gives an accurate answer the data from those channels must be discarded. This method was tried on very conductive field data, but the algorithms were only accurate in the last four channels. The information obtained from the inversion algorithm was therefore inconclusive. In less conductive circumstances this method would provide a good initial guess for a slower more general algorithm - such as GRENDL.

However, if it is possible to include the asymptotic expansion and the integration for resistive overburdens into a routine which can calculate the response at early times for conductive overburden, then in certain circumstances the computation time would be decreased. The inversion could therefore be performed in real time, and interpretation would be significantly easier. The decrease in run times allows more runs to be done in a given time, and thus, for the interpreter to build up a better idea of what the solution space looks like. This would also decrease the interpreter's dependence on the parameter statistics used by GRENDL (see Jupp and Vozoff (1975)).

The strategy outlined in section 5.3 represents a systematic scheme for approaching layered earth inversion, regardless of the

forward problems used. The incorporation of constraints into the inversion routine is recommended because of the advantages it contains.

BIBLIOGRAPHY

Abramowitz, M. and Stegun, I.A. (1970), 'Handbook of Mathematical Functions with Formulas, Graphs, and Mathematical Tables,' **Dover Publications, N.Y.**

Anderson, W.L. (1979), 'Numerical integration of related Hankel transforms of order 0 and 1 by adaptive digital filtering.' **Geophysics**, Vol. 44, p 1287-1305.

Buselli, G. (1974), 'Multichannel transient electromagnetic measurements near Conclurry.' **Aust. Soc. Expl. Geophys. Bulletin**, Vol. 5, p 31-47.

------ (1977), 'Transient electromagnetic Measurements to late delay times over the Woodlawn ore body.' **Aust. Soc. Expl. Geophys. Bulletin**, Vol. 8, p 1-5

------ (1980a), 'The application of SIROTEM in Weathered Terrain.' **Aust. Soc. of Expl. Geophys. Bulletin**, Vol. 11, p 99-109.

------ (1980b), 'Interpretation of SIROTEM data from Elura.' The Geophysics of the Elura orebody Cobar N.S.W.' D.W. Emerson Ed., **Aust. Soc. Expl. Geophys.**

------ (1981), 'An experimental transient electromagnetic system.' Geophysical case study of the Woodlawn orebody New South Wales, Ed. R.J. Whitely, **Permagon Oxford.**

Buselli, G. and O'Neill, B. (1977), 'SIROTEM: A new portable Instrument for Multichannel Transient Electromagnetic Measurements,' **Aust. Soc. Expl. Geophys. Bulletin**, Vol. 8, p 82-87.

C.S.I.R.O. (1978), 'SIROTEM - Transient E.M. system,' a **Commonwealth Scientific and Industrial Research Organization** publication. The Minerals Development Laboratory.

Das, N.C. and Verma, S.K. (1982), 'Electromagnetic response of an arbitrarily shaped three dimensional conductor in a layered earth - numerical results.' **Geophysical J. Roy. Ast. Soc.**, Vol. 68, p 55-66.

Erdelyi, A. (1956), 'Asymptotic Expansions,' **Doves Publications**, N.Y.

Gaver, D.P. (Jr) (1966), 'Observing stochastic processes and approximate transform inversion.' **Operations Research**, Vol. 14, p 444-459.

Grant, F.S. and West, G.F. (1965), 'Interpretation theory in Applied Geophysics,' **McGraw-Hill, Book Coy Inc., N.Y.**

Hoverstein, G.M. and Morrison, H.F. (1982), 'Transient fields of a current loop source above a layered earth.' **Geophysics**, Vol. 47, p 1068-1077.

Jupp, D.J.B. and Vozoff, K. (1975), 'Stable iterative methods for inversion of Geophysical data.' **Geophysical J. Roy. Ast. Soc.**, Vol. 42, p 957-956.

Kamenetski, F.M. (1969), 'Transient processes using combined loops for a two layer section with a non-conducting base,' **Izv. Vuzov. Sect. Geology Prosp.**, Vol. 6, p 108-113.

Kaufman, A.A. (1979), 'Harmonic and transient fields on the surface of a two layered medium.' **Geophysics**, Vol. 44, p 1208-1217.

Knight, J.M. and Raiche, A.P. (1982), 'Transient electromagnetic calculations using the Gaver-Stehfest inverse Laplace transform method.' **Geophysics**, Vol. 47, p 47-50.

Koefoed, O., Ghosh, D.P. and Polman, G.J. (1972), 'Computation of type curves for electromagnetic depth sounding with a horizontal coil by means of a digital linear filter.' **Geophys. Prospecting**, Vol. 20, p 403-420.

Lamontagne, Y.L., Lodha, G.S., Macnae, J.C. and West, G.F. (1980), 'UTEM: wide band time domain EM project 1976-78, reports 1-5.' **Research in Applied Geophysics**, University of Toronto.

Lee, T. (1981), 'The Effect of Displacement Currents on Time Domain Electromagnetic Fields.' **Aust. Soc. Expl. Geophys. Bulletin**, Vol. 12, p 34-37.

------ (1982), 'Asymptotic Expansions for Transient Electromagnetic fields.' **Geophysics**, Vol. 47, p 38-46.

Lee, T. and Lewis, R. (1974), 'Transient EM response of a large loop on a layered ground.' **Geophysical Prospecting**, Vol. 22, p 430-444.

Lewis, R. and Lee, T. (1978), 'The Transient electric fields about a loop on a half-space.' **Aust. Soc. Expl. Geophys. Bulletin**, Vol. 9, p 173-177.

Mallick, K. and Verma, R.K. (1978), 'Time domain electromagnetic sounding with horizontal and vertical, co-planar loops on a multi-layered earth.' **Geoexploration**, Vol. 16, p 291-302.

McCracken, K.G., Hohmann, G.W. and Oristaglio, M.L. (1980) 'Why time domain?' Geophysics of the Elura orebody Cobar N.S.W., **Aust. Soc. of Expl. Geophys.**

Morrison, H.F., Phillips, R.J. and O'Brien, D.P. (1969), 'Quantitative interpretation of transient electromagnetic fields over a layered half space.' **Geophysical prospecting**, Vol. 17, p 82-101.

Nabighan, M.N. (1979), 'Quasistatic Transient Response of a Conductive Half-space - An Approximate Representation.' **Geophysics**, Vol. 44, p 1700-1705.

O'Brien, D.M. and Smith, R.S. (1984), 'Transient electromagnetic response of a layered conducting medium at asymptotically late times.' In press (see appendix).

Olver, F.W.J. (1974), 'Asymptotics and Special Functions.' **Academic Press**, N.Y.

Patterson, T.N.L. (1973), 'Algorithm for automatic numerical integration over a finite interval'. **A.C.M. Comm.**, Vol. 16, p 694-699.

Pelton, W.H., Ward, S.H., Hallof, P.G., Sill, W.R. and Nelson, P.H. (1978), 'Mineral discrimination and removal of inductive coupling with multifrequency I.P.' **Geophysics**, Vol. 43, p 588-609.

Petrick, Wm. R. Jr., Sill, Wm. R. and Ward, S.H. (1981), 'Three dimensional resistivity inversion using alpha centres.' **Geophysics**, Vol. 46, p 1148-1163.

Raiche, A.P. (1983), 'The effect of Ramp function turn-off on the TEM response of a layered earth.' Submitted to **Aust. Soc. Expl. Geophys. Bulletin**, 18.1.83.

Raiche, A.P. and Spies, B.R. (1981), 'Coincident loop transient electromagnetic master curves for interpretation of two layer earths.' **Geophysics**, Vol. 46, p 53-64.

Singh, R.N. (1973), 'Transient electromagnetic response of a conducting sphere in a conducting medium.' **Geophysics**, Vol. 38, p 864-893.

Smith, R.S. (1982), 'The calculation of Transient Electromagnetic responses over a layered earth using asymptotic expansions.' Honours thesis, **Dept. of Econ. Geology**, the University of Adelaide.

Spies, B.R. (1976), 'The Transient Electromagnetic Method in Australia.' **B.M.R. Journal of Australian Geology and Geophysics**, Vol. 1 no. 1, p 23-32.

Spies, B.R., Hone, I.G. and Williams J.W. (1981), 'Geophysical case study of the Woodlawn orebody New South Wales.' Ed. R.J. Whitely, **Permagon, Oxford**, p 281-296.

Stehfest, H. (1970), 'Algorithm 368 Numerical inversion of Laplace transforms.' **A.C.M. Comm.**, Vol. 13, p 47-49.

------ (1970b), 'Remark of algorithm 368.' **A.C.M. Comm.**, Vol. 13, p 624.

Wait, J.R. (1982), 'Geoelectromagnetism.' **Academic Press, N.Y.**

Wannamaker, P.E., Hohmann, G.W. and San Filipo, W.A. (1984), 'Electromagnetic modelling of three dimensional bodies in layered earths using integral equations.' **Geophysics**, Vol. 49, p 60-74.

Ward, S.H. (1967), 'Electromagnetic Theory for Geophysical Applications.' Mining Geophysics Volume II - Theory. **The Society for Exploration Geophysicists.**

Weidelt, P. (1982), 'Response characteristics of coincident loop transient electromagnetic systems.' **Geophysics**, Vol. 47, p 1325-1330.

Appendix

The Joint Paper

O'Brien and Smith

(1984)

Submitted to the Journal of the Australian Mathematical Society, Series B.

TRANSIENT ELECTROMAGNETIC RESPONSE OF A LAYERED CONDUCTING MEDIUM AT ASYMPTOTICALLY LATE TIMES.

D.M. O'Brien

* R.S. Smith

November 1983.

Department of Economic Geology

University of Adelaide

Adelaide

South Australia 5000

Australia

* Present address:

Department of Physics

University of Toronto

Toronto

Ontario

Canada M5S 1A7

Short title: ASYMPTOTIC EM RESPONSE.

0. ABSTRACT.

In this paper we consider a pair of horizontal conducting loops in the air above a horizontally layered ground. The transmitting loop is driven by a current source which rises from zero at time zero to a final constant value at time τ. We firstly compute the emf induced in the receiving loop and derive an asymptotic series for the emf at late times. Secondly, we estimate the error in truncating the asymptotic series at N terms and design a reliable numerical algorithm for summing the asymptotic series.

1. INTRODUCTION.

In this paper we consider the transient electromagnetic (TEM) response of a horizontally layered medium such as that shown in figure 1.

FIGURE 1.

This subject has been studied by many authors, in particular, by authors interested in the application of electromagnetic techniques to the detection of minerals. An excellent guide to the literature is contained in the book on geo-electromagnetism published recently by Wait [21]. In principle, the TEM response is completely known, because the electromagnetic Green's tensor for a layered conducting medium reduces to an elementary expression after Laplace (or Fourier) transformation of the time variable and Hankel transformation of the radial cylindrical coordinate, but in practice the numerical inversion of the two integral transforms poses a problem. Morrison, Phillips and O'Brien [16] gave an early solution which used the trapezoidal quadrature rule for the inverse Hankel transform and the fast Fourier algorithm for the inverse Fourier transform. After the development of digital filters for the Hankel transform of arbitrary order ν , several new programs were written which used digital filters for the Hankel transform and possibly also for the Fourier transform, since the latter can be formulated as a Hankel transform with order ν =1/2. These programs were considerably more efficient. (Koefoed [10], Mallick and Verma [15], Anderson [2].) Knight and Raiche [9] made a further significant improvement in efficiency by reversing the order of the inverse integral transforms, and applied the Gaver - Stehfest

[6, 18, 19] algorithm to the inverse Laplace transform followed by an adaptive version of Patterson's [17] algorithm for Gaussian quadrature to evaluate the Hankel transform. The success of Knight and Raiche's strategy is due to the gain in speed and accuracy of the Gaver - Stehfest algorithm when applied to functions known analytically rather than numerically. Knight and Raiche's algorithm is currently the best available.

Complementary to these computer programs, which attempt to invert the integral transforms numerically, is the work on asymptotic expansions of the TEM response at both early and late times. Lee and Lewis [14] established that at early or late times the TEM response approaches that of a half space whose conductivity is equal to that of the top layer or the bottom layer, respectively. Lee [13] also developed a two term asymptotic expansion valid for late times, which subsumed earlier results by Kamenetski [7] and Kaufman [8]. In addition to their simplicity and speed, the asymptotic expansions often have the useful property that they work best when the more general computer programs are most costly. For example, Knight and Raiche's algorithm seems to be slowest at late times, precisely when Lee's asymptotic formula is applicable.

If the object were to compute the TEM response of a single layered medium, then many of the refinements above would not be necessary, because even the most basic algorithm will obtain the TEM response for relatively little cost. However, in practice we want to infer the structure of a layered ground from observations of its TEM response, and to do so we employ an optimisation algorithm which adjusts the model in order to minimise a cost function which measures the discrepancy between the actual data and the data predicted by the model. The

optimisation algorithm will be iterative and will proceed from an initial guess for the model to a final 'solution', which is a local minimiser of the cost function. The 'solution' is dependent upon the initial guess, so, in addition to all the iterations of the optimisation algorithm, it is essential to experiment with different initial guesses. If all this calculation is to be performed in real time, so that a geophysicist can immediately interpret his survey data, then the computer code which calculates the TEM response of the layered ground must employ every known time saving device.

With this motivation, we now turn to the content of this paper.

We develop a late time asymptotic expansion for the TEM response of the layered conducting ground depicted in figure 1, and we establish the region of usefulness of the expansion. The terms of the expansion are easily computed and can be programmed on almost any micro - computer. The expansion may be used on its own for a very rapid first interpretation of field data, or may be coupled with existing software such as the TEM program of Knight and Raiche [9], to produce faster inversion programs.

The transmitting and receiving loops must be horizontal, but otherwise their shapes and positions are arbitrary, although in practice we will require the loops to be either circular or rectangular. In particular, the loops may be either coincident or distinct. We assume that the transmitting loop carries a current density

$$\underline{J}(\underline{x},t) = \underline{M}(\underline{x})\, I(t)\ , \qquad (1.1)$$

where $\underline{M}$ is horizontal, divergence free and has compact support, and I is the ramp function

$$I(t) = \begin{cases} 0 & \text{if} \quad t < 0 \\ t/\tau & \text{if } 0 \leqslant t \leqslant \tau \\ 1 & \text{if } \tau < t \end{cases} \qquad (1.\ 2)$$

Such a temporal variation models the UTEM prospecting system (Lamontagne, Lodha, Macnae and West [12]), the PEM prospecting system (Crone [5]), and also models SIROTEM (Buselli and O'Neill [3]) in the limit $\tau \rightarrow 0$.

We will work exclusively with scaled, dimensionless variables, defined as follows.

Quantity	Unit
length	λ
conductivity	σ_{n+1}
time	$\sigma_{n+1} \mu \lambda^2$
permittivity	$\sigma_{n+1}^2 \mu \lambda^2$
electric field intensity	volts/unit scaled length
current density	amps/unit scaled area

Here λ denotes any typical length chosen as the unit of length, such as the radius or side length of the transmitting loop. We will compute the dimensionless quantity

$$Z(t) = \lambda \sigma_{n+1} V/I_p \quad , \qquad (1.\ 3)$$

where V is the emf induced in the receiving loop, measured in volts, and I_p is the peak value of the current in the transmitting loop, measured in amps. $Z(t)$ is clearly related to the mutual impedance of the transmitting and receiving loops over the layered medium.

The key to the asymptotic analysis of the TEM response lies in the treatment of the inverse Laplace transform. We examine the singularities of the function to be transformed and show that the contour of integration may be deformed around a cut along the negative real axis. Then $Z(t)$ has the asymptotic form

$$Z(t) \sim [B_1(t) - B_1(t - \tau)]/\tau \quad , \qquad (1.\ 4)$$

where

$$B_i(t) = \pi^{-2} \int_0^\infty dx \, \exp(-x^2 t) \, x^{2(i-1)} S(x) \quad , \qquad (1.5)$$

and

$$S(x) = x^2 \int_0^1 dm \, (1 - m^2)^{1/2} \, m \, P(mx)/Q(m,x) \quad . \qquad (1.6)$$

Here P is a function which we call the loop function, because it depends solely on the disposition of the loops and not on the structure of the layered medium, whereas the function Q has the opposite dependence. Watson's lemma (Copson [4]) can be applied to $B_i(t)$ and we obtain the asymptotic expansion

$$B_i(t) \sim A_i(t) = (2\pi^2)^{-1} \sum_{r=0}^\infty S_r \, \Gamma((r+1)/2 + i) \, t^{-((r+1)/2 + i)} \quad , \qquad (1.7)$$

where S_0 , S_1 , ... are the coefficients in a power series for S convergent for small x:

$$S(x) = x^2 \sum_{r=0}^\infty S_r \, x^r \quad . \qquad (1.8)$$

The coefficients S_0 , S_1 , ... depend upon both the geometry of the loops and the structure of the medium, but are independent of time. Consequently, the coefficients only need be computed once if the mutual impedance is required at several times. If the time variation of the source current is a step rather than a ramp, then the appropriate asymptotic expansion is obtained in the limit as $\tau \rightarrow 0$, namely,

$$Z(t) \sim -A_2(t) \quad . \qquad (1.9)$$

Listed below are the times taken to compute the coefficients by

the CYBER machine at the University of Adelaide.

Number of layers.	Time to compute S_0, ... S_{15}.
1	36 msec
2	49 msec
3	66 msec
4	99 msec
5	181 msec

The extra time required to sum the asymptotic series is negligible, approximately 1 msec per time.

In all practical prospecting systems, the quantity that is actually measured is not the mutual impedance at a particular time, but rather the average of this quantity over a time channel

$$t_0 < t < t_1 \quad .$$

Thus, the observed quantity is

$$Z(t_0,t_1) = (t_1 - t_0)^{-1} \int_{t_0}^{t_1} dt\, Z(t) \quad . \tag{1.10}$$

Provided that both t_0 and t_1 are sufficiently late, then the asymptotic expansion may be substituted for $Z(t)$ and integrated termwise to give

$$Z(t_0,t_1) = \begin{cases} \dfrac{A_0(t_0) - A_0(t_1) - A_0(t_0 - \tau) + A_0(t_1 - \tau)}{\tau\,(t_1 - t_0)} & , \tau > 0 \quad , \\ \dfrac{A_1(t_1) - A_1(t_0)}{(t_1 - t_0)} & , \tau = 0 \quad . \end{cases} \tag{1.11}$$

The asymptotic series in (1.7) above is divergent (except for the degenerate case of a half space without overburden), but, for any fixed number of terms, will provide any desired accuracy for sufficiently late times. However, before

the asymptotic series can be used successfully, the problems of chosing the number of terms and of deciding how late is 'sufficiently late' must be addressed. We will show that

$$\left| B_i(t) - B_i^N(t) \right| < K \ \xi^{2(i+1)} F(N + 2(i+1), \xi t^{1/2}) \quad , \qquad (1.12)$$

where B_i^N is the sum to N terms of the asymptotic series and

$$F(m,z) = \Gamma(m/2)/z^m \quad .$$

The number ξ is computable exactly in principle, but in practice is given sufficiently accurately by the following expression

$$\xi^{-1} = \begin{cases} d\,|\theta_1|(1 + |\chi|^{1/2}) & , \ \chi \leqslant 0 \ , \\ d\,|\theta_1|(1 + \chi)^{1/2} & , \ \chi \geqslant 0 \ , \end{cases} \qquad (1.13)$$

where

$$\chi = (\theta_1 + \theta_2)/\theta_1^2$$

$$\theta_1 = d^{-1} \sum_{i=1}^{n} (1 - \sigma_i)\, d_i \qquad (1.14)$$

$$\theta_2 = d^{-2} \sum_{i=1}^{n} (1 - \sigma_i)\, d_i (d_1 + \ldots + d_{i-1} - d_{i+1} - \ldots - d_n)$$

and finally

$$d = \sum_{i=1}^{n} d_i \quad . \qquad (1.15)$$

If $\xi^2 t > 1$, then the bound, regarded as a function of N, decreases at first, passes through a minimum, and then diverges. If $\xi^2 t \leqslant 1$, the bound simply diverges. The minimum of F(m,z) occurs when

$$\Psi(m/2) = 2 \log z \quad , \qquad (1.16)$$

where Ψ is the psi function, and typical values of F at the minimum are listed below.

z	m at minimum	F(m,z) at the minimum
2	9	2.27×10^{-2}
3	19	1.03×10^{-4}
4	33	7.03×10^{-8}
5	51	6.95×10^{-12}

On the basis of these results, a reasonable strategy for truncating the asymptotic series might be as follows.

(1) Compute χ and ξ from formulae (1.14) and (1.13).

(2) Check whether

$$\xi^2 t > 3 \quad . \tag{1.17}$$

If not, set a warning flag to indicate that the time is too early.

(3) Find the closest integer N to the solution of (1.16). This is easily done as the values of the psi function can be generated by recursion and then stored.

(4) Sum the asymptotic series to N terms.

We implemented this strategy and found it successful but too conservative, no doubt because the estimate (1.12) is not sufficiently sharp. Instead we adopted the following pragmatic strategy.

(1) Compute a running average of the moduli of two terms.

(2) Choose N corresponding to the minimum of the running average.

(3) Take the average of the moduli of the last term and the first omitted term as a measure of the error.

We found the running average necessary because the odd and even order terms occasionally had different orders of magnitude. The success of the strategy is shown in figure 2 where we plot contours of the error for a medium with a single conductive layer with unit thickness above the basement. The prospecting system is SIROTEM with coincident circular loops with unit radius and a step function current source driving the transmitter loop. The variables in the plot are time and the conductivity of the layer. The errors were computed by comparison of the asymptotic series with the program of Knight and Raiche [9]. Also shown on the plot are the theoretical curve

$$\xi^2 t = 3 \qquad (1.18)$$

and the curve along which the pragmatic algorithm believes it has achieved an accuracy of 1%. The algorithm clearly is reliable.

FIGURE 2.

2. DERIVATION OF Z(s).

We begin the analysis with the following expressions for the Laplace transform of the emf induced in the receiving loop:

$$V(s) = \int_R d\underline{x} \cdot \underline{E}(\underline{x},s) \quad , \tag{2. 1}$$

$$\underline{E}(\underline{x},s) = \frac{-s}{\lambda\sigma_{n+1}} \int_T d^3x' \; g(\underline{x},\underline{x}',s) \; \underline{J}(\underline{x}',s) \quad , \tag{2. 2}$$

and

$$g(\underline{x},\underline{x}',s) = (4\pi)^{-1}\int_0^\infty dl\,(l/k_0)\; J_0(l\,|\underline{r} - \underline{r}'|)\,[\exp(-k_0\,|z - z'|\,) + \exp(-k_0(z + z')\,)\; b/a] \tag{2. 3}$$

Here V and $\underline{E}$ denote the induced emf and the electric field intensity. The variables $k_0, k_1, \ldots, k_{n+1}$ are defined by

$$k_i = (\varepsilon_i s^2 + \sigma_i s + l^2)^{1/2}, \tag{2. 4}$$

and a and b are elements of the matrix A defined as follows:

$$A = \begin{pmatrix} a & b \\ c & d \end{pmatrix} = \begin{pmatrix} \exp(k_{n+1}d) & 0 \\ 0 & \exp(-k_{n+1}d) \end{pmatrix} \begin{pmatrix} 1 & k_{n+1} \\ 1 & -k_{n+1} \end{pmatrix} T_n \cdots T_1 \begin{pmatrix} 1 & k_0 \\ 1 & -k_0 \end{pmatrix}^{-1}$$

where (2. 5)

$$T_i = \begin{pmatrix} \cosh k_i d_i & k_i \sinh k_i d_i \\ k_i^{-1} \sinh k_i d_i & \cosh k_i d_i \end{pmatrix}. \tag{2. 6}$$

This result may be derived along the lines followed by Morrison, Phillips and O'Brien [16]. Alternatively, one can

prove that the special properties of the source current density $\underline{J}$, that it be horizontal and divergence free, imply that there are no charge distributions on the interfaces between the layers and that Maxwell's equations reduce to the telegraph equation for a single scalar field. The telegraph equation separates in rectangular coordinates into ordinary differential operators, whose spectral kernels can be constructed by standard techniques. Convolution of these kernels yields the spectral kernel for the telegraph operator from which Green's function g is constructed. The remaining steps which lead to V are then trivial.

The function g represents the effect at $\underline{x}$ of a source at $\underline{x}'$ and contains geometrical optics terms which must be isolated and treated separately. To do so, let $\tilde{\underline{x}}'$ represent the reflection of $\underline{x}'$ in the plane $z = 0$. Then

$$g(\underline{x},\underline{x}',s) = g_0(|\underline{x} - \underline{x}'|,s) + p\, g_0(|\underline{x} - \tilde{\underline{x}}'|,s) + f(\underline{x},\underline{x}',s) \quad (2.7)$$

where

$$g_0(r,s) = \exp(-(\varepsilon_0 s^2 + \sigma_0 s)^{1/2} r) / (4\pi r) \quad (2.8)$$

and

$$f(\underline{x},\underline{x}',s) = (4\pi)^{-1} \int_0^\infty dl\ (1/k_0)\ J_0(l\,|\underline{r} - \underline{r}'|)\ \exp(-k_0(z + z'))\ .[b/a - p] \quad . \quad (2.9)$$

The constant p is ultimately fixed by boundary conditions, but its actual value will not concern us because it will cancel from the asymptotic expansion. The interpretation of g_0 becomes apparent after we compute its inverse Laplace transform:

$$g_0(r,t) = \frac{\exp(-t/t_0)}{4\pi r}\ [\delta(t - r/c) +$$

$$\frac{H(t - r/c)\; r\; I_1((t^2 - r^2/c^2)^{1/2}/t_0)]}{ct_0 \quad (t^2 - r^2/c^2)^{1/2}} \qquad (2.10)$$

where

$$t_0 = 2\varepsilon_0/\sigma_0 \quad ,$$
$$c = \varepsilon_0^{-1/2} \quad , \qquad (2.11)$$

and H is the step function,

$$H(t) = \begin{cases} 0 & \text{if } t < 0 \\ 1/2 & \text{if } t = 0 \\ 1 & \text{if } t > 0 \end{cases} \qquad (2.12)$$

The case of most interest is that obtained by setting $\sigma_0 = 0$, so that the air is a perfect insulator, for then

$$g_0(r,t) = \delta(t - r/c)/(4\pi r) \quad . \qquad (2.13)$$

Here c is the speed of light in air (in scaled variables!), so the first term in (2.7) represents the passage of a wave front directly from $\underline{x}$ to $\underline{x}'$, whereas the second represents the wave front reflected from the interface between the air and the earth.

In the application to geoprospecting systems, the contributions from the g_0 terms occur at times too early to measure. Indeed, if $\underline{E}_0$ denotes the contribution to $\underline{E}$ from g_0, then

$$\underline{E}_0(\underline{x},t) = -(\lambda\sigma_{n+1})^{-1}\int_0^t dt' \int_T d^3x' \; g_0(r,t-t')\; \dot{\underline{J}}(\underline{x}',t')$$
$$= -(\lambda\sigma_{n+1}\tau)^{-1}\int_T d^3x' \; \underline{M}(\underline{x}')\; H(t - r/c)\; H(\tau - (t - r/c))/(4\pi r) \qquad (2.14)$$

Since the speed of light in air is so large compared with the separation of the source and receiver, the terms involving c may be dropped to give

$$\underline{E}_0(\underline{x},t) = -(\lambda\sigma_{n+1}\tau)^{-1} H(\tau - t)\int_T d^3x' \quad \underline{M}(\underline{x}') \;/\; (4\pi r) \quad . \qquad (2.15)$$

Consequently, $\underline{E}_0$ vanishes for times later than τ. Since our aim is to analyse the signal at late times, we may discard the g_0 terms throughout the rest of the paper

If we combine formulae (2.1), (2.2) and (2.3), we obtain

$$Z(s) = -(4\pi)^{-1} sI(s) \int_0^\infty dl \; (1/k_0) \; P(l) \; \exp[-(k_0 - l)(z + z')] \; . [b/a - p] \qquad (2.16)$$

where

$$P(l) = \int_R d\underline{x} \cdot \int_T d^3x' \; J_0(l|\underline{r} - \underline{r}'|) \; \underline{M}(\underline{x}') \; \exp[-l(z + z')] \quad . (2.17)$$

We call P the loop function, because all the geometric information concerning the disposition of the loops is embodied in P. So far we have not restricted $\underline{M}$, apart from requiring $\underline{M}$ to be horizontal and divergence free, but we will now impose the 'thin wire approximation' in which we assume that $\underline{M}$ is concentrated on the axis of the transmitting loop. Thus, we now let T denote the axis of the transmitting loop, rather than its volume, and parametrise T by the curve

$$q \longmapsto \underline{x}'(q) , \qquad 0 < q < |T| ,$$

where $|T|$ is the circumference of T. Then $d\underline{x}'/dq$ is a unit vector tangential to T and

$$\underline{M} = d\underline{x}'/dq \quad . \qquad (2.18)$$

Hence,

$$P(l) = \int_R d\underline{x} \cdot \int_T dq \; J_0(l|\underline{r} - \underline{r}'|) \; \exp[-l(z + z')] \; d\underline{x}'/dq \quad . \; (2.19)$$

An alternative expression for P can be obtained by repeated

application of Stokes' theorem to formula (2.19):

$$P(l) = \int_R \int_T l^2 \; J_0(l|\underline{r} - \underline{r}'|) \exp[-l(z + z')] \quad , \qquad (2.20)$$

where the integrations are now over the areas of the loops. This form for P is generally more convenient for calculation because it involves only scalar quantities. For example, when the transmitting and receiving loops are circular, with radii a and b, and centres separated by a distance d, repeated application of the addition theorem for Bessel functions gives

$$P(l) = 4\pi^2 \, ab \, J_1(la) \, J_1(lb) \, J_0(ld). \qquad (2.21)$$

The TEM response of the layered medium is obtained from Z(s) by inverse Laplace transform,

$$Z(t) = (2\pi i)^{-1} \int_C ds \; Z(s) \exp(st) \quad , \qquad (2.22)$$

where C is a contour parallel to the imaginary s axis and which lies entirely to the right of the singularities of Z(s). Our strategy is to locate these singularities and deform the contour about them in such a way that Watson's lemma can be applied to the integral representation of Z(t).

3. SINGULARITIES OF Z(s).

We observe that sI(s) is an entire function of s, namely,

$$sI(s) = [1 - \exp(-s\tau)]/(s\tau) \quad , \qquad (3.1)$$

so we can focus upon the functions a and b which appear in the matrix A.

Each factor T which appears in the expansion of A is

an entire function of

$$k_i^2 = \varepsilon_i s^2 + \sigma_i s + l^2 \quad , \quad 1 \leqslant i \leqslant n \quad , \quad (3.\ 2)$$

and so is necessarily entire in both s and l. Consequently A is a holomorphic function of s except when

$$k_0^2 = \varepsilon_0 s^2 + l^2 \leqslant 0$$

or (3. 3)

$$k_{n+1}^2 = \varepsilon_{n+1} s^2 + \sigma_{n+1} s + l^2 \leqslant 0 \ .$$

A short analysis shows that, for any fixed l, A is holomorphic in the variable s throughout the plane cut as shown in figure 3.

FIGURE 3.

Note that the endpoints shown for the cut on the real axis are only correct asymptotically as $\varepsilon_{n+1} \longrightarrow 0$.

Let us compute the discontinuity of b/a across the cut on the real axis. To do so we establish the convention that the value of k_i on its associated cut is taken to be its boundary value from above. Let

$$s = u + iv \quad ,$$

and define for u on the cut

$$D(u) = (2\pi i)^{-1} \lim_{v \to 0+} [(b/a - p)(u - iv) - (b/a - p)(u + iv)] \quad . \quad (3.\ 4)$$

Since the sign of k_{n+1} reverses when s crosses the cut, and since

$$b(-k_{n+1}) = d(k_{n+1}) \quad ,$$

$$a(-k_{n+1}) = c(k_{n+1}) \quad , \quad (3.\ 5)$$

we find that

$$D(u) = (2\pi i)^{-1} \lim_{v \to 0+} [d/c - b/a](u + iv) \quad (3.\ 6)$$

$$= (2\pi i)^{-1} \lim_{v \to 0+} [(ad - bc)/(ac)](u + iv) \quad . \quad (3.\ 7)$$

Now

$$ad - bc = \det A = k_{n+1}/k_0 \quad , \quad (3.\ 8)$$

so

$$D(u) = k_{n+1}/(2\pi i k_0 ac) \quad , \qquad (3.9)$$

where the limit sign has been omitted on the understanding that all quantities are defined on the cut by their boundary values from above.

The analytic structure of A simplifies if we now introduce the quasi-static approximation which sets

$$\varepsilon_i = 0 \quad , \qquad i = 0, 1, \ldots, n+1. \qquad (3.10)$$

The cuts parallel to the imaginary axis recede to infinity, as does the left hand endpoint of the cut on the real axis. Thus, for fixed l, A is holomorphic in the whole s plane, with the exception of a cut along the real axis from $-\infty$ to $-l^2$. The discontinuity of b/a across this cut is

$$D(u) = (l^2 + u)^{1/2}/(2\pi i\, l\, ac) \qquad (3.11)$$

since

$$k_0 = l \qquad (3.12)$$

and

$$k_{n+1} = (l^2 + u)^{1/2} \qquad (3.13)$$

in the quasi-static approximation.

The quasi-static approximation is nearly always used in the analysis of geoprospecting systems because observations are made long after the wave fronts have passed the observer. Under these circumstances, the fields evolve according to a diffusion equation rather than a wave equation. We will now keep the quasi-static approximation for the rest of the paper.

In addition to the singularities of Z(s) associated with the branch cuts of k_0 and k_{n+1}, there will also be poles at the zeros of a. These zeros correspond to eigenvalues of the operator

$$L = -d^2/dz^2 + q \quad , \qquad (3.14)$$

where

$$q = \varepsilon s^2 + \sigma s \quad , \tag{3.15}$$

on the Sobolev space $W^{2,2}(\mathbb{R})$. That this should be so emerges naturally from the construction of Green's function g along the lines sketched at the beginning of section 2, but since most of the steps are fairly routine and would require us to introduce extensive notation, we will omit them here. From the positivity of the operator $-d^2/dz^2$, it is easy to show that

$$(u^2 - v^2)(f, \varepsilon f) + u(f, \sigma f) + l^2 \leqslant 0 \quad , \tag{3.16}$$

$$v[\, 2u(f, \varepsilon f) + (f, \sigma f)\,] = 0 \quad , \tag{3.17}$$

where $s = u + iv$ and f is the normalised eigenfunction corresponding to the zero of a. In the quasi - static approximation, these inequalities reduce to

$$u(f, \sigma f) + l^2 \leqslant 0 \quad , \tag{3.18}$$

$$v(f, \sigma f) = 0 \quad . \tag{3.19}$$

From (3.18) and (3.19) we conclude that the zeros of a lie on the negative real axis. Since the continuous spectrum of L is the interval $(-\infty, -l^2]$, and since L cannot have eigenvalues embedded in its continuous spectrum, it follows that the zeros of a are confined to the interval $[-l^2, 0]$. Finally, consider the special case of a resistive overburden, for which

$$\sigma(z) \leqslant 1 \quad \text{for } z \leqslant 0 \quad .$$

Then

$$(f, \sigma f) \leqslant 1$$

and so (3.18) implies that

$$u \leqslant -l^2 \quad .$$

This is a contradiction and so the function a cannot have any zeros if the overburden is resistive.

The conclusion of the analysis is that (in the quasi-static approximation) the singularities of b/a for any

fixed l consist of a square - root branch point at $-l^2$, whose associated cut lies on the segment $(-\infty, -l^2]$ of the negative real axis, together with a finite number of simple poles in the segment $[-l^2, 0]$. Consequently, the contour C for the inverse Laplace transform can be any vertical line in the right hand s plane.

4. DERIVATION OF Z(t).

The TEM response of the layered medium is

$$Z(t) = -(8\pi^2 i)^{-1} \int_C ds\, \exp(st)\, sI(s) \int_0^\infty dl\, F(l)\, [b/a - p](l,s) \quad . \quad (4.1)$$

Interchange the order of integration, and deform the contour C around the negative real axis. Then

$$Z(t) = -(8\pi^2 i)^{-1} \int_0^\infty dl\, F(l) \Big\{ \int_{-\infty}^{-l^2} ds\, \exp(st)\, sI(s) \lim_{v \to 0+} [\, [b/a - p](u - iv) - [b/a - p](u + iv)\,] + (2\pi i) \sum_{k=1}^{n(l)} \text{residue}_{s = s_k(l)} [\exp(st)\, sI(s)\, (b/a - p)] \Big\} \quad . \quad (4.2)$$

Here $s_k(l)$ denotes the k^{th} zero of a, regarded as a function of s with l as parameter. The number of such zeros also depends on l, indicated by the notation n(l), but n(l) is zero for sufficiently small l. Hence, the zeros $s_k(l)$ are strictly negative for all l and are bounded away from zero, from which it follows that the contributions of the pole terms are all exponentially damped in time. Since we are interested in late times, we discard these

terms and obtain

$$Z(t) = -(4\pi)^{-1} \int_0^{\infty} dl\, P(l) \int_{-\infty}^{-l^2} ds\, \exp(st)\, sI(s)\, D(s) \qquad (4.3)$$

Reverse the order of integration again and substitute

$$s = -x^2 \quad \text{and} \quad l = mx \,. \qquad (4.4)$$

Then

$$Z(t) = [B_1(t) - B_1(t-\tau)]/\tau \,, \qquad (4.5)$$

where

$$B_l(t) = \pi^{-2} \int_0^{\infty} dx\, \exp(-x^2 t)\, x^{2(l-1)}\, S(x) \,, \qquad (4.6)$$

$$S(x) = x^2 \int_0^{1} dm\, (1-m^2)^{1/2}\, m\, P(mx)/Q(m,x) \,, \qquad (4.7)$$

and

$$Q(m,x) = 4\, l^2 ac. \qquad (4.8)$$

In the limit as $\tau \longrightarrow 0$, we find

$$Z(t) = -B_2(t). \qquad (4.9)$$

5. ASYMPTOTIC ANALYSIS OF $B_l(t)$.

We now apply Watson's lemma (Copson [4]) to (4.6) to obtain an asymptotic expansion for $B_l(t)$ at late times. We develop S as a convergent power series for small x,

$$S(x) = x^2 \sum_{r=0}^{\infty} S_r\, x^r \,, \qquad (5.1)$$

substitute this into (4.6) and integrate termwise to obtain

$$B_i(t) \sim A_i(t) = (2\pi^2)^{-1} \sum_{r=0}^{\infty} S_r \Gamma((r+1)/2 + i)\, t^{-((r+1)/2+i)} \quad (5.2)$$

In this section we will develop two expressions for the Taylor coefficients S_r, the first of which will be a convenient tool for the analysis but unsuited to numerical computation, whereas the second will have the opposite properties.

The first step is to develop Q in power series for small x, which we achieve by expanding the factors in the matrix A in series and then multiplying the series together. Next we develop P in series and compute the ratio P/Q. Finally we integrate over m.

The matrix T has the series representation

$$T_r = \sum_{i_r=0}^{\infty} \frac{(k_r d_r)^{2i_r}}{(2i_r)!} T_r^{i_r} \quad , \quad (5.3)$$

where

$$T_r^{i_r} = \begin{pmatrix} 1 & 2i_r/d_r \\ d_r/(2i_r+1) & 1 \end{pmatrix} . \quad (5.4)$$

If we let $X = T_n T_{n-1} \ldots T_1$, then

$$X = \sum_{r=0}^{\infty} X_r x^{2r} \quad , \quad (5.5)$$

where

$$X_r = \sum_{|i|=r} (m^2 - \sigma_1)^{i_1} \ldots (m^2 - \sigma_n)^{i_n} X_r^i \quad , \quad (5.6)$$

$$X_r^i = \frac{d_1^{2i_1} \ldots d_n^{2i_n}}{(2i_1)! \ldots (2i_n)!} T_n^{i_n} \ldots T_1^{i_1} \quad , \quad (5.7)$$

and

$$i = (i_1, \ldots, i_n) \quad ,$$

$$|i| = i_1 + \ldots + i_n \quad . \quad (5.8)$$

Let

$$X = \begin{pmatrix} \alpha & \beta \\ \gamma & \delta \end{pmatrix} \quad , \qquad X_r = \begin{pmatrix} \alpha_r & \beta_r \\ \gamma_r & \delta_r \end{pmatrix} \quad . \tag{5. 9}$$

A short calculation yields that

$$Q = (\alpha 1 + \beta)^2 + x^2(1 - m^2)\,(\gamma 1 + \delta)^2 \quad , \tag{5.10}$$

so we obtain the series for Q by further multiplication.

$$\begin{aligned} (\alpha 1 + \beta) &= m \sum_{r=0}^{\infty} \alpha_r x^{2r+1} + \sum_{r=0}^{\infty} \beta_r x^{2r} = \sum_{r=0}^{\infty} \mu_r x^{r+1} \\ (\gamma 1 + \delta) &= m \sum_{r=0}^{\infty} \gamma_r x^{2r+1} + \sum_{r=0}^{\infty} \delta_r x^{2r} = \sum_{r=0}^{\infty} \nu_r x^{r} \end{aligned} \tag{5.11}$$

where

$$\begin{aligned} \mu_{2r} &= m\,\alpha_r & \qquad \nu_{2r+1} &= m\,\gamma_r \\ \mu_{2r-1} &= \beta_r & \qquad \nu_{2r} &= \delta_r \quad . \end{aligned} \tag{5.12}$$

Hence,

$$Q(m,x) = x^2 \sum_{r=0}^{\infty} Q_r x^r \quad , \tag{5.13}$$

where

$$Q_r = \sum_{p+q=r} [\mu_p \mu_q + (1 - m^2)\nu_p \nu_q] \quad . \tag{5.14}$$

Note that $Q_0 = 1$ and hence is independent of m. Since X_r is a polynomial in m of degree 2r, it follows trivially that

$$\text{degree}(\mu_{2r}) = 2r + 1 \quad , \quad \text{degree}(\nu_{2r}) = 2r \quad ,$$

$$\text{degree}(\mu_{2r-1}) = 2r \quad , \quad \text{degree}(\nu_{2r+1}) = 2r + 1 \quad ,$$

and hence that the degree of Q_r does not exceed r + 2. In fact,

$$\text{degree}(Q_r) = r \quad . \tag{5.15}$$

To prove this, firstly observe that α_r, β_r, γ_r and δ_r are polynomials in m^2, and then establish by induction on r that Q_{2r}

and $m^{-1} Q_{2r+1}$ must also be polynomials in m^2. Thus, Q_r will have degree r if the coefficient of m^{r+2} is zero. But this coefficient is independent of $\sigma_1, \ldots, \sigma_n$, so we set

$$\sigma_1 = \sigma_2 = \ldots = \sigma_n = 1$$

and find that

$$Q(m,x) = x^2 ,$$

which clearly demonstrates that the coefficient of m^{r+2} is always zero if $r > 0$.

It is quite apparent that formulae (5.6) and (5.7) are unsuited to numerical computation, because the number of terms in the summation for X_r becomes extremely large for more than two layers and the cost of computing the partitions of r and the matrix products is excessive. Fortunately, it is not difficult to prove by induction that

$$X = \sum_{\varepsilon_2,\cdots,\varepsilon_n} C_\varepsilon \begin{pmatrix} \cosh B_\varepsilon & k_1^{-1} \sinh B_\varepsilon \\ (\varepsilon_n k_n)^{-1} \sinh B_\varepsilon & k_1 (\varepsilon_n k_n)^{-1} \cosh B_\varepsilon \end{pmatrix} \quad (5.16)$$

where

$$B_\varepsilon = k_1 d_1 + \varepsilon_2 k_2 d_2 + \ldots + \varepsilon_n k_n d_n ,$$

$$C_\varepsilon = 2^{1-n} (1 + \varepsilon_2 k_2/k_1)(1 + \varepsilon_3 k_3/\varepsilon_2 k_2) \ldots (1 + \varepsilon_n k_n/\varepsilon_{n-1} k_{n-1}) \quad (5.17)$$

The summation is over the signs $\varepsilon_i = \pm$, so the number of terms in the summation is 2^{n-1}.

The ratios k_{i+1}/k_i which appear in C_ε are independent of x, so it is only necessary to expand the hyperbolic functions in order to obtain the series development of X. A short calculation gives

$$X = \sum_{r=0}^{\infty} x^{2r} \sum_{\varepsilon} X_r^{(\varepsilon)} , \quad (5.18)$$

where

$$X_r^{(\varepsilon)} = \frac{C_\varepsilon K_\varepsilon^{2r}}{(2r)!} \begin{pmatrix} 1 & 2rp_1/K_\varepsilon \\ K_\varepsilon/(\varepsilon_n p_n(2r+1)) & p_1/(\varepsilon_n p_n) \end{pmatrix} \tag{5.19}$$

and

$$p_i = (m^2 - \sigma_i)^{1/2} , \tag{5.20}$$

$$K_\varepsilon = p_1 d_1 + \varepsilon_2 p_2 d_2 + \ldots + \varepsilon_n p_n d_n . \tag{5.21}$$

Note that the earlier expression for X_r indicated that its elements were polynomials in m, but the present formula does not even show clearly that the elements are real! Nonetheless, formula (5.18) is well suited for computation for the following reason. Let

$$X_r^{(\varepsilon)} = \begin{pmatrix} \alpha_r^{(\varepsilon)} & \beta_r^{(\varepsilon)} \\ \gamma_r^{(\varepsilon)} & \delta_r^{(\varepsilon)} \end{pmatrix} \tag{5.22}$$

and define

$$\mu_{2r}^{(\varepsilon)} = m\,\alpha_r^{(\varepsilon)} , \qquad \nu_{2r+1}^{(\varepsilon)} = m\,\gamma_r^{(\varepsilon)} ,$$

$$\mu_{2r-1}^{(\varepsilon)} = \beta_r^{(\varepsilon)} , \qquad \nu_{2r}^{(\varepsilon)} = \delta_r^{(\varepsilon)} , \tag{5.23}$$

so that

$$\mu_r = \sum_\varepsilon \mu_r^{(\varepsilon)} , \qquad \nu_r = \sum_\varepsilon \nu_r^{(\varepsilon)} . \tag{5.24}$$

Then $\mu_r^{(\varepsilon)}$ and $\nu_r^{(\varepsilon)}$ satisfy the following recursion formula,

$$\mu_{r+2}^{(\varepsilon)} = \mu_r^{(\varepsilon)} K_\varepsilon^2/[(r+1)(r+2)] ,$$

$$\nu_{r+2}^{(\varepsilon)} = \nu_r^{(\varepsilon)} K_\varepsilon^2/[(r+1)(r+2)] , \tag{5.25}$$

with the initial values

$$\mu_0^{(\varepsilon)} = m\,C_\varepsilon , \qquad \nu_0^{(\varepsilon)} = C_\varepsilon\, p_1/(\varepsilon_n p_n) ,$$

$$\mu_1^{(\varepsilon)} = p_1 C_\varepsilon K_\varepsilon , \qquad \nu_1^{(\varepsilon)} = C_\varepsilon K_\varepsilon\, m/(\varepsilon_n p_n) . \tag{5.26}$$

This recursion formula is easy to program and fast in execution.

The loop function is also an entire function and from

the representation (2.20) it is clear that it has a series development of the form

$$P(mx) = m^2x^2 \sum_{r=0}^{\infty} P_r (mx)^r \quad . \tag{5.27}$$

Expressions for the coefficients P_r are given for coincident circular loops and arbitrary rectangular loops in appendix 1.

Both P and Q have a zero of the second order at x = 0, so provided that x is less than the modulus of the closest non-zero zero of Q, the series for P and Q can be manipulated as follows. Let

$$F = P/Q \tag{5.28}$$

$$= m^2 \sum_{r=0}^{\infty} F_r x^r \quad , \tag{5.29}$$

where

$$F_0 = P_0 \tag{5.30}$$

and

$$F_r = m^r P_r - \sum_{p=1}^{r} Q_p F_{r-p} \quad , \; r > 0 \quad . \tag{5.31}$$

It is easy to prove by induction on r that F_r is a polynomial in m, that

$$\text{degree}(F_r) \leqslant r \quad , \tag{5.32}$$

and that F_{2r} and $m^{-1} F_{2r+1}$ are polynomials in m^2.

Within the region of convergence of the series (5.29), we may integrate termwise over m to obtain

$$S(x) = x^2 \sum_{r=0}^{\infty} S_r x^r \quad , \tag{5.33}$$

where

$$S_r = \int_0^1 dm \; (1 - m^2)^{1/2} m^3 F_r(m) \quad . \tag{5.34}$$

To evaluate S_r two options are open.

(1) For odd orders, F_{2r+1} has the form

$$F_{2r+1} = m \cdot \text{polynomial in } m^2 .$$

Hence,

$$S_{2r+1} = 2 \int_{-1}^{+1} dm \, (1 - m^2)^{1/2} \, m^3 \, F_{2r+1}(m) \quad . \qquad (5.35)$$

These integrals can be evaluated exactly by Gaussian quadrature with weight $(1 - m^2)^{1/2}$, interval $[-1,+1]$, and Chebyshev polynomials of the second kind. (Stroud and Secrest [20].) To evaluate the even orders, let

$$w = m^2$$

and obtain

$$S_{2r} = 2^{-1} \int_{0}^{1} dw \, (1 - w)^{1/2} w \, F_{2r}(w^{1/2}) \quad . \qquad (5.36)$$

Recall that $F_{2r}(w^{1/2})$ will be a polynomial in w. Thus, S_{2r} may be evaluated exactly by Gaussian quadrature with weight $(1 - w)^{1/2}$, interval $[0,1]$ and Jacobi polynomials. (Krylov, Lugin and Yanovich [11].)

(2) Alternatively, quadrature rules may be developed for the interval $[0,1]$ with weight $(1 - m^2)^{1/2} m^3$, so that both the odd and even order S_r may be evaluated exactly with the same quadrature rule. This approach leads to a simpler program and is the one we have followed. We computed Gaussian rules with from one to twenty points. In order to compute S_r exactly for

$$0 \leqslant r \leqslant N = 2M - 1 \quad ,$$

we chose the rule with M points:

$$S_r = \sum_{i=1}^{M} w_i \, F_r(m_i) \quad ,$$

where w_i and m_i are the computed weights and nodes. In appendix 2 are tabulated the weights and nodes for the 8 point rule, sufficient to give the first 16 terms of the asymptotic expansion.

The algorithm for computing the coefficients S_r is summarised in the flow chart below.

Compute P_0, P_1, ... P_N for the loop configuration.

Set $S_r = 0$, $r = 0, 1, \ldots, N$.

Set m_i to the first quadrature node.

Label 1: Set $\mu_r = 0$ and $\nu_r = 0$.

Set $\varepsilon_2 = +$, $\varepsilon_3 = +$, ... , $\varepsilon_n = +$.

Label 2: Compute B_ε and C_ε.

Compute $\mu_0^{(\varepsilon)}$, $\mu_1^{(\varepsilon)}$ and $\nu_0^{(\varepsilon)}$, $\nu_1^{(\varepsilon)}$.

Compute $\mu_r^{(\varepsilon)}$ and $\nu_r^{(\varepsilon)}$ by recursion.

Increment μ_r and ν_r. $\mu_r := \mu_r + \mu_r^{(\varepsilon)}$, $\nu_r := \nu_r + \nu_r^{(\varepsilon)}$.

If not finshed all sign combinations, go to 2.

Compute Q_0, Q_1, ... , Q_N from μ_r and ν_r.

Compute F_0, F_1, ... , F_N recursively from P_r and Q_r.

Increment S_r. $S_r := S_r + w_i F_r(m_i)$.

If not finished all quadrature points, go to 1.

Stop.

6. THIN LAYER APPROXIMATIONS.

At this point we can establish the relation between our asymptotic expansion and the expansion to two terms obtained by Lee [13]. To do so, let

$$Q^{(K)} = x^2 \sum_{r=0}^{k} Q_r \, x^r \quad , \tag{6. 1}$$

and call $Q^{(k)}$ the k^{th} thin layer approximation to Q. Since X_r contains a factor $d_1^{2i_1} \ldots d_n^{2i_n}$, it is clear that the terms in the expansion of X (and hence of Q) will become very small if the layers are thin, so it is reasonable to truncate the series as in (6.1) above. Explicit calculation yields

$$\begin{aligned} Q_0 &= 1 \\ Q_1 &= 2md\theta_1 \\ Q_2 &= d^2[(\theta_1 + \theta_2)(2m^2 - 1) + \theta_1^2] \end{aligned} \tag{6. 2}$$

where θ_1 and θ_2 are given by (1.14).

If the series for Q is truncated at the first term, then the recurrence formula (5.31) degenerates to

$$F_r = m^r P_r \tag{6. 3}$$

from which we obtain

$$S_r = c_r P_r \quad , \tag{6. 4}$$

where

$$c_r = \int_0^1 dm \, (1 - m^2)^{1/2} \, m^{3+r} \quad ,$$

$$= \frac{\Gamma(3/2) \, \Gamma((r + 4)/2)}{2 \, \Gamma((r + 7)/2)} \quad . \tag{6. 5}$$

Thus,

$$A_i(t) = (2\pi^2)^{-1} \sum_{r=0}^{\infty} c_r P_r \Gamma((r+1)/2+i)\, t^{-((r+1)/2+i)} \quad . \qquad (6.6)$$

This is the response of a uniform half space with the conductivity of the basement, as expected because all information concerning the layers was contained in the terms dropped from Q.

The first order thin layer approximation gives

$$Q^{(1)} = x^2 [1 + 2mxd\theta_1] \quad . \qquad (6.7)$$

Note that $Q^{(1)}$ can vanish if $\theta_1 < 0$, corresponding to a conductive overburden, so the thin layer approximation has introduced a spurious zero on the x axis. The recurrence relation for F_r can again be solved explicitly, because equation (5.31) reduces to

$$\begin{aligned} F_0 &= P_0 \\ F_r &= m^r P_r - Q_1 F_{r-1} \quad , \end{aligned} \qquad (6.8)$$

which has the solution

$$\begin{aligned} F_r &= \sum_{p=0}^{r} (-Q_1)^p m^{r-p} P_{r-p} \quad , \\ &= m^r L_r \quad , \end{aligned} \qquad (6.9)$$

where

$$L_r = \sum_{p=0}^{r} (-2d\theta_1)^p P_{r-p} \quad . \qquad (6.10)$$

Thus,

$$S_r = c_r L_r$$

and

$$A_i(t) = (2\pi^2)^{-1} \sum_{r=0}^{\infty} c_r L_r \Gamma((r+1)/2+i)\, t^{-((r+1)/2+i)} \quad . \qquad (6.11)$$

Lee [13] obtained the first two terms of this asymptotic expansion for the case of coincident circular transmitting and receiving loops.

7. ERROR ESTIMATES.

If the function Q never vanished for non-zero x, then the series for S would converge for all x and the asymptotic expansion would be a convergent series. This happens only for the case of a uniform half-space, for which

$$Q = x^2 ,$$

so in principle the transient response of the half space could be calculated with arbitrary accuracy by summing sufficiently many terms of the series. (In practice, however, the series is so slowly convergent at early times that the finite word length of the computer causes large cancellation errors when many terms of the series are summed.) In all other cases, Q is an entire function of order 1/2, and so has an infinite number of isolated zeros. The proximity of these zeros to the origin limits the radius of convergence of the series for S, and hence reduces the range of times for which the asymptotic series is useful. For low conductivity contrasts or thin layers, the zeros of Q are well away from the origin, and the asymptotic series 'converges' well, but, for larger conductivities and thicker layers, the zeros of Q crowd in around the origin and the 'convergence' of the asymptotic series is poor.

To make these intuitive ideas precise, we will develop an estimate for the error in chopping the asymptotic series at N terms. The estimate will be in terms of the quantity

$$\xi = \inf_{0 \leq m \leq 1} \xi(m) ,$$

where (7. 1)

$$\xi(m) = \inf_{k \geq 1} |x_k(m)| ,$$

and

$$0 = x_0(m) , x_1(m) , x_2(m) , \ldots$$

are the distinct zeros of Q, regarded as a function of x with parameter m. Clearly ξ is the closest approach to the origin of all the zeros of Q as m is allowed to vary over the range [0,1]. In principle ξ is computable, because Q is an elementary combination of hyperbolic functions and its zeros can be found by a number of well established algorithms. However, the cost of such a search is not justified, firstly because the pragmatic algorithm works well, and secondly because we can approximate ξ by the quantity $\xi^{(k)}$, defined analogously as the closest approach to the origin of the zeros of $Q^{(k)}$. It is easy to see that

$$1/\xi^{(1)} = 2d|\theta_1| \quad , \qquad (7.2)$$

and a rather lengthy, but straightforward, calculation yields

$$1/\xi^{(2)} = \begin{cases} d|\theta_1|(1 + |\chi|^{1/2}) & , \quad \chi \leq 0 \\ d|\theta_1|(1 + \chi)^{1/2} & , \quad \chi \geq 0 \end{cases} \quad . \qquad (7.3)$$

This is the approximation quoted in the introduction. Higher order approximations could be computed numerically, but again the cost is unwarranted. To illustrate this, the figures below compare $\xi^{(1)}$, $\xi^{(2)}$ and ξ in the case of a single conductive layer over a basement, for which ξ can be computed exactly:

$$\xi = \log[(\sigma_1^{1/2} + 1) / (\sigma_1^{1/2} - 1)] / (2\sigma_1^{1/2} d_1) \quad . \qquad (7.4)$$

	$\sigma_1 = 10,\ d_1 = 0.1$	$\sigma_1 = 1000,\ d_1 = 1$
$\xi^{(1)}$	0.556	0.500×10^{-3}
$\xi^{(2)}$	0.833	1.000×10^{-3}
ξ	1.035	1.000×10^{-3}

These figures also illustrate the general rule that the zeros crowd in around the origin as the product of conductivity and thickness increases.

We now turn to the derivation of the error estimate.

Let

$$F^N = m^2 \sum_{r=0}^{N} F_r \, x^r \qquad (7.5)$$

and

$$S^N = x^2 \int_0^1 dm \, (1 - m^2)^{1/2} \, m \, F^N(m) \quad . \qquad (7.6)$$

Lemma.

There exists a constant K such that for all x

$$|S(x) - S^N(x)| < K \, x^3 (x/\xi)^N / |x - \xi| \quad . \qquad (7.7)$$

Proof.

For each m, F has only simple poles, so the sequence

$$\xi(m)^r |F_r(m)| \quad , \quad r=0, 1, 2, \ldots$$

is bounded. Hence, there exists a constant C(m) such that

$$\xi(m)^r |F_r(m)| < C(m) \qquad \text{for all } r.$$

Since $\xi < \xi(m)$ for all m, it follows that

$$|F_r(m)| < C(m)/\xi^r \qquad \text{for all } r.$$

Consider $x < \xi$. Since the series for F is convergent for such x,

$$S(x) - S^N(x) = x^2 \int_0^1 dm \, (1 - m^2)^{1/2} \, m^3 \sum_{r=N+1}^{\infty} F_r(m) \, x^r \quad ,$$

and

$$|S(x) - S^N(x)| < x^2 \int_0^1 dm \, (1 - m^2)^{1/2} \, m^3 \sum_{r=N+1}^{\infty} C(m) \, (x/\xi)^r$$

$$= x^2 \, C \, (x/\xi)^{N+1} / (1 - x/\xi) \quad ,$$

where

$$C = \int_0^1 dm \, (1 - m^2)^{1/2} \, m^3 \, C(m) \quad .$$

Thus, (7.7) holds with K = C.

Now consider $x > \xi$. The series is no longer convergent, but it is certainly true that

$$|S(x) - S^N(x)| < x^2 \int_0^1 dm\ (1 - m^2)^{1/2}\ m\ |F(m,x)| +$$

$$x^2 \int_0^1 dm\ (1 - m^2)^{1/2}\ m^3 \sum_{r=0}^{N} |F_r(m)|\ x^r \quad .$$

Since $|J_0| \leqslant 1$, it follows from (2.20) that

$$|P(1)| \leqslant 1^2\,|T|\,|R| \quad ,$$

where $|T|$ and $|R|$ denote the areas of the transmitting and receiving loops. The function

$$(1 - m^2)^{1/2}\ m^3\ x^2/Q(m,x)$$

has at worst an integrable singularity in m, so there exists a constant L such that

$$\int_0^1 dm\ (1 - m^2)^{1/2}\ m\ |P(mx)/Q(m,x)| \leqslant L \quad \text{for all } x \geqslant \xi \quad .$$

Hence,

$$|S(x) - S^N(x)| < x^2 L + x^2 \int_0^1 dm\ (1 - m^2)^{1/2}\ m^3 C(m) \sum_{r=0}^{N} (x/\xi)^r$$

$$= x^2 [L + C\ (1 - (x/\xi)^{N+1})\ /\ (1 - x/\xi)] \quad .$$

Choose K so that

$$L + C\ (x/\xi)^{N+1}\ /(x/\xi - 1) < K\ (x/\xi)^{N+1}\ /(x/\xi - 1) \quad ,$$

a condition which will be satisfied provided that

$$K > C + L\ N^N/(N + 1)^{N+1} \quad .$$

Then

$$|S(x) - S^N(x)| < x^2 K\ (x/\xi)^{N+1}\ /(x/\xi - 1) \quad .$$

Again (7.7) holds and the proof is complete. ■

Define

$$B_i^N(t) = \pi^{-2} \int_0^\infty dx\ \exp(-x^2 t)\ x^{2(i-1)}\ S^N(x) \quad .$$

Choose any small positive number ε, split the integration into three ranges, $[0, \xi - \varepsilon]$, $[\xi - \varepsilon, \xi + \varepsilon]$ and $[\xi + \varepsilon, \infty)$, and use the estimate for $|S(x) - S^N(x)|$ in the first and last ranges.

$$\begin{aligned}
\pi^2 |B_i(t) - B_i^N(t)| < & \int_0^{\xi-\varepsilon} dx\ \exp(-x^2 t)\ x^{2(i-1)}\ K\ x^3 (x/\xi)^N / (\xi - x) \\
& + \int_{\xi-\varepsilon}^{\xi+\varepsilon} dx\ \exp(-x^2 t)\ x^{2(i-1)} |S(x) - S^N(x)| \\
& + \int_{\xi+\varepsilon}^{\infty} dx\ \exp(-x^2 t)\ x^{2(i-1)}\ K\ x^3 (x/\xi)^N / (x - \xi) \\
< \varepsilon^{-1} K & \int_0^\infty dx\ \exp(-x^2 t)\ x^{2i+1}\ (x/\xi)^N \\
& + \int_{\xi-\varepsilon}^{\xi+\varepsilon} dx\ \exp(-x^2 t)\ x^{2(i-1)} |S(x) - S^N(x)| \quad .
\end{aligned}$$

The first integral is trivial. Apply the mean value theorem to the second integral.

$$\begin{aligned}
\pi^2 |B_i(t) - B_i^N(t)| < & \ (2\varepsilon)^{-1} K \xi^{2(i+1)} \Gamma(N/2 + i + 1) / (\xi t^{1/2})^{N+2i+2} \\
& + 2\varepsilon\ \exp(-z^2 t)\ z^{2(i-1)} |S(z) - S^N(z)| \quad ,
\end{aligned}$$

where z is a point in the interval $[\xi - \varepsilon, \xi + \varepsilon]$. Provided that $0 < \varepsilon < \xi$ and also that ξ is not too small, then the dominant term is the first. In any case, we can always increase the constant K in order to obtain the following bound.

$$|B_i(t) - B_i^N(t)| < (2\pi^2 \varepsilon)^{-1} K \xi^{2(i+1)} \Gamma(N/2 + i + 1) / (\xi t^{1/2})^{N+2i+2} \quad .$$

This is the bound mentioned in the introduction.

8. APPENDIX 1.

We assume that both the transmitting and receiving loops lie on the surface of the ground, so that $z = z' = 0$.

Consider firstly the case of concident circular transmitting and receiving loops with radius a. Formula (2.21) for the loop function reduces to

$$P(l) = [2\pi a J_1(la)]^2 \quad . \tag{8. 1}$$

Insert the series for J_1^2 given in formula (9.1.14) of Abramowitz and Stegun [1]to obtain

$$P_{2r+1} = 0 \quad ,$$

$$P_{2r} = (2\pi a)^2 \frac{(-1)^r (a/2)^{2r+2} (2r+2)!}{r! [(r+1)!]^2 (r+2)!} \quad . \tag{8. 2}$$

The sequence of P_r is best computed by recursion, since

$$P_{2r+2} = -P_{2r} a^2 (2r+3)/[2(r+1)(r+2)(r+3)] \quad , \tag{8. 3}$$

and

$$P_0 = \pi^2 a^4 \quad . \tag{8. 4}$$

Now consider rectangular transmitting and receiving loops with sides parallel to the x and y axes. Suppose that the transmitting loop encloses the area

$$a' \leqslant x \leqslant b'$$

$$c' \leqslant y \leqslant d' \tag{8. 5}$$

and that the receiving loop encloses the area

$$a \leqslant x \leqslant b$$

$$c \leqslant y \leqslant d \quad . \tag{8. 6}$$

Insert the series for J_0 (Abramowitz and Stegun [1], formula (9.1.10)) to obtain

$$P(l) = l^2 \sum_{r=0}^{\infty} P_r \, l^r \quad , \tag{8. 7}$$

where

$$P_{2r+1} = 0 \tag{8. 8}$$

$$P_{2r} = (-1)^r V_r / [2^{2r} (r!)^2] \tag{8. 9}$$

and

$$V_r = \int_R \int_T |\underline{r} - \underline{r}'|^{2r} \qquad (8.10)$$

The integrations in (8.10) are over the areas of the loops. For the rectangular loops,

$$V_r = \int_a^b dx \int_c^d dy \int_{a'}^{b'} dx' \int_{c'}^{d'} dy' \quad [\,(x - x')^2 + (y - y')^2\,]^r . \qquad (8.11)$$

Use the binomial theorem on the power to reduce the integrand to a sum of multinomials which can then be integrated trivially. Thus,

$$V_r = \sum_{k=0}^{r} \binom{r}{k} U_k(a,b,a',b')\, U_{r-k}(c,d,c',d') \qquad (8.12)$$

where

$$U_k(a,b,a',b') = [\,(b - a')^{2k+2} - (a - a')^{2k+2} - (b - b')^{2k+2} + (a - b')^{2k+2}\,]/[(2k + 1)(2k + 2)] . \qquad (8.13)$$

Formulae (8.8), (8.12) and (8.13) give an easily computable expression for the sequence P_r.

9. APPENDIX 2.

Listed below are the points and weights for a Gaussian quadrature rule with weight $(1 - m^2)^{1/2} m^3$ on the interval (0,1).

	Points	Weights
1	0.90824874853396784 8D+00	0.27885965427471749 9D-01
2	0.97653238030076067 7D+00	0.93419146430268078 9D-02
3	0.80132260515933598 5D+00	0.37945315843912497 6D-01
4	0.66544563671505275 1D+00	0.32202010044121320 7D-01

5	0.51298670112517667 6D+00	0.18096542080283412 4D-01
6	0.35791468609859386 3D+00	0.64889592666668865 5D-02
7	0.21455094914825976 0D+00	0.12822342339086755 9D-02
8	0.96079995503882680 7D-01	0.90391793941982743 5D-04

10. REFERENCES.

[1] M. Abramowitz and I.A. Stegun, 'Handbook of mathematical functions' (Dover, New York, 1965).

[2] W.L. Anderson, 'Numerical integration of related Hankel transforms of orders 0 and 1 by adaptive digital filtering', Geophysics 44 (1979), 1287 - 1305.

[3] G. Buselli and B. O'Neill, 'SIROTEM: A new portable instrument for multichannel transient electromagnetic measurements', ASEG Bulletin 8 (1977), 82 - 87.

[4] E.T. Copson, 'Asymptotic expansions' (Cambridge University Press, Cambridge, 1971).

[5] J.D. Crone, 'Ground pulse EM - examples of survey results in the search for massive sulphides and new developments with the Crone PEM equipment', Paper presented by the author at the 25th international geological congress, Sydney, Australia, August 1976.

[6] D.P. Gaver Jr., 'Observing stochastic processes and approximate transform inversion', Operations Research 14 (1966), 444 - 459.

[7] F.M. Kamenetski, 'Transient processes using combined loops for a two layer section with a non conducting base', Izv. Vuzov. Section Geology Prosp. 6 (1969), 108 - 113.

[8] A.A. Kaufman, 'Harmonic and transient fields on the surface of a two layered medium', Geophysics 44 (1979), 1208 - 1217.

[9] J.H. Knight and A.P. Raiche, 'Transient electromagnetic calculations using the Gaver - Stehfest inverse Laplace transform method', Geophysics 47 (1982), 47 - 50.

[10] O. Koefoed, D.P. Ghosh and G.J. Polman, 'Computation of type curves for electromagnetic depth sounding with a horizontal coil by means of a digital linear filter', Geophys. Prosp. 20 (1972), 403 - 420.

[11] V.J. Krylov, V.V. Lugin and L.A. Yanovich, 'Tables for integration of functions with power singularities

$$\int_0^1 x^{\beta} (1 - x)^{\alpha} f(x)\, dx \quad .'$$

(Minsk: Izdat. Akad. Nauk BSSR, 1963).

[12] Y.L. Lamontagne, G.S. Lodha, J.C. Macnae and G.F. West, 'UTEM: Wideband time domain EM project 1976 - 78, reports 1-5', Research in applied geophysics # 11, Geophysics laboratory, Department of physics, University of Toronto, 1980.

[13] T. Lee, 'Asymptotic expansions for transient electromagnetic fields', Geophysics 47 (1982), 38 - 46.

[14] T. Lee and R. Lewis, 'Transient EM response of a large loop on a layered ground', Geophys. Prosp. 22 (1974), 430 - 444.

[15] K. Mallick and R.K. Verma, 'Time domain electromagnetic sounding with horizontal and vertical coplanar loops on a multilayered earth', Geoexploration 16 (1978), 291 - 302.

[16] H.F. Morrison, R.J. Phillips and D.P. O'Brien, 'Quantitative interpretation of transient electromagnetic fields over a layered half space', Geophys. Prosp. 17 (1968), 82 - 101.

[17] T.N.L. Patterson, 'Algorithm for automatic numerical integration over a finite interval', Commun. ACM 16 (1973), 694 - 699.

[18] H. Stehfest, 'Algorithm 368. Numerical inversion of Laplace transforms', Commun. ACM 13 (1970), 47 - 49.

[19] H. Stehfest, 'Remark on algorithm 368', Commun. ACM 13 (1970), 624.

[20] A.H. Stroud and D. Secrest, 'Gaussian quadrature formulas' (Prentice-Hall, Englewood Cliffs, N.J., 1966).

[21] J.R. Wait, 'Geoelectromagnetism' (Academic Press, New York, 1982).

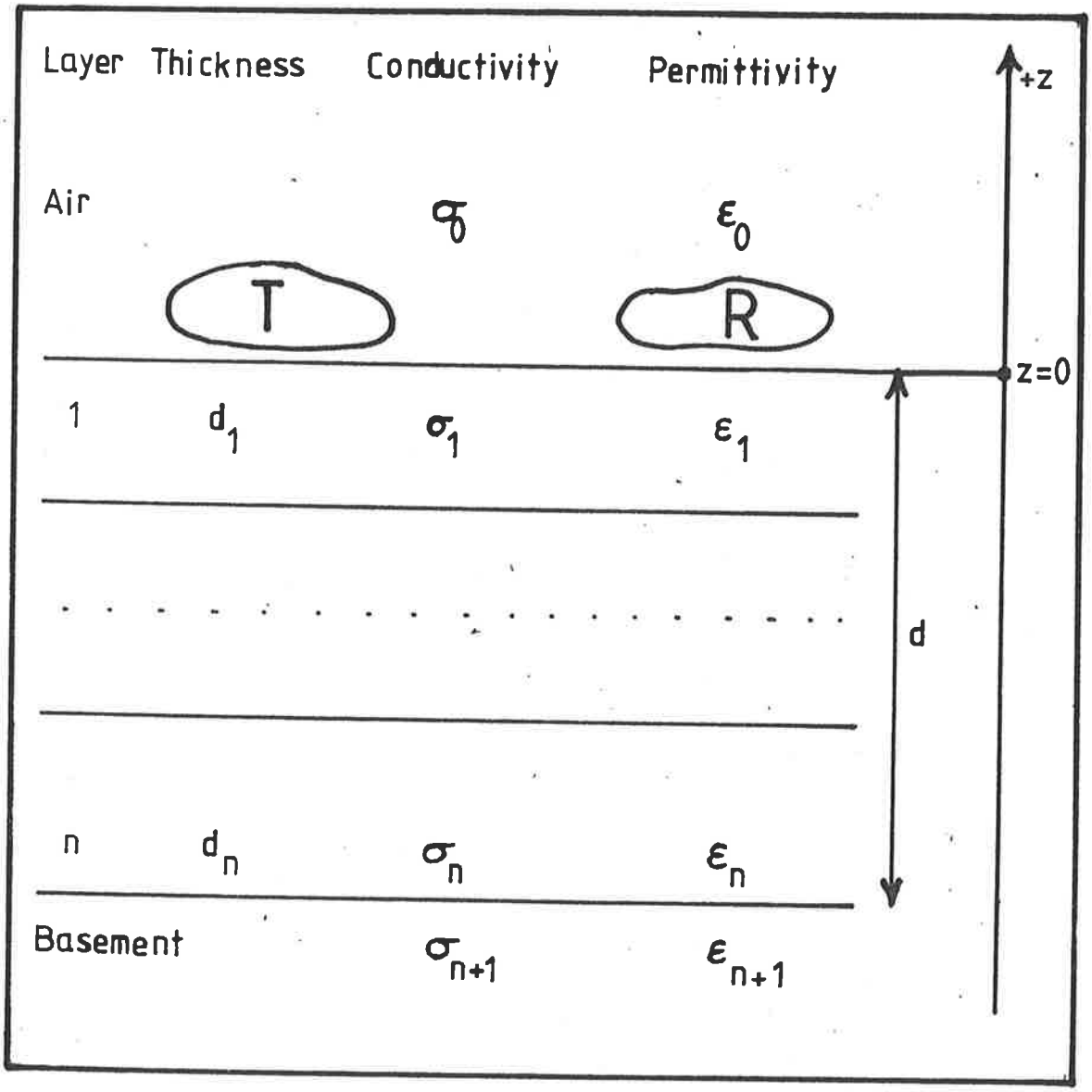
Layer
Thickness
Conductivity
Permittivity
+z
Air
σ_0
ε_0
T
R
z=0
1
d_1
σ_1
ε_1
d
n
d_n
σ_n
ε_n
Basement
σ_{n+1}
ε_{n+1}

Figure 1.

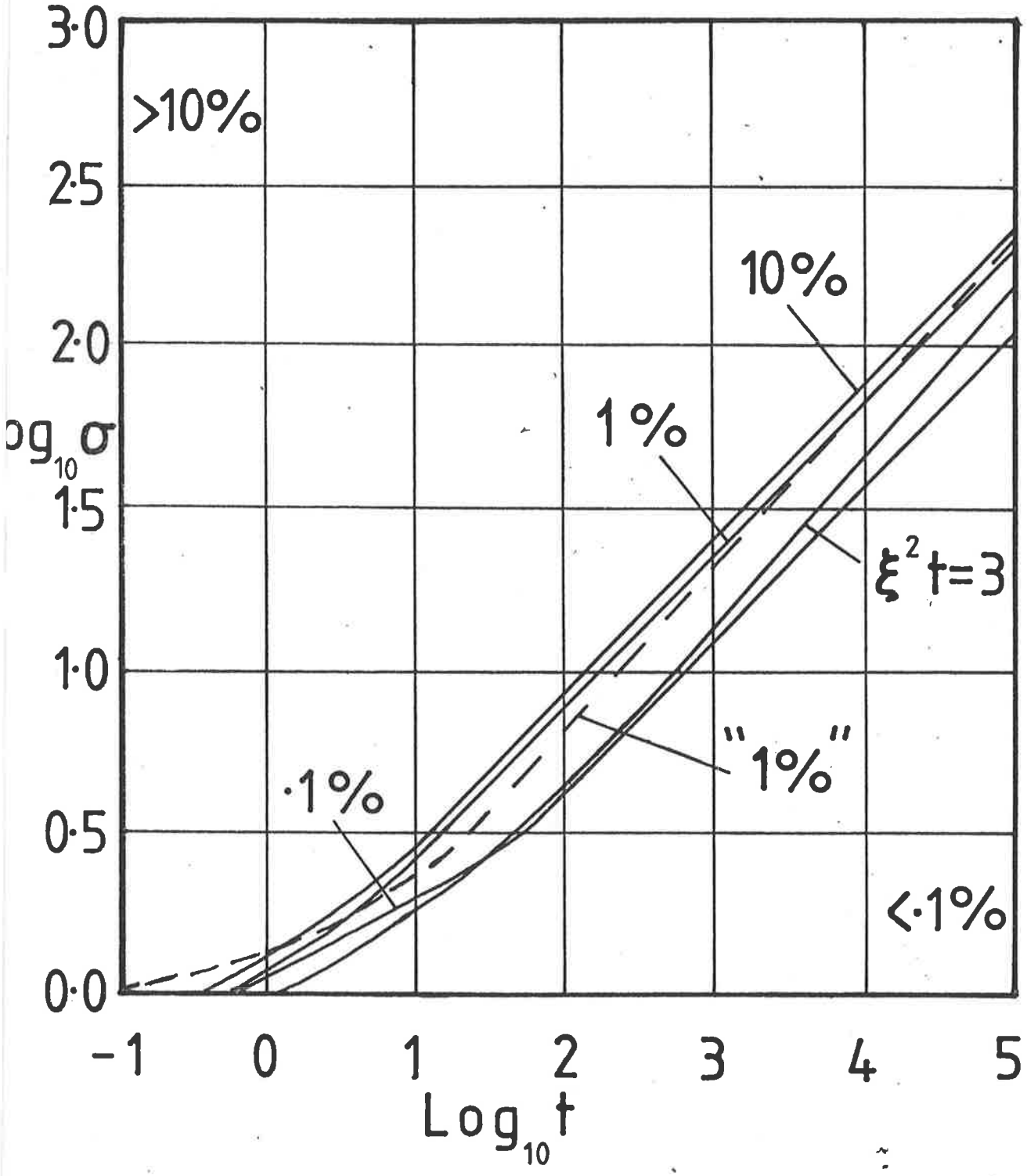

Figure 2.

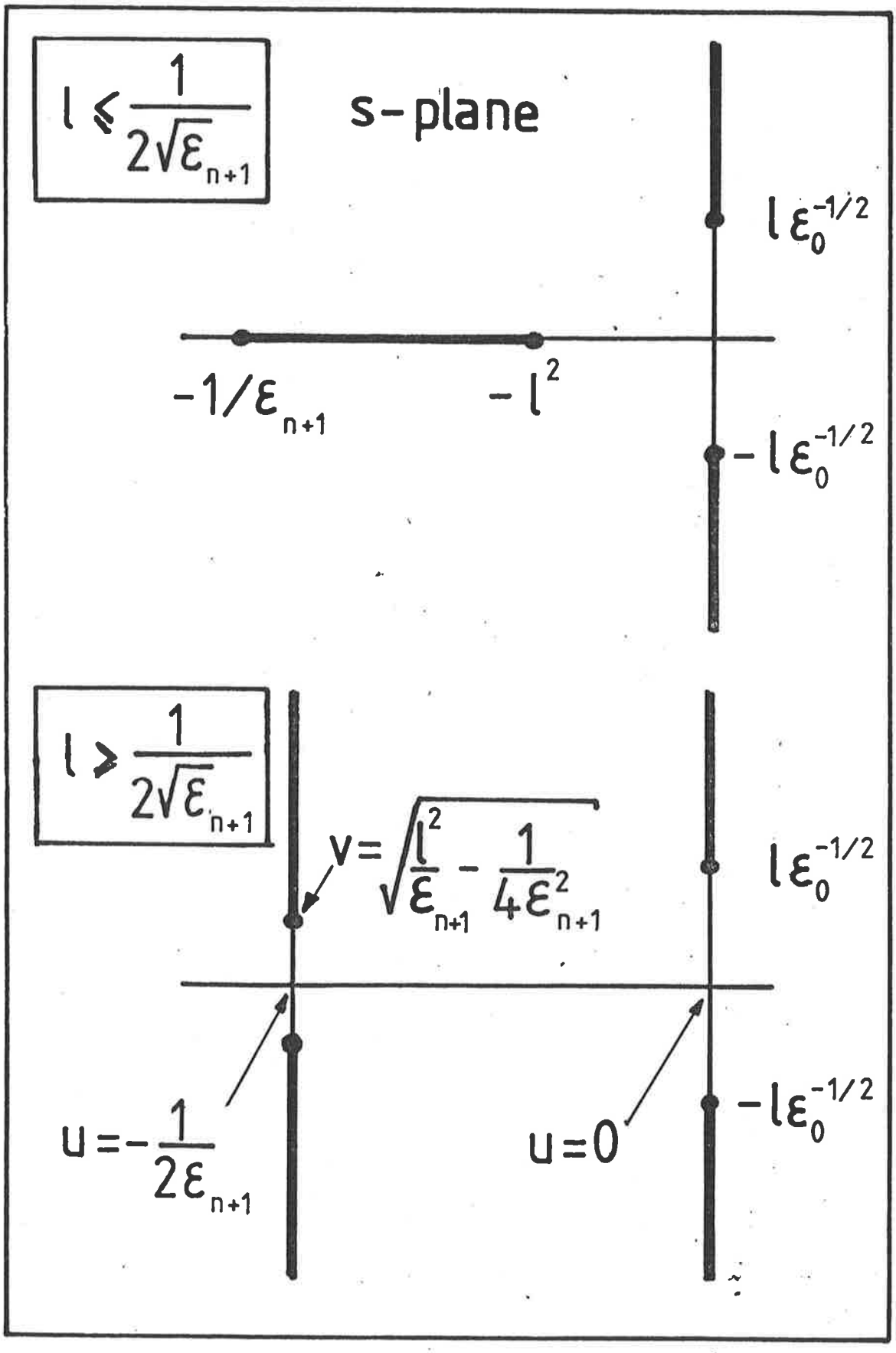
$l \leqslant \frac{1}{2\sqrt{\varepsilon_{n+1}}}$
s-plane
$l\,\varepsilon_0^{-1/2}$
$-1/\varepsilon_{n+1}$
$-l^2$
$-l\,\varepsilon_0^{-1/2}$
$l > \frac{1}{2\sqrt{\varepsilon_{n+1}}}$
$v = \sqrt{\frac{l^2}{\varepsilon_{n+1}} - \frac{1}{4\varepsilon_{n+1}^2}}$
$l\,\varepsilon_0^{-1/2}$
$u = -\frac{1}{2\varepsilon_{n+1}}$
$u = 0$
$-l\,\varepsilon_0^{-1/2}$

Figure 3.

transform and the fast Fourier algorithm for the inverse Fourier transform. After the development of digital filters for the Hankel transform of arbitrary order ν, several new programs were written which used digital filters for the Hankel transform and possibly also for the Fourier transform, since the latter can be formulated as a Hankel transform with order $\nu = \frac{1}{2}$. These programs were considerably more efficient. (Koefoed [10], Mallick and Verma [15], Anderson [2].) Knight and Raiche [9] made a further significant improvement in efficiency by reversing the order of the inverse integral transforms, and applied the Gaver-Stehfest [6, 19, 20] algorithm to the inverse Laplace transform followed byan adaptive version of Patterson's [17] algorithm for Gaussian quadrature to evaluate the Hankel transform. The success of Knight and Raiche's strategy is due to the gain in speed and accuracy of the Gaver-Stehfest algorithm when applied to functions known analytically rather than numerically. After publication of their paper, Knight and Raiche replaced Patterson's integration with a digital filter, and their modified algorithm is currently the best available.

Complementary to these computer programs, which attempt to invert the integral transforms numerically, is the work on asymptotic expansions of the TEM response at both early and late times. Lee and Lewis [14] established that at early or late times the TEM response approaches that of a half space whose conductivity is equal to that of the top layer or the bottom layer, respectively. Lee [13] also developed a two term asymptotic expansion valid for late times, which subsumed earlier results by Kamenetski [7] and Kaufman [8]. In addition to their simplicity and speed, the asymptotic expansions often have the useful property that they work best when the more general computer programs are most costly. For example, Knight and Raiche's algorithm seems to be slowest at late times, precisely when Lee's asymptotic formula is applicable.

If the object were to compute the TEM response of a single layered medium, then many of the refinements above would not be necessary, because even the most basic algorithm will obtain the TEM response for relatively little cost. However, in practice we want to infer the structure of a layered ground from observations of its TEM response, and to do so we employ an optimisation algorithm which adjusts the model in order to minimise a cost function which measures the discrepancy between the actual data and the data predicted by the model. The optimisation algorithm will be iterative and will proceed from an initial guess for the model to a final 'solution', which is a local minimiser of the cost function. The 'solution' is dependent upon the initial guess, so, in addition to all the iterations of the optimisation algorithm, it is essential to experiment with different initial guesses. If all this calculation is to be performed in real time, so that a geophysicist can immediately interpret his survey data, then the computer code which calculates the TEM response of the layered ground must employ every known time saving device.

With this motivation, we now turn to the content of this paper.

We develop a late time asymptotic expansion for the TEM response of the layered conducting ground depicted in Figure 1, and we establish the region of usefulness of the expansion. The terms of the expansion are easily computed and can be programmed on almost any microcomputer. The expansion may be used on its own for a very rapid first interpretation of field data, or may be coupled with existing software such as the TEM program of Knight and Raiche [9], to produce faster inversion programs.

The transmitting and receiving loops must be horizontal, but otherwise their shapes and positions are arbitrary, although in practice we will require the loops to be either circular or rectangular. In particular, the loops may be either coincident or distinct. We assume that the transmitting loop carries a current density

$$\mathbf{J}(\mathbf{x}, t) = \mathbf{M}(\mathbf{x}) I(t), \tag{1.1}$$

where $\mathbf{M}$ is horizontal, divergence free and has compact support, and I is the ramp function

$$I(t) = \begin{cases} 0 & \text{if } t < 0 \\ t/\tau & \text{if } 0 \leqslant t \leqslant \tau \\ 1 & \text{if } \tau < t. \end{cases} \tag{1.2}$$

Such a temporal variation models the UTEM prospecting system (Lamontagne, Lodha, Macnae and West [12]), the PEM prospecting system (Crone [5]), and also models SIROTEM (Buselli and O'Neill [3]) in the limit $\tau \to 0$.

It is worth noting that the extension of the analysis to receiving loops which are not horizontal is straightforward, and only requires the introduction of a new loop function. However, the extension to transmitters other than horizontal loops requires more substantial changes. For such sources two complications arise: firstly, the electric field intensity has a nonzero vertical component which is discontinuous across the interfaces between the layers; and secondly, a tensor rather than scalar Green's function is needed. Nevertheless, the analysis is the same in principle, although more cumbersome in practice.

We will work exclusively with variables scaled as follows:

coordinates	$\mathbf{x} \to \mathbf{x}/l$	(dimensionless);
conductivity	$\sigma \to \sigma/\sigma_{n+1}$	(dimensionless);
time	$t \to t/(l^2\mu\sigma_{n+1})$	(dimensionless);
permittivity	$\varepsilon \to \varepsilon/(l^2\mu\sigma_{n+1}^2)$	(dimensionless);
electric field	$\mathbf{E} \to \mathbf{E}l$	(volts/unit scaled length);
current density	$\mathbf{J} \to \mathbf{J}l^2$	(amps./unit scaled area).

Here l denotes any typical length chosen as the unit of length, such as the radius or side length of the transmitting loop. We will compute the dimensionless quantity

$$Z(t) = l\sigma_{n+1}V/I_p, \tag{1.3}$$

where V is the e.m.f. induced in the receiving loop, measured in volts, and I_p is the peak value of the current in the transmitting loop, measured in amps. $Z(t)$ is clearly related to the mutual impedance of the transmitting and receiving loops over the layered medium.

The key to the asymptotic analysis of the TEM response lies in the treatment of the inverse Laplace transform. We examine the singularities of the function to be transformed and show that the contour of integration maybe deformed around a cut along the negative real axis. Then $Z(t)$ has the asymptotic form

$$Z(t) \sim [B_1(t) - B_1(t-\tau)]/\tau, \tag{1.4}$$

where

$$B_i(t) = \pi^{-2}\int_0^\infty dx \exp(-x^2 t)x^{2(i-1)}S(x), \tag{1.5}$$

and

$$S(x) = x^2\int_0^1 dm(1-m^2)^{1/2}mP(mx)/Q(m,x). \tag{1.6}$$

Here P is a function which we call the loop function, because it depends solely on the disposition of the loops and not on the structure of the layered medium, whereas the function Q has the opposite dependence. Watson's lemma (Copson [4]) can be applied to $B_i(t)$ and we obtain the asymptotic expansion

$$B_i(t) \sim A_i(t) = (2\pi^2)^{-1}\sum_{r=0}^{\infty} S_r\Gamma((r+1)/2+i)t^{-((r+1)/2+i)}, \tag{1.7}$$

where $S_0, S_1, \ldots$ are the coefficients in a power series for S convergent for small x:

$$S(x) = x^2\sum_{r=0}^{\infty} S_r x^r. \tag{1.8}$$

The coefficients $S_0, S_1, \ldots$ depend upon both the geometry of the loops and the structure of the medium, but are independent of time. Consequently, the coefficients only need be computed once if the mutual impedance is required at several times. If the time variation of the source current is a step rather than a ramp, then the appropriate asymptotic expansion is obtained in the limit as $\tau \to 0$, namely

$$Z(t) \sim -A_2(t). \tag{1.9}$$

Listed in Table 1 are the times taken to compute the coefficients by the CYBER 173 machine at the University of Adelaide.

TABLE 1.

Number of Layers	Time to compute $S_0, \cdots S_{15}$
1	36 msec.
2	49 msec.
3	66 msec.
4	99 msec.
5	181 msec.

The extra time required to sum the asymptotic series is negligible, approximately 1 msec per time.

In all practical prospecting systems, the quantity that is actually measured is not the mutual impedance at a particular time, but rather the average of this quantity over a time channel

$$t_0 < t < t_1 \quad .$$

Thus, the observed quantity is

$$Z(t_0, t_1) = (t_1 - t_0)^{-1} \int_{t_0}^{t_1} dt Z(t). \tag{1.10}$$

Provided that both t_0 and t_1 are sufficiently late, then the asymptotic expansion may be substituted for $Z(t)$ and integrated termwise to give

$$Z(t_0, t_1) = \begin{cases} \dfrac{A_0(t_0) - A_0(t_1) - A_0(t_0 - \tau) + A_0(t_1 - \tau)}{\tau(t_1 - t_0)}, & \tau > 0, \\ \dfrac{A_1(t_1) - A_1(t_0)}{(t_1 - t_0)}, & \tau = 0. \end{cases} \tag{1.11}$$

The asymptotic series in (1.7) above is divergent (except for the degenerate case of a half space without overburden), but, for any fixed number of terms, will provide any desired accuracy for sufficiently late times. However, before the asymptotic series can be used successfully, the problems of chosing the number of terms and of deciding how late is 'sufficiently late' must be addressed. We will show that

$$|B_i(t) - B_i^N(t)| < K\xi^{2(i+1)} F(N + 2(i+1), \xi t^{1/2}), \tag{1.12}$$

where B_i^N is the sum to N terms of the asymptotic series and

$$F(m, z) = \Gamma(m/2)/z^m.$$

The number ξ is computable exactly in principle, but in practice is given sufficiently accurately by the following expression

$$\xi^{-1} = \begin{cases} d|\theta_1|\left(1 + |\chi|^{1/2}\right), & \chi \leqslant 0, \\ d|\theta_1|(1 + \chi)^{1/2}, & \chi \geqslant 0, \end{cases} \tag{1.13}$$

where 218

$$\chi = (\theta_1 + \theta_2)/\theta_1^2$$

$$\theta_1 = d^{-1} \sum_{i=1}^{n} (1 - \sigma_i)\, d_i$$

$$\theta_2 = d^{-2} \sum_{i=1}^{n} (1 - \sigma_i)\, d_i (d_1 + \cdots + d_{i-1} - d_{i+1} - \cdots - d_n) \tag{1.14}$$

and finally 226

$$d = \sum_{i=1}^{n} d_i. \tag{1.15}$$

If $\xi^2 t > 1$, then the bound, regarded as a function of N, decreases at first, passes through a minimum, and then diverges. If $\xi^2 t \leqslant 1$, the bound simply diverges. The minimum of $F(m, z)$ occurs when 231

$$\psi(m/2) = 2 \log z, \tag{1.16}$$

where ψ is the psi function, and typical values of F at the minimum are listed in Table 2. 234

TABLE 2.

z	m at minimum	$F(m, z)$ at the medium
2	9	2.27×10^{-2}
3	19	1.03×10^{-4}
4	33	7.03×10^{-8}
5	51	6.95×10^{-12}

242

On the basis of these results, a reasonable strategy for truncating the asymptotic series might be as follows. 244

(1) Compute χ and ξ from formulae (1.14) and (1.13). 245

(2) Check whether 246

$$\xi^2 t > 3. \tag{1.17}$$

If not, set a warning flag to indicate that the time is too early. 248

(3) Find the closest integer N to the solution of (1.16). This is easily done as the values of the psi function can be generated by recursion and then stored. 251

(4) Sum the asymptotic series to N terms. We implemented this strategy and

found it successful but too conservative, no doubt because the estimate (1.12) is not sufficiently sharp. Instead we adopted the following pragmatic strategy.

(1) Compute a running average of the moduli of two terms.

(2) Choose N corresponding to the minimum of the running average.

(3) Take the average of the moduli of the last term and the first omitted term as a measure of the error. We found the running average necessary because the odd and even order terms occasionally had different orders of magnitude. The success of the strategy is shown in Figure 2 where we plot contours of the error for a medium with a single conductive layer with unit thickness above the basement. The prospecting system is SIROTEM with coincident circular loops with unit radius and a step function current source driving the transmitter loop. The variables in the plot are time and the conductivity of the layer. The errors were computed by comparison of the asymptotic series with the program of Knight and Raiche [9]. Also shown on the plot are thetheoretical curve

$$\xi^2 t = 3 \tag{1.18}$$

and the curve along which the pragmatic algorithm believes it has achieved an accuracy of 1%. The algorithm clearly is reliable.

Fig 2

16700255

2. Derivation of $Z(s)$

We begin the analysis with the following expressions for the Laplace transform of the e.m.f. induced in the receiving loop:

$$V(s) = \int_R d\mathbf{x} \cdot \mathbf{E}(\mathbf{x}, s), \tag{2.1}$$

$$\mathbf{E}(\mathbf{x}, s) = \frac{-s}{I\sigma_{n+1}} \int_T d^3x' g(\mathbf{x}, \mathbf{x}', s)\mathbf{J}(\mathbf{x}', s), \tag{2.2}$$

and

$$g(\mathbf{x}, \mathbf{x}', s) = (4\pi)^{-1} \int_0^\infty d\lambda (\lambda/k_0) J_0(\lambda|r - r'|)\left[\exp\left(-k_0|z - z'|\right) + \exp\left(-k_0(z + z')\right) b/a\right] \tag{2.3}$$

Here V and $\mathbf{E}$ denote the induced e.m.f. and the electric field intensity. The variables $k_0, k_1, \ldots, k_{n+1}$ are defined by

$$k_i = \left(\varepsilon_i s^2 + \sigma_i s + \lambda^2\right)^{1/2}, \tag{2.4}$$

and a and b are elements of the matrix A defined as follows:

$$A = \begin{bmatrix} a & b \\ c & d \end{bmatrix} = \begin{bmatrix} \exp(k_{n+1}d) & 0 \\ 0 & \exp(-k_{n+1}d) \end{bmatrix} \begin{bmatrix} 1 & k_{n+1} \\ 1 & -k_{n+1} \end{bmatrix} T_n \cdots T_1 \begin{bmatrix} 1 & k_0 \\ 1 & -k_0 \end{bmatrix}^{-1} \tag{2.5}$$

where

$$T_i = \begin{bmatrix} \cosh k_i d_i & k_i \sinh k_i d_i \\ k_i^{-1} \sinh k_i d_i & \cosh k_i d_i \end{bmatrix}. \tag{2.6}$$

This result may be derived along the lines followed by Morrison, Phillips and O'Brien [16]. Alternatively, one can prove that the special properties of the source current density **J**, that it be horizontal and divergence free, imply that there are no charge distributions on the interfaces between the layers and that Maxwell's equations reduce to the telegraph equation for a single scalar field. The telegraph equation separates in rectangular coordinates into ordinary differential operators, whose spectral kernels can be constructed by standard techniques. Convolution of these kernels yields the spectral kernel for the telegraph operator from which Green's function g is constructed. The remaining steps which lead to V are then trivial.

The function g represents the effect at $\mathbf{x}$ of a source at $\mathbf{x}'$ and contains geometrical optics terms which must be isolated and treated separately. To do so, let $\tilde{\mathbf{x}}'$ represent the reflection of $\mathbf{x}'$ in the plane $z = 0$. Then

$$g(\mathbf{x}, \mathbf{x}', s) = g_0(|\mathbf{x} - \mathbf{x}'|, s) + p g_0(|\mathbf{x} - \tilde{\mathbf{x}}'|, s) + f(\mathbf{x}, \mathbf{x}', s), \tag{2.7}$$

where

$$g_0(r, s) = \exp\left[-(\varepsilon_0 s^2 + \sigma_0 s)^{1/2} r\right]/(4\pi r) \tag{2.8}$$

and

$$f(\mathbf{x}, \mathbf{x}', s) = (4\pi)^{-1} \int_0^\infty d\lambda (\lambda/k_0) J_0(\lambda |\mathbf{r} - \mathbf{r}'|) \exp\left(-k_0 (z + z')\right) [b/a - p]. \tag{2.9}$$

The first g_0 term is usually called the primary field in the geophysical TEM literature, and is the field that would remain if the earth were removed, whereas the second g_0 term is a reflection from the air-earth interface. The constant p is ultimately fixed by boundary conditions, but its actual value will not concern us because it will cancel from the asymptotic expansion. The interpretation of g becomes apparent after we compute its inverse Laplace transform:

$$g_0(r, t) = \frac{\exp(-t/t_0)}{4\pi r} \left[\delta(t - r/c) + \frac{H(t - r/c) r I_1\left((t^2 - r^2/c^2)^{1/2}/t_0\right)}{c t_0 (t^2 - r^2/c^2)^{1/2}} \right] \tag{2.10}$$

where

$$t_0 = 2\varepsilon_0/\sigma_0,$$
$$c = \varepsilon_0^{-1/2}, \tag{2.11}$$

and H is the step function, 346

$$H(t) = \begin{cases} 0 & \text{if } t < 0, \\ \frac{1}{2} & \text{if } t = 0, \\ 1 & \text{if } t > 0. \end{cases} \tag{2.12}$$

The case of most interest is that obtained by setting $\sigma_0 = 0$, so that the air is a perfect insulator, for then 351

$$g_0(r, t) = \delta(t - r/c)(4\pi r). \tag{2.13}$$

Here c is the speed of light in air (in scaled variables!), so the first term in (2.7) represents the passage of a wave front directly from $\mathbf{x}$ to $\mathbf{x}'$, whereas the second represents the wave front reflected from the interface between the air and the earth. 356

In the application to geoprospecting systems, the contributions from the g_0 terms occur at times too early to measure. Indeed, if $\mathbf{E}_0$ denotes the contribution to $\mathbf{E}$ from g_0, then 359

$$\begin{aligned} \mathbf{E}_0(\mathbf{x}, t) &= -(l\sigma_{n+1})^{-1} \int_0^t dt' \int_T d^3x' g_0(r, t - t') \dot{\mathbf{J}}(\mathbf{x}', t') \\ &= -(l\sigma_{n+1}\tau)^{-1} \int_T d^3x' \mathbf{M}(\mathbf{x}') H(t - r/c) H(\tau - (t - r/c))/(4\pi r) \end{aligned} \tag{2.14}$$

Since the speed of light in air is so large compared with the separation of the source and receiver, the terms involving c may be dropped to give 369

$$\mathbf{E}_0(\mathbf{x}, t) = -(l\sigma_{n+1}\tau)^{-1} H(\tau - t) \int_T d^3x' \mathbf{M}(\mathbf{x}')/(4\pi r). \tag{2.15}$$

Consequently, $\mathbf{E}_0$ vanishes for times later than τ. Since our aim is to analyse the signal at late times, we may discard the g_0 terms throughout the rest of the paper. 375

If we combine formulae (2.1), (2.2) and (2.3), we obtain 376

$$Z(s) = -(4\pi)^{-1} sI(s) \int_0^\infty d\lambda (\lambda/k_0) \mathrm{P}(\lambda) \exp[-(k_0 - \lambda)(z + z')][b/a - p] \tag{2.16}$$

where 382

$$\mathrm{P}(\lambda) = \int_R d\mathbf{x} \cdot \int_T d^3x' J_0(\lambda|\mathbf{r} - \mathbf{r}'|) \mathbf{M}(\mathbf{x}') \exp[-\lambda(z + z')]. \tag{2.17}$$

We call P the loop function, because all the geometric information concerning the

disposition of the loops is embodied in P. So far we have not restricted $\mathbf{M}$, apart from requiring $\mathbf{M}$ to be horizontal and divergence free, but we will now impose the 'thin wire approximation' in which we assume that $\mathbf{M}$ is concentrated on the axis of the transmitting loop. Thus, we now let T denote the axis of the transmitting loop, rather than its volume, and parametrise T by the curve

$$q \mapsto \mathbf{x}'(q), \quad 0 \leqslant q \leqslant |T|.$$

where $|T|$ isthe circumference of T. Then $d\mathbf{x}'/dq$ is a unit vector tangential to T and

$$\mathbf{M} = d\mathbf{x}'/dq. \tag{2.18}$$

Hence,

$$P(\lambda) = \int_R d\mathbf{x} \cdot \int_T dq J_0(\lambda|\mathbf{r} - \mathbf{r}'|)\exp[-\lambda(z + z')]\, d\mathbf{x}'/dq. \tag{2.19}$$

An alternative expression for P can be obtained by repeated application of Stokes' theorem to formula (2.19):

$$P(\lambda) = \int_R \int_T \lambda^2 J_0(\lambda|\mathbf{r} - \mathbf{r}'|)\exp[-\lambda(z + z')], \tag{2.20}$$

where the integrations arenow over the areas of the loops. This form for P is generally more convenient for calculation because it involves only scalar quantities. For example, when the transmitting and receiving loops are circular, with radii a and b, and centres separated by a distance d, repeated application of the addition theorem for Bessel functions gives

$$P(\lambda) = 4\pi^2 ab J_1(\lambda a) J_1(\lambda b) J_0(\lambda d). \tag{2.21}$$

The TEM response of the layered medium is obtained from $Z(s)$ by inverse Laplace transform,

$$Z(t) = (2\pi i)^{-1} \int_C ds Z(s)\exp(st). \tag{2.22}$$

where C is a contour parallel to the imaginary s axis and which lies entirely to the right of the singularities of $Z(s)$. Our strategy is to locate these singularities and deform the contour about them in such a way that Watson's lemma can be applied to the integral representation of $Z(t)$.

3. Singularities of $Z(s)$

We observe that $sI(s)$ is an entire function of s, namely,

$$sI(s) = [1 - \exp(-s\tau)]/(s\tau), \tag{3.1}$$

so we can focus upon the functions a and b which appear in the matrix A.

Each factor T which appears in the expansion of A is an entire function of

$$k_i^2 = \varepsilon_i s^2 + \sigma_i s + \lambda^2, \quad 1 \leqslant i \leqslant n, \tag{3.2}$$

and so is necessarily entire in both s and λ. Consequently A is a holomorphic function of s except when

$$k_0^2 = \varepsilon_0 s^2 + \lambda^2 \leqslant 0 \tag{3.3}$$

or

$$k_{n+1}^2 = \varepsilon_{n+1} s^2 + \sigma_{n+1} s + \lambda^2 \leqslant 0.$$

A short analysis shows that, for any fixed λ, A is holomorphic in the variable s throughout the plane cut as shown in Figure 3.

Note that the endpoints shown for the cut on the real axis are only correct asymptotically as $\varepsilon_{n+1} \to 0$.

Let us compute the discontinuity of b/a across the cut on the real axis. To do so we establish the convention that the value of k_i on its associated cut is taken to be its boundary value from above. Let

$$s = u + iv,$$

and define for u on the cut

$$D(u) = (2\pi i)^{-1} \lim_{v \to 0^+} [(b/a - p)(u - iv) - (b/a - p)(u + iv)]. \tag{3.4}$$

Since the sign of k_{n+1} reverses when s crosses the cut, and since

$$\begin{aligned} b(-k_{n+1}) &= d(k_{n+1}), \\ a(-k_{n+1}) &= c(k_{n+1}), \end{aligned} \tag{3.5}$$

we find that

$$D(u) = (2\pi i)^{-1} \lim_{v \to 0^+} [d/c - b/a](u + iv) \tag{3.6}$$

$$= (2\pi i)^{-1} \lim_{v \to 0^+} [(ad - bc)/(ac)](u + iv). \tag{3.7}$$

Now

$$ad - bc = \det A = k_{n+1}/k_0, \tag{3.8}$$

so

$$D(u) = k_{n+1}/(2\pi i k_0 ac), \tag{3.9}$$

where the limit sign has been omitted on the understanding that all quantities are defined on the cut by their boundary values from above.

The analytic structure of A simplifies if we now introduce the quasistatic approximation which sets

$$\varepsilon_i = 0, \quad i = 0, 1, \ldots, n+1. \tag{3.10}$$

The cuts parallel to the imaginary axis recede to infinity, as does the left hand endpoint of the cut on the real axis. Thus, for fixed λ, A is holomorphic in the whole s plane, with the exception of a cut along the real axis from $-\infty$ to $-\lambda^2$. The discontinuity of b/a across this cut is

$$D(u) = (\lambda^2 + u)^{1/2}/(2\pi i \lambda ac) \tag{3.11}$$

since

$$k_0 = \lambda \tag{3.12}$$

and

$$k_{n+1} = (\lambda^2 + u)^{1/2} \tag{3.13}$$

in the quasistatic approximation.

The quasistatic approximation is nearly always used in the analysis of geoprospecting systems because observations are made long after the wave fronts have passed the observer. Under these circumstances, the fields evolve according to a diffusion equation rather than a wave equation. We will now keep the quasistatic approximation for the rest of the paper.

In addition to the singularities of $Z(s)$ associated with the branch cuts of k_0 and k_{n+1}, there will also be poles at the zeros of a. Here we regard a as a function of s with parameter λ, and we denote the number of zeros by $n(\lambda)$ and their positions by $s_1(\lambda), \ldots, s_{n(\lambda)}(\lambda)$. These zeros correspond to eigenvalues of the operator

$$L = -d^2/dz^2 + q, \tag{3.14}$$

where

$$q = \varepsilon s^2 + \sigma s, \tag{3.15}$$

on the Sobolev space $H^2(\mathbf{R})$. That this should be so emerges naturally from the construction of Green's function g along the lines sketched at the beginning of Section 1, but since most of the steps are fairly routine and would require us to introduce extensive notation, we will omit them here. Instead, we will show that the zeros must lie in the interval $[-\lambda^2, 0]$, and that $n(\lambda)$ is zero if λ is sufficiently small.

From the positivity of the operator $-d^2/dz^2$, it is easy to show that

$$(u^2 - v^2)(f, \varepsilon f) + u(f, \sigma f) + \lambda^2 \leqslant 0, \tag{3.16}$$

$$v[2u(f, \varepsilon f) + (f, \sigma f)] = 0, \tag{3.17}$$

where $s = u + iv$ and f is the normalised eigenfunction corresponding to the zero of a. In the quasistatic approximation, these inequalities reduce to

$$u(f,\sigma f) + \lambda^2 \leqslant 0, \tag{3.18}$$

$$v(f,\sigma f) = 0. \tag{3.19}$$

From (3.18) and (3.19) we conclude that the zeros of a lie on the negative real axis. Since the point $-\lambda^2$ will lie in the continuous spectrum of L if s is in the interval $(-\infty, -\lambda^2]$, and since L cannot have eigenvalues embedded in its continuous spectrum, it follows that the zeros of a are confined to the interval $[-\lambda^2, 0]$.

We obtain an upper bound on the zeros of a by comparing the spectrum of L with the spectrum of a related operator L_*, whose conductivity function has only a single layer above the basement.

LEMMA. *Let $\bar{\sigma}$ denote the maximum value of σ, and suppose that $\bar{\sigma}$ is greater than 1. Then $n(\lambda)$ is zero if*

$$\lambda^2 < M = \pi^2/[4d^2(\bar{\sigma} - 1)]. \tag{3.20}$$

Any zeros of a must satisfy

$$s_i(\lambda) < -M. \tag{3.21}$$

PROOF. We will restrict s to be real and negative, and show that, when $|s|$ is less than M, L cannot have any eigenvalues. Consequently, a cannot have any zeros. Equivalently, any zeros of a must satisfy the inequality (3.21). Since all zeros of a lie in the interval $[-\lambda^2, 0]$, then $|s| < M$ whenever (3.20) is true, so $n(\lambda)$ must be zero.

Let q_* denote the 'potential' with σ replaced by the function

$$\sigma_*(z) = \begin{cases} 1, & z < -d, \\ \bar{\sigma}, & -d \leqslant z \leqslant 0, \\ 0, & 0 < z, \end{cases} \tag{3.22}$$

and let L_* denote the differential operator with q replaced by q_*. Then L and L_* have the same essential spectrum, namely, the interval $[s, \infty)$ (Schechter [18], Theorem 5.8.1), and, if L_* does not have any eigenvalues, then neither can L. Indeed, if L has an eigenvalue ζ below the essential spectrum, with normalised eigenfunction f, then

$$(f, L_* f) + (f, [q - q_*] f) = \zeta < s.$$

Since $q - q_*$ is both bounded and positive, it follows that

$$(f, L_* f) \leqslant \zeta < s,$$

which implies that L_* also has an eigenvalue (Schechter [18], Corollary 4.4.1), and we have a contradiction. Lastly, it is a standard result from quantum mechanics that L_* does not have any eigenvalues if $|s| < M$ (Schechter [18], Corollary 3.3.1).

Finally, we note the special case of a resistive overburden, for which

$$\sigma(z) \leqslant 1 \quad \text{for } z \leqslant 0.$$

Then

$$(f, \sigma f) \leqslant 1$$

and so (3.18) implies that

$$u \leqslant -\lambda^2.$$

This is a contradiction and so the function a cannot have any zeros if the overburden is resistive.

The conclusion of the analysis is that the singularities of b/a consist of a square-root branch point at the point $-\lambda^2$ and a finite number of simple poles in the segment $[-\lambda^2, 0]$. The branch cut for the square root lies along the segment $(-\infty, -\lambda^2]$ of the negative real axis. Consequently, the contour C for the inverse Laplace transform can be any vertical line in the right hand s plane.

In the next section we will deform the contour C around the negative real axis of the s plane. It is interesting to note here the role of the quasistatic approximation, without which the three cuts would pinch on the origin of the s plane as $\lambda \to 0$. Whether or not the contour C could be deformed would become quite a delicate question.

4. Derivation of $Z(t)$

The TEM response of the layered medium is

$$Z(t) = -(8\pi^2 i)^{-1} \int_C ds \exp(st) sI(s) \int_0^\infty d\lambda P(\lambda)[b/a - p](\lambda, s). \quad (4.1)$$

With the contour C in the right half plane, we may interchange the order of integration. Having done so, we deform the contour C around the negative real axis. Then

$$Z(t) = -(8\pi^2 i)^{-1} \int_0^\infty d\lambda P(\lambda) \Bigg\{ \int_{-\infty}^{-\lambda^2} ds \exp(st) sI(s) \lim_{u \to 0^+} [[b/a - p](u - iv) - [b/a - p](u + iv)]$$

$$+ (2\pi i) \sum_{i=1}^{n(\lambda)} \operatorname*{residue}_{s = s_i(\lambda)} [\exp(st) sI(s)(b/a - p)] \Bigg\}. \quad (4.2)$$

Because the zeros $s_i(\lambda)$ are strictly negative for all λ and are bounded away from zero, it follows that the contributions of the pole terms are all exponentially damped in time. In fact, the second term in (4.2) is bounded by

$$(4\pi)^{-1} \exp(-Mt) \int_0^\infty d\lambda \left| P(\lambda) \sum_{i=1}^{n(\lambda)} \operatorname*{residue}_{s = s_i(\lambda)} [sI(s)(b/a - p)] \right|.$$

Since we are interested in late times, we discard these terms and obtain

$$Z(t) = -(4\pi)^{-1}\int_0^\infty d\lambda P(\lambda)\int_{-\infty}^{-\lambda^2} ds \exp(st)sI(s)D(s). \tag{4.3}$$

Reverse the order of integration again and substitute

$$s = -x^2 \text{ and } \lambda = mx. \tag{4.4}$$

Then

$$Z(t) = [B_1(t) - B_1(t-\tau)]/\tau, \tag{4.5}$$

where

$$B_i(t) = \pi^{-2}\int_0^\infty dx \exp(-x^2 t)x^{2(i-1)}S(x), \tag{4.6}$$

$$S(x) = x^2\int_0^1 dm(1-m^2)^{1/2}mP(mx)/Q(m,x), \tag{4.7}$$

and

$$Q(m,x) = 4\lambda^2 ac. \tag{4.8}$$

In the limit as $\tau \to 0$, we find

$$Z(t) = -B_2(t). \tag{4.9}$$

5. Asymptotic analysis of $B_i(t)$

We now apply Watson's lemma (Copson [4]) to (4.6) to obtain an asymptotic expansion for $B_i(t)$ at late times. We develop S as a convergent power series for small x,

$$S(x) = x^2\sum_{r=0}^{\infty} S_r x^r, \tag{5.1}$$

substitute this into (4.6) and integrate termwise to obtain

$$B_i(t) \sim A_i(t) = (2\pi^2)^{-1}\sum_{r=0}^{\infty} S_r\Gamma((r+1)/2+i)t^{-((r+1)/2+i)}. \tag{5.2}$$

In this section we will develop two expressions for the Taylor coefficients S_r, the first of which will be a convenient tool for the analysis but unsuited to numerical computation, whereas the second will have the opposite properties.

The first step is to develop Q in power series for small x, which we achieve by expanding the factors in the matrix A in series and then multiplying the series together. Next we develop P in series and compute the ratio P/Q. Finally we integrate over m.

The matrix T_r has the series representation

$$T_r = \sum_{i_r=0}^{\infty} \frac{(k_r d_r)^{2i_r}}{(2i_r)!} T_r^{i_r}, \tag{5.3}$$

where

$$T_r^{i_r} = \begin{bmatrix} 1 & 2i_r/d_r \\ d_r/(2i_r+1) & 1 \end{bmatrix}. \tag{5.4}$$

If we let $X = T_n T_{n-1} \cdots T_1$, then

$$X = \sum_{r=0}^{\infty} X_r x^{2r}, \tag{5.5}$$

where

$$X_r = \sum_{|i|=r} (m^2 - \sigma_1)^{i_1} \cdots (m^2 - \sigma_n)^{i_n} X_r^i, \tag{5.6}$$

$$X_r^i = \frac{d_1^{2i_1} \cdots d_n^{2i_n}}{(2i_1)! \cdots (2i_n)!} T_n^{i_n} \cdots T_1^{i_1}, \tag{5.7}$$

and

$$i = (i_1, \ldots, i_n),$$
$$|i| = i_1 + \cdots + i_n. \tag{5.8}$$

Let

$$X = \begin{bmatrix} \alpha & \beta \\ \gamma & \delta \end{bmatrix}, \qquad X_r = \begin{bmatrix} \alpha_r & \beta_r \\ \gamma_r & \delta_r \end{bmatrix}. \tag{5.9}$$

A short calculation yields that

$$Q = (\alpha\lambda + \beta)^2 + x^2(1 - m^2)(\gamma\lambda + \delta)^2, \tag{5.10}$$

so we obtain the series for Q by further multiplication.

$$(\alpha\lambda + \beta) = m \sum_{r=0}^{\infty} \alpha_r x^{2r+1} + \sum_{r=0}^{\infty} \beta_r x^{2r} = \sum_{r=0}^{\infty} \mu_r x^{r+1}$$
$$(\gamma\lambda + \delta) = m \sum_{r=0}^{\infty} \gamma_r x^{2r+1} + \sum_{r=0}^{\infty} \delta_r x^{2r} = \sum_{r=0}^{\infty} \nu_r x^r \tag{5.11}$$

where

$$\mu_{2r} = m\alpha_r, \quad \nu_{2r+1} = m\gamma_r,$$
$$\mu_{2r-1} = \beta_r, \quad \nu_{2r} = \delta_r. \tag{5.12}$$

Hence,

$$Q(m, x) = x^2 \sum_{r=0}^{\infty} Q_r x^r, \tag{5.13}$$

where

682

$$Q_r = \sum_{p+q=r} \left[\mu_p \mu_q + (1-m^2)\nu_p \nu_q\right]. \tag{5.14}$$

Note that $Q_0 = 1$ and hence is independent of m. Since X_r is a polynomial in m of degree $2r$, it follows trivially that

687

$$\begin{aligned} &\text{degree}(\mu_{2r}) = 2r+1, \quad &&\text{degree}(\nu_{2r}) = 2r, \\ &\text{degree}(\mu_{2r-1}) = 2r, \quad &&\text{degree}(\nu_{2r+1}) = 2r+1, \end{aligned}$$

and hence that the degree of Q_r does not exceed $r+2$. In fact,

692

$$\text{degree}(Q_r) = r. \tag{5.15}$$

To prove this, firstly observe that α_r, β_r, γ_r and δ_r are polynomials in m^2, and then establish by induction on r that Q_{2r} and $m^{-1}Q_{2r+1}$ must also be polynomials in m^2. Thus, Q_r will have degree r if the coefficient of m^{r+2} is zero. But this coefficient is independent of $\sigma_1, \ldots, \sigma_r$, so we set

16700644

699

$$\sigma_1 = \sigma_2 = \cdots = \sigma_n = 1$$

and find that

701

$$Q(m, x) = x^2,$$

which clearly demonstrates that the coefficient of m^{r+2} is always zero if $r > 0$.

704

It is quite apparent that formulae (5.6) and (5.7) are unsuited to numerical computation, because the number of terms in the summation for X_r becomes extremely large for more than two layers and the cost of computing the partitions of r and the matrix products is excessive. Fortunately, it is not difficult to prove by induction that

709

$$X = \sum_{\varepsilon_2, \ldots, \varepsilon_n} C_\varepsilon \begin{bmatrix} \cosh B_\varepsilon & k_1 \sinh B_\varepsilon \\ (\varepsilon_n k_n)^{-1} \sinh B_\varepsilon & k_1(\varepsilon_n k_n)^{-1} \cosh B_\varepsilon \end{bmatrix} \tag{5.16}$$

where

715

$$B_\varepsilon = k_1 d_1 + \varepsilon_2 k_2 d_2 + \cdots + \varepsilon_n k_n d_n,$$

$$C_\varepsilon = 2^{1-n}(1 + \varepsilon_2 k_2/k_1)(1 + \varepsilon_3 k_3/\varepsilon_2 k_2) \cdots (1 + \varepsilon_n k_n/\varepsilon_{n-1} k_{n-1}). \tag{5.17}$$

The summation is over the signs $\varepsilon_i = \pm$, so the number of terms in the summation is 2^{n-1}.

723

The ratios k_{i+1}/k_i which appear in C_ε are independent of x, so it is only necessary to expand the hyperbolic functions in order to obtain the series development of X. A short calculation gives

726

$$X = \sum_{r=0}^{\infty} x^{2r} \sum_{\varepsilon} X_r^{(\varepsilon)}, \tag{5.18}$$

where

729

$$X_r^{(\varepsilon)} = \frac{C_\varepsilon k_\varepsilon^{2r}}{(2r)!}\begin{bmatrix} 1 & 2rp_1/K_\varepsilon \\ K_\varepsilon/(\varepsilon_n p_n(2r+1)) & p_\ell/(\varepsilon_n p_n) \end{bmatrix} \tag{5.19}$$

and

$$p_i = (m^2 - \sigma_i)^{1/2}, \tag{5.20}$$

$$K_\varepsilon = p_1 d_1 + \varepsilon_2 p_2 d_2 + \cdots + \varepsilon_n p_n d_n. \tag{5.21}$$

Note that the earlier expression for X_r indicated that its elements were polynomials in m, but the present formula does not even show clearly that the elements are real! Nonetheless, formula (5.18) is well suited for computation for the following reason. Let

$$X_r^{(\varepsilon)} = \begin{bmatrix} \alpha_r^{(\varepsilon)} & \beta_r^{(\varepsilon)} \\ \gamma_r^{(\varepsilon)} & \delta_r^{(\varepsilon)} \end{bmatrix}, \tag{5.22}$$

and define

$$\begin{aligned} \mu_{2r}^{(\varepsilon)} &= m\alpha_r^{(\varepsilon)}, & \nu_{2r+1}^{(\varepsilon)} &= m\gamma_r^{(\varepsilon)}, \\ \mu_{2r-1}^{(\varepsilon)} &= \beta_r^{(\varepsilon)}, & \nu_{2r}^{(\varepsilon)} &= \delta_r^{(\varepsilon)}, \end{aligned} \tag{5.23}$$

so that

$$\mu_r = \sum_\varepsilon \mu_r^{(\varepsilon)}, \qquad \nu_r = \sum_\varepsilon \nu_r^{(\varepsilon)}. \tag{5.24}$$

Then $\mu_r^{(\varepsilon)}$ and $\nu_r^{(\varepsilon)}$ satisfy the following recursion formula,

$$\begin{aligned} \mu_{r+2}^{(\varepsilon)} &= \mu_r^{(\varepsilon)} K_\varepsilon^2/[(r+1)(r+2)], \\ \nu_{r+2}^{(\varepsilon)} &= \nu_r^{(\varepsilon)} K_\varepsilon^2/[(r+1)(r+2)], \end{aligned} \tag{5.25}$$

with the initial values

$$\begin{aligned} \mu_0^{(\varepsilon)} &= mC_\varepsilon, & \nu_0^{(\varepsilon)} &= C_\varepsilon p_1/(\varepsilon_n p_n), \\ \mu_1^{(\varepsilon)} &= p_1 C_\varepsilon K_\varepsilon, & \nu_1^{(\varepsilon)} &= C_\varepsilon K_\varepsilon m/(\varepsilon_n p_n). \end{aligned} \tag{5.26}$$

This recursion formula is easy to program and fast in execution.

The loop function is also an entire function and from the representation (2.20) it is clear that it has a series development of the form

$$P(mx) = m^2 x^2 \sum_{r=0}^{\infty} P_r (mx)^r. \tag{5.27}$$

Expressions for the coefficients P_r are given for coincident circular loops and arbitrary rectangular loops in Appendix 1.

Both P and Q have a zero of the second order at $x = 0$, so provided that x is less than the modulus of the closest nonzero zero of Q, the series for P and Q can be manipulated as follows. Let

$$F = P/Q \tag{5.28}$$

$$= m^2 \sum_{r=0}^{\infty} F_r x^r, \tag{5.29}$$

where

$$F_0 = P_0 \tag{5.30}$$

and

$$F_r = m^r P_r - \sum_{p=1}^{r} Q_p F_{r-p}, \qquad r > 0. \tag{5.31}$$

It is easy to prove by induction on r that F_r is a polynomial in m, that

$$\text{degree}(F_r) \leqslant r, \tag{5.32}$$

and that F_{2r} and $m^{-1}F_{2r+1}$ are polynomials in m^2.

Within the region of convergence of the series (5.29), we may integrate termwise over m to obtain

$$S(x) = x^2 \sum_{r=0}^{\infty} S_r x^r, \tag{5.33}$$

where

$$S_r = \int_0^1 dm(1 - m^2)^{1/2} m^3 F_r(m). \tag{5.34}$$

To evaluate S_r two options are open.

(1) For odd orders, F_{2r+1} has the form

$$F_{2r+1} = m \cdot \text{polynomial in } m^2.$$

Hence,

$$S_{2r+1} = 2^{-1} \int_{-1}^{+1} dm(1 - m^2)^{1/2} m^3 F_{2r+1}(m). \tag{5.35}$$

These integrals can be evaluated exactly by Gaussian quadrature with weight $(1 - m^2)^{1/2}$, interval $[-1, +1]$, and Chebyshev polynomials of the second kind. (Stroud and Secrest [21]). To evaluate the even orders, let

$$w = m^2$$

and obtain

$$S_{2r} = 2^{-1} \int_0^1 dw(1 - w)^{1/2} w F_{2r}(w^{1/2}). \tag{5.36}$$

Recall that $F_{2r}(w^{1/2})$ will be a polynomial in w. Thus, S_{2r} may be evaluated exactly by Gaussian quadrature with weight $(1 - w)^{1/2}$, interval $[0, 1]$ and Jacobi polynomials. (Krylov, Lugin and Yanovich [11].)

(2) Alternatively, quadrature rules may be developed for the interval $[0, 1]$ with

weight $(1 - m^2)^{1/2}m^3$, so that both the odd and even order S_r may be evaluated exactly with the same quadrature rule. This approach leads to a simpler program and is the one we have followed. We computed Gaussian rules with from one to twenty points. In order to compute S_r exactly for

$$0 \leqslant r \leqslant N = 2M - 1,$$

we chose the rule with M points: 827

$$S_r = \sum_{i=1}^{M} w_i F_r(m_i),$$

where w_i and m_i are the computed weights and nodes. In Appendix 2 are tabulated the weights and nodes for the 8 point rule, sufficient to give the first 16 terms of the asymptotic expansion. 831

The algorithm for computing the coefficients S_r is summarised in the flow chart below.

Compute $P_0, P_1, \cdots, P_N$ for the loop configuration.
Set $S_r = 0$, $r = 0, 1, \ldots, N$.
Set m_i to the first quadrature node.
Label 1: Set $\mu_r = 0$ and $\nu_r = 0$.
Set $\varepsilon_2 = +, \varepsilon_3 = +, \ldots, \varepsilon_n = +$.
16700766 Label 2: Compute B_ε and C_ε.
Compute $\mu_0^{(\varepsilon)}, \mu_1^{(\varepsilon)}$ and $\nu_0^{(\varepsilon)}, \nu_1^{(\varepsilon)}$.
Compute $\mu_r^{(\varepsilon)}$ and $\nu_r^{(\varepsilon)}$ by recursion.
Increment μ_r and ν_r. $\mu_r := \mu_r + \mu_r^{(\varepsilon)}$, $\nu_r := \nu_r + \nu_r^{(\varepsilon)}$
If not finished all sign combinations, go to 2.
Compute $Q_0, Q_1, \ldots, Q_n$ from μ_r and ν_r.
Compute $F_0, F_1, \ldots, F_N$ recursively from P_r and Q_r.
Increment S_r. $S_r := S_r + w_i F_r(m_i)$.
If not finished all quadrature points, go to 1.
Stop.

851

6. Thin layer approximations

At this point we can establish the relation between our asymptotic expansion and the expansion to two terms obtained by Lee [13]. To do so, let 855

$$Q^{(k)} = x^2 \sum_{r=0}^{k} Q_r x^r, \tag{6.1}$$

and call $Q^{(k)}$ the kth thin layer approximation to Q. Since X_r contains a factor $d_1^{2i_1} \cdots d_n^{2i_n}$, it is clear that the terms in the expansion of X (and hence of Q) will become very small if the layers are thin, so it is reasonable to truncate the series as in (6.1) above. Explicit calculation yields

$$\begin{aligned} Q_0 &= 1 \\ Q_1 &= 2md\theta_1 \\ Q_2 &= d^2\left[(\theta_1 + \theta_2)(2m^2 - 1) + \theta_1^2\right] \end{aligned} \tag{6.2}$$

where θ_1 and θ_2 are given by (1.14).

If the series for Q is truncated at the first term, then the recurrence formula (5.31) degenerates to

$$F_r = m^r P_r \tag{6.3}$$

from which we obtain

$$S_r = c_r P_r, \tag{6.4}$$

where

$$\begin{aligned} c_r &= \int_0^1 dm(1 - m^2)^{1/2} m^{3+r}, \\ &= \frac{\Gamma(3/2)\Gamma((r+4)/2)}{2\Gamma((r+7)/2)}. \end{aligned} \tag{6.5}$$

Thus,

$$A_i(t) = (2\pi^2)^{-1} \sum_{r=0}^{\infty} c_r P_r \Gamma((r+1)/2 + i) t^{-((r+1)/2+i)}. \tag{6.6}$$

This is the response of a uniform half space with the conductivity of the basement, as expected, because all information concerning the layers was contained in the terms dropped from Q.

The first order thin layer approximation gives

$$Q^{(1)} = x^2[1 + 2mxd\theta_1]. \tag{6.7}$$

Note that $Q^{(1)}$ can vanish if $\theta_1 < 0$, corresponding to a conductive overburden, so the thin layer approximation has introduced a spurious zero on the x axis. The recurrence relation for F_r can again be solved explicitly, because equation (5.31) reduces to

$$\begin{aligned} F_0 &= P_0 \\ F_r &= m^r P_r - Q_1 F_{r-1}, \end{aligned} \tag{6.8}$$

which has the solution

$$F_r = \sum_{p=0}^{r} (-Q_1)^p m^{r-p} P_{r-p},$$

$$= m^r L_r, \tag{6.9}$$

where

$$L_r = \sum_{p=0}^{r} (-2d\theta_1)^p P_{r-p}. \tag{6.10}$$

Thus,

$$S_r = c_r L_r$$

and

$$A_i(t) = (2\pi^2)^{-1} \sum_{r=0}^{\infty} c_r L_r \Gamma((r+1)/2 + i) t^{-((r+1)/2+i)}. \tag{6.11}$$

Lee [13] obtained the first two terms of this asymptotic expansion for the case of coincident circular transmitting and receiving loops.

7. Error estimates

If the function Q never vanishedfor nonzero x, then the series for S would converge for all x and the asymptotic expansion would be a convergent series. This happens only for the case of a uniform half space, for which

$$Q = x^2,$$

so in principle the transient response of the half space could be calculated with arbitrary accuracy by summing sufficiently many terms of the series. (In practice, however, the series is so slowly convergent at early times that the finite word length of the series are summed.) In all other cases, Q is an entire function of order $\frac{1}{2}$, and so has an infinite number of isolated zeros. The proximity of these zeros to the origin limits the radius of convergence for the series for S, and hence reduces the range of times for which the asymptotic series is useful. For low conductivity contrasts or thin layers, the zeros of Q are well away from the origin, and the asymptotic series 'converges' well, but, for larger conductivities and thicker layers, the zeros of Q crowd in around the origin and the 'convergence' of the asymptotic series is poor.

To make these intuitive ideas, precise we will develop an estimate for the error in chopping the asymptotic series at N terms. The estimate will be in terms of the quantity

$$\xi = \inf_{0 \leq m \leq 1} \xi(m), \tag{7.1}$$

where

$$\xi(m) = \inf_{k \geq 1} |x_k(m)|,$$

and

$$0 = x_0(m), x_1(m), x_2(m), \cdots$$

are distinct zeros of Q, regarded as a function of x with parameter m. Clearly ξ is the closest approach to the origin of all the zeros of Q as m is allowed to vary over the range $[0, 1]$. In principle ξ is computable, because Q is an elementary combination of hyperbolic functions and its zeros can be found by a number of well established algorithms. However, the cost of such a search is not justified, firstly because the pragmatic algorithm works well, and secondly because we can approximate ξ by the quantity $\xi^{(k)}$, defined analogously as the closest approach to the origin of the zeros of $Q^{(k)}$. It is easy to see that

$$1/\xi^{(1)} = 2d|\theta_1|, \tag{7.2}$$

and a rather lengthy, but straightforward, calculation yields

$$1/\xi^{(2)} = \begin{cases} d|\theta_1|\left(1+|\chi|^{1/2}\right), \chi \leq 0 \\ d|\theta_1|(1+\chi)^{1/2}, \chi \geq 0. \end{cases} \tag{7.3}$$

This is the approximation quoted in the introduction. Higher order approximations could be computed numerically, but again the cost is unwarranted. To illustrate this, the figures in Table 3 compare $\xi^{(1)}$, $\xi^{(2)}$ and ξ in the case of a single conductive layer over a basement, for which ξ can be computed exactly:

$$\xi = \log\left[\left(\sigma_1^{1/2}+1\right)/\left(\sigma_1^{1/2}-1\right)\right]/\left(2\sigma_1^{1/2}d_1\right). \tag{7.4}$$

TABLE 3.

	$\sigma_1 = 10, d_1 = 0.1$	$\sigma_1 = 1000, d_1 = 1$
$\xi^{(1)}$	0.556	0.500×10^{-3}
$\xi^{(2)}$	0.833	1.000×10^{-3}
ξ	1.035	1.000×10^{-3}

These figures also illustrate the general rule that the zeros crowd in around the origin as the product of conductivity and thickness increases.

We now turn to the derivation of the error estimate. Let

$$F^N = m^2 \sum_{r=0}^{N} F_r x^r \tag{7.5}$$

and

$$S^N = x^2 \int_0^1 dm(1-m^2)^{1/2} m F^N(m). \tag{7.6}$$

LEMMA. *There exists a constant K such that for all x*

$$|S(x) - S^N(x)| < Kx^3(x/\xi)^N/|x - \xi|. \tag{7.7}$$

PROOF. For each m, F has only simple poles, so the sequence

$$\xi(m)^r|F_r(m)|, r = 0, 1, 2, \cdots$$

is bounded. Hence, there exists a constant $C(m)$ such that

$$\xi(m)^r|F_r(m)| < C(m) \quad \text{for all } r.$$

Since $\xi < \xi(m)$ for all m, it follows that

$$|F_r(m)| < C(m)/\xi^r \quad \text{for all } r.$$

Consider $x < \xi$. Since the series for F is convergent for such x,

$$S(x) - S^N(x) = x^2\int_0^1 dm(1 - m^2)^{1/2}m^3 \sum_{r=N+1}^{\infty} F_r(m)x^r,$$

and

$$|S(x) - S^N(x)| < x^2\int_0^1 dm(1 - m^2)^{1/2}m^3 \sum_{r=N+1}^{\infty} C(m)(x/\xi)^r$$

$$= x^2C(x/\xi)^{N+1}/(1 - x/\xi),$$

where

$$C = \int_0^1 dm(1 - m^2)^{1/2}m^3C(m).$$

Thus, (7.7) holds with $K = C$.

Now consider $x > \xi$. The series is no longer convergent, but it is certainly true that

$$|S(x) - S^N(x)| < x^2\int_0^1 dm(1 - m^2)^{1/2}m|F(m, x)|$$

$$+x^2\int_0^1 dm(1 - m^2)^{1/2}m^3 \sum_{r=0}^{N} |F_r(m)|x^r$$

Since $|J_0| \leqslant 1$, it follows from (2.20) that

$$|P(\lambda)| \leqslant \pi^2|T|\,|R|,$$

where $|T|$ and $|R|$ denote the areas of the transmitting and receiving loops. The function

$$(1 - m^2)^{1/2}m^3x^2/Q(m, x)$$

has at worst an integrable singularity in m, so there exists a constant L such that

$$\int_0^1 dm(1 - m^2)^{1/2}m|P(mx)/Q(m, x)| \leqslant L \quad \text{for all } x \geqslant \xi.$$

Hence,

$$|S(x) - S^N(x)| < x^2 L + x^2 \int_0^1 dm(1-m^2)^{1/2} m^3 C(m) \sum_{r=0}^{N} (x/\xi)^r$$

$$= x^2 \left[L + C\left(1 - (x/\xi)^{N+1}\right)/(1 - x/\xi) \right].$$

Choose K so that

$$L + C(x/\xi)^{N+1}/(x/\xi - 1) < K(x/\xi)^{N+1}/(x/\xi - 1),$$

a condition which will be satisfied provided that

$$K > C + LN^N/(N+1)^{N+1}.$$

Then

$$|S(x) - S^N(x)| < x^2 K(x/\xi)^{N+1}/(x/\xi - 1).$$

Again (7.7) holds and the proof is complete.

Define

$$B_i^N(t) = \pi^{-2} \int_0^\infty dx \exp(-x^2 t) x^{2(i-1)} S^N(x).$$

Choose any small positive number ε, split the integration into three ranges, $[0, \xi - \varepsilon]$, $[\xi - \varepsilon, \xi + \varepsilon]$ and $[\xi + \varepsilon, \infty)$, and use the estimate for $|S(x) - S^N(x)|$ in the first and last ranges.

$$\pi^2 |B_i(t) - B_i^N(t)| < \int_0^{\xi-\varepsilon} dx \exp(-x^2 t) x^{2(i-1)} K x^3 (x/\xi)^N/(\xi - x)$$

$$+ \int_{\xi-\varepsilon}^{\xi+\varepsilon} dx \exp(-x^2 t) x^{2(i-1)} |S(x) - S^N(x)|$$

$$+ \int_{\xi+\varepsilon}^{\infty} dx \exp(-x^2 t) x^{2(i-1)} K x^3 (x/\xi)^N/(x - \xi)$$

$$< \varepsilon^{-1} K \int_0^\infty dx \exp(-x^2 t) x^{2i+1} (x/\xi)^N$$

$$+ \int_{\xi-\varepsilon}^{\xi+\varepsilon} dx \exp(-x^2 t) x^{2(i-1)} |S(x) - S^N(x)| \quad .$$

The first integral is trivial. Apply the mean value theorem to the second integral.

$$\pi^2 |B_i(t) - B_i^N(t)| < (2\varepsilon)^{-1} K \xi^{2(i+1)} \Gamma(N/2 + i + 1)/\left(\xi t^{1/2}\right)^{N+2i+2}$$

$$+ 2\varepsilon \exp(-z^2 t) z^{2(i-1)} |S(z) - S^N(z)|,$$

where z is a point in the interval $[\xi - \varepsilon, \xi + \varepsilon]$. Provided that $0 < \varepsilon < \xi$ and also that ξ is not too small, then the dominant term is the first. In any case, we can always increase the constant K in order to obtain the following bound.

$$|B_i(t) - B_i^N(t)| < (2\pi^2\varepsilon)^{-1} K\xi^{2(i+1)}\Gamma(N/2 + i + 1)/(\xi t^{1/2})^{N+2i+2}.$$

This is the bound mentioned in the introduction.

1088

Appendix 1

We assume that both the transmitting and receiving loops lie on the surface of the ground, so that $z = z' = 0$. 1091

Consider firstly the case of concident circular transmitting and receiving loops with radius a. Formula (2.21) for the loop function reduces to 1093

$$P(\lambda) = [2\pi a J_1(\lambda a)]^2. \tag{8.1}$$

Insert the series for J_1^2 given in formula (9.1.14) of Abramowitz and Stegun [1] to obtain 1096

$$P_{2r+1} = 0,$$

$$P_{2r} = (2\pi a)^2 \frac{(-1)^r (a/2)^{2r+2}(2r+2)!}{r![(r+1)!]^2(r+2)!}. \tag{8.2}$$

The sequence of P_r is best computed by recursion, since 1101

$$P_{2r+2} = -P_{2r} a^2(2r+3)/[2(r+1)(r+2)(r+3)], \tag{8.3}$$

and 1104

$$P_0 = \pi^2 a^4. \tag{8.4}$$

Now consider rectangular transmitting and receiving loops with sides parallel to the x and y axes. Suppose that the transmitting loop encloses the area 1108

$$\begin{aligned} a' &\leqslant x \leqslant b', \\ c' &\leqslant y \leqslant d' \end{aligned} \tag{8.5}$$

and that the receiving loop encloses the area 1111

$$\begin{aligned} a &\leqslant x \leqslant b \\ c &\leqslant y \leqslant d. \end{aligned} \tag{8.6}$$

Insert the series for J_0 (Abramowitz and Stegun [1], formula (9.1.10)) to obtain 1115

$$P(\lambda) = \lambda^2 \sum_{r=0}^{\infty} P_r \lambda^r, \tag{8.7}$$

where 1118

$$P_{2r+1} = 0 \tag{8.8}$$

$$P_{2r} = (-1)^r V_r / [2^{2r}(r!)^2] \tag{8.9}$$

and

$$V_r = \int_R \int_T |\mathbf{r} - \mathbf{r}'|^{2r}. \tag{8.10}$$

The integrations in (8.10) are over the areas of the loops. For the rectangular loops,

16701010

$$V_r = \int_a^b dx \int_c^d dy \int_{a'}^{b'} dx' \int_{c'}^{d'} dy' \left[(x - x')^2 + (y - y')^2\right]^r. \tag{8.11}$$

Use the binomial theorem on the power to reduce the integrand to a sum of multinomials which can then be integrated trivially. Thus,

$$V_r = \sum_{k=0}^{r} \binom{r}{k} U_k(a, b, a', b') U_{r-k}(c, d, c', d') \tag{8.12}$$

where

$$U_k(a, b, a', b') = \left[(b - a')^{2k+2} - (a - a')^{2k+2} - (b - b')^{2k+2} + (a - b')^{2k+2}\right] / [(2k + 1)(2k + 2)]. \tag{8.13}$$

Formulae (8.8), (8.12) and (8.13) give an easily computable expression for the sequence P_r.

Appendix 2

Listed in Table 4 are the points and weights for a Gaussian quadrature rule with weight $(1 - m^2)^{1/2} m^3$ on the interval (0, 1).

TABLE 4

	Points	Weights
1	0.908248748533967848*D* + 00	0.278859654274717499*D*–01
2	0.9765 32380300760677*D* + 00	0.934191464302680789*D*–02
3	0.801322605159335985*D* + 00	0.379453158439124976*D*–01
4	0.665445636715052751*D* + 00	0.322020100441213207*D*–01
5	0.512986701125[illegible]6676*D* + 00	0.180965420802834124*D*–01
6	0.357914686098593863*D* + 00	0.648895926666688655*D*–02
7	0.21455094914825976*D* + 00	0.128223423390867559*D*–02
8	0.960799955038826807*D*–01	0.903917939419827435*D*–04

References

[1] M.Abramowitz and I. A. Stegun, *Handbook of mathematical functions* (Dover, New York, 1965). 1171

[2] W. L. Anderson, "Numerical integration of related Hankel transforms of orders 0 and 1 by adaptive digital filtering", *Geophysics* 44 (1979), 1287–1305. 1173

[3] G. Buselli and B. O'Neill, "SIROTEM: A new portable instrument for multichannel transient electromagnetic measurements", *ASEG Bull.* 8 (1977), 82–87. 1176

[4] E. T. Copson, *Asymptotic expansions* (Cambridge University Press, Cambridge, 1971). 1179

[5] J. D. Crone, "Ground pulse EM—examples of survey results in the search for massive sulphides and new developments with the Crone PEM equipment", Paper presented by the author at the 25th international geological congress, Sydney, Australia (August, 1976). 1181

[6] D. P. Gaver, Jr., "Observing stochastic processes and approximate transform inversion", *Oper. Res.* 14 (1966), 444–459. 1185

[7] F. M. Kamenetski, "Transient processes using combined loops for a two layer section with a nonconducting base", *Izv. Vuzov. Section Geology Prosp.* 6 (1969), 108–113. 1187

[8] A. A. Kaufman, "Harmonic and transient fields on the surface of a two layered medium", *Geophysics* 44 (1979), 1208–1217. 1190

[9] J. H. Knight and A. P. Raiche, "Transient electromagnetic calculations using the Gaver-Stehfest inverse Laplace transform method", *Geophysics* 47 (1982), 47–50. 1192

[10] O. Koefoed, D. P. Ghosh and G. J. Polman, "Computation of type curves for electromagnetic depth sounding with a horizontal coil by means of a digital linear filter", *Geophys. Prosp.* 20 (1972), 403–420. 1195

[11] V. J. Krylov, V. V. Lugin and L. A. Yanovich, *Tables for integration of functions with power singularities* $\int_0^1 x^\beta (1-x)^\alpha f(x)\,dx$ (Izdat. Akad. Nauk BSSR, Minsk, 1963). 1198

[12] Y. L. Lamontagne, G. S. Lodha, J. C. Macnae and G. F. West, "UTEM: Wideband time domain EM project 1976–78, reports 1–5", *Research in applied geophysics* #11, Geophysics laboratory, Department of Physics, University of Toronto (1980). 1201

[13] T. Lee, "Asymptotic expansions for transient electromagnetic fields", *Geophysics* 47 (1982), 38–46. 1205

[14] T. Lee and R. Lewis, "Transient EM response of a large loop on a layered ground", *Geophys. Prosp.* 22 (1974), 430–444. 1207

[15] K. Mallick and R. K. Verma, "Time domain electromagnetic sounding with horizontal and vertical coplanar loops on a multilayered earth", *Geoexploration* 16 (1978), 291–302. 1209

[16] H. F. Morrison, R. J. Phillips and D. P. O'Brien, "Quantitative interpretation of transient electromagnetic fields over a layered half space", *Geophys. Prosp.* 17 (1968), 82–101. 1212

[17] T. N. L. Patterson, "Algorithm for automatic numerical integration over a finite interval", *Comm. ACM* 16 (1973), 694–699. 1215

[18] M. Schechter, *Operator methods in quantum mechanics* (North Holland, New York, 1981). 1217

[19] H. Stehfest, "Algorithm 368. Numerical inversion of Laplace transforms", *Comm. ACM* 13 (1970), 47–49. 1219

[20] H. Stehfest, "Remark on algorithm 368", *Comm. ACM* 13 (1970), 624. 1221

[21] A. H. Stroud and D. Secrest, *Gaussian quadrature formulas* (Prentice-Hall, Englewood Cliffs, N.J., 1966). 1223

[22] J. R. Wait, *Geoelectromagnetism* (Academic Press, New York, 1982). 1225

---

[2]Present address: Department of Physics, Univerisity of Toronto, Toronto, Ontario, Canada M5S 1A7.

1233

FIGURE 1

FIGURE 2

FIGURE 3

D. M. O'Brien[1] and R. S. Smith[2]

Asymptotic EM response

1. CSIRO
DIVISION OF ATMOSPHERIC RESEARCH
PRIVATE BAG 1
MORDIALLOC, VICTORIA 3195